

ELECTRON TRANSFER REACTIONS OF CYTOCHROMES C

ELECTRON TRANSFER REACTIONS
OF
CYTOCHROMES C

By

BRANKO F. PETERMAN, Dip. Ing., M.Sc.

A Thesis

Submitted to the School of Graduate Studies
in Partial Fulfilment of the Requirements
for the Degree
Doctor of Philosophy

McMaster University

DOCTOR OF PHILOSOPHY (1976)
(Biology)

McMASTER UNIVERSITY
Hamilton, Ontario

TITLE: Electron Transfer Reactions of Cytochromes c

AUTHOR: Branko F. Peterman, Dipl. Ing. (University of
Ljubljana, Ljubljana,
Yugoslavia)
M.Sc. (University of Saskatchewan,
Regina)

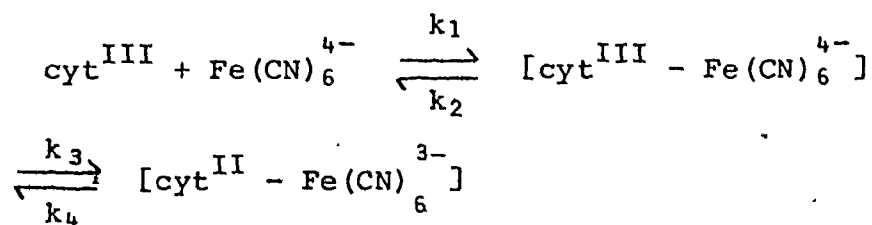
SUPERVISOR: Professor R.A. Morton

NUMBER OF PAGES: xvii, 189.

ABSTRACT

In the work described in this thesis we undertook studies of the electron transfer between cytochromes c and iron hexacyanides, a reaction which serves as a simple, well defined model for electron transfer *in vivo*. In particular, we were interested in the following aspects of electron transfer: the mechanism of the oxidation of ferrocytochrome c by ferricyanide, the mechanism of reduction of ferricytochrome c by ferrocyanide, the effect of charges on the protein and the ionic strength of the medium on electron transfer, and the effect of ions which bind to cytochrome c on oxidation and reduction. Since ion binding to cytochrome c has been observed by several techniques, cytochrome c preparations in this study were electrodialed, whenever possible, in order to remove contaminating bound ions.

The results of our work indicate that the oxidation of ferrocytochrome c by ferricyanide in non-binding (tris-cacodylate) buffer follows irreversible second-order kinetics. The reduction of ferricytochrome by ferrocyanide was found consistent with the following reaction scheme:



Our data suggests that there are different pathways for reduction and oxidation of cytochrome c when iron hexacyanides are used.

The effect of the ionic strength on the bimolecular rate for the oxidation of horse heart and *P. aeruginosa* ferrocytochromes in non-binding buffer was analyzed using Debye-Hückel theory, and suggested that the oxidation of horse heart ferrocytochrome c proceeds at nearly the diffusion-controlled rate. From this analysis an effective charge of +7.8 units for horse heart cytochrome c was obtained. The oxidation of *P. aeruginosa* cytochrome c was much slower and was not consistent with a diffusion-controlled reaction. The ionic strength dependence of the rate of oxidation for *M. denitrificans* ferrocytochrome c could not be fitted to Debye-Hückel theory.

The ionic strength was also found to affect the reduction of ferricytochrome c by ferrocyanide. The measurements revealed that the dissociation constant K_d ($= k_1/k_2$) and the rate constant k_4 in the above mechanism are ionic strength dependent.

Analysis of the effect of binding ions on the rate of oxidation for horse heart ferrocytochrome c

indicated that more than one chloride, phosphate, potassium and picrate ion were bound to horse heart ferrocytochrome c. The bound ion slowed the rate of oxidation.

The reduction of ferricytochrome c by ferrocyanide was approximated by a reversible second-order reaction, and the overall reduction and oxidation rates were derived. The ratios of these rate constants, measured in various buffers, were used to estimate the number of ions bound to ferricytochrome c and their respective binding constants. Approximately one chloride ion and almost two picrate ions were bound to horse heart ferricytochrome c. The rate of reduction of ferricytochrome c having bound ion(s) was also slower than normal.

Chemical modification (guanidination) of all the lysine residues of cytochrome c showed that positive charges and not lysines are necessary for efficient electron transfer between cytochrome c and iron hexacyanides.

To my wife Marjana
for her help and sacrifice

3
ACKNOWLEDGEMENTS

I wish to express my deepest appreciation to my supervisor Dr. R.A. Morton for his guidance and assistance throughout the course of this work. It has been rewarding to have a teacher of his capacities.

I would like to thank Dr. S.T. Bayley, Dr. B. Hillcoat and Dr. P. Nicholls (Brock University) for helpful discussions and suggestions during this investigation.

I am grateful to Mr. David Vogt for training me in machining skills and Mr. Robert Gillies for helping me to solve many electronics problems.

I am indebted to the National Research Council of Canada for the awards of Student Scholarships from 1972 to 1975.

TABLE OF CONTENTS

	Page
1. INTRODUCTION	1
1.1 Biological function of cytochromes c	1
1.2 Structure of cytochromes c	3
1.3 Mechanism of electron transfer reactions.	6
1.3.1. Chemical basis of electron transfer	6
1.3.2. Electron transfer of heme proteins.	8
1.3.3. Electron transfer of cytochrome c	10
1.4 Binding of ions to cytochrome c	15
1.5 Nature and scope of this work	18
2. MATERIALS AND METHODS.	23
2.1 Chemicals	23
2.2 Purification of cytochromes c	23
2.3 Electrodialysis of horse heart cytochrome c	25
2.4 Preparation of ferricytochrome c in D ₂ O	26
2.5 Guanidination of horse heart cytochrome c	28
2.6 Determination of lysine content of guanidinated cytochrome c	29
2.7 Preparation of buffers.	31
2.8 Determination of apparent equilibrium constant.	33
2.9 Stopped-flow measurements	35
3. EXPERIMENTAL RESULTS	37
3.1 Measurements of the apparent equilibrium constant	37

TABLE OF CONTENTS (cont'd)

	Page
3.2 Oxidation of ferrocytochrome c	40
3.2.1. Mechanism of oxidation of ferrocytochrome c .	43
3.2.2. The effect of ionic strength on the oxidation of ferrocytochrome c	50
3.2.3. Specific anion effects on the oxidation of ferrocytochrome c	53
3.2.3.1. The oxidation of the ferrocytochrome c in potassium phosphate buffer.	53
3.2.3.2. The effect of phosphate and chloride anions on the oxidation of ferrocytochrome c	56
3.2.3.3. The effect of picrate on the oxidation of ferrocytochrome c	57
3.2.3.4. The effect of ferrocyanide on the oxidation of ferrocytochrome c	61
3.2.4. Specific cation effects on the oxidation of ferrocytochrome c	63
3.2.4.1. The effect of potassium on the oxidation of ferrocytochrome c	63
3.2.5. Effect of D ₂ O on the oxidation of ferrocytochrome c	63
3.3 Reduction of ferricytochrome c with potassium ferrocyanide	65
3.3.1. Mechanism of reduction of ferricytochrome c .	67
3.3.2. The effect of the ionic strength on the reduction of ferricytochrome c	81
3.3.3. Specific anion effects on the reduction of ferricytochrome c	81
3.3.3.1. The effect of Cl ⁻ and phosphate on the reduction of ferricytochrome c	81
3.3.3.2. The effect of picrate on the reduction of ferricytochrome c	85

TABLE OF CONTENTS (cont'd)

	Page
3.4 Guanidinated cytochrome c	88
3.4.1. Oxidation of guanidinated ferrocytochrome c	88
3.4.2. Reduction of guanidinated ferricytochrome c	90
3.4.3. The effect of Cl^- on the reduction of guanidinated cytochrome c	93
4. ANALYSIS OF EXPERIMENTAL RESULTS AND DISCUSSION	95
4.1 Mechanism of electron transfer	95
4.1.1. Oxidation of ferrocytochrome c	95
4.1.2. Reduction of ferricytochrome c	96
4.2 Involvement of electric charges on cytochrome in electron transfer	104
4.2.1. Effect of ionic strength on oxidation	104
4.2.2. Effect of ionic strength on reduction	114
4.3 Specific ion effects on electron transfer.	116
4.3.1. Effects of ions on oxidation.	116
4.3.2. Effects of ions on reduction.	126
4.4 Comparison between guanidinated and unmodified cytochrome c	131
5. SUMMARY AND CONCLUSIONS	134
5.1 Oxidation of ferrocytochrome by ferricyanide	134
5.2 Reduction of ferricytochrome c by ferrocyanide	136
5.3 Modification of the lysine residues of cytochrome c	137
APPENDIX I	139
Rotating Dialyzer.	139
APPENDIX II	142

TABLE OF CONTENTS (cont'd)

	Page
Electrodialysis.	142
II.1. Principles of electrodialysis.	142
II.2. Apparatus.	143
APPENDIX III.	148
Stopped-flow Photometer.	148
III.1. Apparatus	148
III.1.1. Principle of operation.	148
III.1.2. Flow system	151
III.1.3. Optical system.	157
III.1.4. Electronics	159
III.2. Evaluation of performance	161
III.2.1. Applicability of Beer-Lambert law	161
III.2.2. Mixing efficiency	164
III.2.3. Dead time	165
III.2.4. Summary of performance.	166
APPENDIX IV	172
IV.1. Analysis of the kinetic runs	172
REFERENCES.	181

Descriptive Note	ii
Abstract	iii
Preface	vi
Acknowledgements	vii
Table of Contents	viii
List of Figures	xii
List of Tables	xvii

LIST OF FIGURES

		Page
Figure 2.1.	Electrodialysis of ferricytochrome c.	27
Figure 3.1.	Variation of $-\log_{10} K_{eq}$ versus $f(I)$, where $f(I)$ is defined as $\sqrt{I} / (1 + 6\sqrt{I})$.	38
Figure 3.2.	Comparison between the apparent equilibrium constants measured with dialyzed cytochrome c and electrodialed cytochrome c.	41
Figure 3.3.	Absorption spectra of reduced and oxidized horse heart cytochrome c.	44
Figure 3.4.	Computer-calculated averaged absorbancy differences as a function of time ($\Delta A(t)$ vs t) for the reaction between ferrocytochrome c and ferricyanide.	45
Figure 3.5.	Computer fitting of the experimental $\Delta A(t)$ vs t curve.	46
Figure 3.6.	Variation of the second-order rate constant for the oxidation of ferrocytochrome c as a function of ferricyanide concentration.	48
Figure 3.7.	Variation of the second-order rate constant for the oxidation of ferrocytochrome c as a function of ferrocytochrome c concentration.	49
Figure 3.8.	Effect of the ionic strength on the rate of oxidation ($\log k_{ox}$ vs \sqrt{I}) for cytochromes: (Δ) cHo^{II} ; (\square) cMn^{II} ; (o) cPs^{II} .	52

LIST OF FIGURES (cont'd)

	Page	
Figure 3.9.	Comparison of $\log k_{\text{Ox}}$ vs \sqrt{I} in tris-cacodylate and potassium phosphate buffer.	55
Figure 3.10. A and B	Effect of chloride (A) and phosphate (B) on the rate of oxidation of horse heart ferrocyanochrome c.	58
Figure 3.11.	Effect of picrate on oxidation of ferrocyanochrome c.	60
Figure 3.12.	Effect of potassium ferrocyanide on the rate of oxidation and on the rate of reduction as measured by the oxidation of ferrocyanochrome c.	62
Figure 3.13.	Effect of potassium ion on the rate of oxidation of ferrocyanochrome c.	64
Figure 3.14.	Ionic strength dependence of the rate constant for oxidation of cHoII in D_2O .	66
Figure 3.15. A and B	Relationship between the observed first-order rate constant for reduction of ferricytochrome c and the concentration of potassium ferrocyanide at several ionic strengths.	69
Figure 3.16. A and B	Double reciprocal plots of the observed first-order rate constant and the concentration of potassium ferrocyanide ($1/k_{\text{obs}}$ vs $1/\text{potassium ferrocyanide}$).	72
Figure 3.17.	The plots of $1/(k_{\text{obs}} - k_4)$ vs $1/(\text{Fe}(\text{CN})_6^-)$ at several different ionic strengths.	75
Figure 3.18A.	Variation of the overall second-order rate constant for reduction ($k_{\text{red}}^{\text{F}}$) of ferricytochrome c as a function of potassium ferrocyanide concentration.	79

LIST OF FIGURES (cont'd)

	Page	
Figure 3.18B.	Variation of the overall second-order rate constant for oxidation (k_{Ox}^r) as a function of potassium ferrocyanide concentration.	80
Figure 3.19.	Ionic strength dependence of the observed first-order rate constant for reduction of ferricytochrome c at different concentrations of potassium ferrocyanide.	82
Figure 3.20.	Effect of phosphate on the reduction of ferricytochrome c.	84
Figure 3.21.	Effect of chloride on the reduction of ferricytochrome c.	86
Figure 3.22.	Effect of picrate and chloride on the overall rate constants for reduction (o, Δ) and oxidation (+, \bullet).	87
Figure 3.23.	Comparison of the ionic strength dependence of the oxidation rate constant between modified and unmodified ferrocycytochrome c.	89
Figure 3.24.	Observed first-order rate for reduction of unmodified and modified ferricytochrome c as a function of potassium ferrocyanide concentration.	91
Figure 3.25.	Variation of the overall forward and reverse rate constants derived from reduction kinetics of modified ferricytochrome c as a function of potassium ferrocyanide concentration.	92
Figure 3.26.	Effect of chloride on the reduction of guanidinated ferricytochrome c.	94

LIST OF FIGURES (cont'd)

	Page
Figure 4.1. Variation of $\log k_{OX}$ vs $f(I) = \frac{\sqrt{I}}{1 + 6\sqrt{I}}$ for horse heart cytochrome c.	106
Figure 4.2. Variation of $\log k_{OX}$ vs $f(I) = \frac{\sqrt{I}}{1 + 6\sqrt{I}}$ for <i>P. aeruginosa</i> cytochrome c.	111
Figure 4.3. Plot of $\log H(k_{OX})$ vs $\log (A)$ for chloride (o), phosphate (+), potassium (Δ) and picrate (Δ).	120
Figure 4.4. Assumed location of binding sites for chloride and phosphate on cytochrome c.	124
Figure 4.5. Plot of $\log [(K_{ap} - K_{ap}^O) / K_{ap}^O]$ vs $\log (A)$ for picrate at ionic strength of 0.0485M(+) and chloride at the ionic strength of 0.194M(o) and 0.0485 M (Δ).	128
Figure I.1. Rotating dialyzer.	140
Figure II.1. Apparatus for electro dialysis.	145
Figure II.2A. Cross sectional drawing of electrode compartment.	146
Figure II.2B. Cross sectional drawing of sample compartment.	146
Figure III.1. Stopped-flow system.	149
Figure III.2. Flow system.	150
Figure III.3. Mounting of syringes.	152
Figure III.4A. Diagramatic view of the mixer.	154
Figure III.4B. Stopping syringe assembly.	154
Figure III.5. Actuating and triggering circuit.	156

3

LIST OF FIGURES (cont'd)

	Page
Figure III.6. Optical system.	158
Figure III.7. Current-to-voltage converter.	160
Figure III.8. Calculated light path as a function of absorbancy measured by the stopped-flow photometer.	163
Figure III.9. Computer analysis of a kinetic run.	167
Figure III.10. Transmittance changes during discharge.	169
Figure IV.1A. Schematic representation of a stopped-flow experiment.	174
Figure IV.1B. Schematic representation of the computer fitting of the experimental curve.	174

LIST OF TABLES

		Page
Table 1	Kinetic parameters K_d , k_3 and k_4 at different ionic strengths.	76
Table 2	Kinetic parameters ($K_d = k_2/k_1$, k_3 , k_4 , $K'_d = k_5/k_6$ and K_{eq}) for reduction of ferricytochrome c at several ionic strengths.	98
Table 3	The number of ions bound to cyt^{II} (n) and their association constants (K_a) as estimated from plots (Figure 4.3) based on measured oxidation rate constants.	121
Table 4	The number of ions bound to cyt^{III} (n) and their association constants (K_a) as determined from Hill plots (Figure 4.5) based on measurements of ($k_{\text{red}}^r/k_{\text{ox}}^r$).	129
Table 5	Comparison between kinetic parameters $K_d = k_2/k_1$, k_3 , k_4 and $K'_d = k_5/k_6$ for guanidinated and unmodified cytochrome c (I = 0.1 M).	132
Table III.1.	First-order rate constants and dead times for reduction of ferricyanide (0.1 mM) by ascorbate in 0.1 M phosphate buffer pH 7.0, 24°C.	171

1. INTRODUCTION

1.1 Biological function of cytochromes c

Since its isolation in 1930 by Keilin cytochrome c has been extensively used to study biological electron transfer. The work presented here involves a study of the electron transfer properties of three different cytochromes (horse heart, *Pseudomonas aeruginosa* and *Micrococcus denitrificans*) as observed when iron hexacyanides are used as electron donors or acceptors. In this section the biological functions of mammalian (horse heart) and bacterial (*Pseudomonas*, *Micrococcus*) are discussed and compared.

Mammalian cytochrome c is a component of the mammalian electron transport chain - a series of electron transferring proteins located on the mitochondrial membrane of all aerobic organisms. In the last stage of the biological oxidation of energy-rich organic molecules the electrons, removed from the various intermediates of the tricarboxylic acid cycle, are fed into the electron transport chain. When the electrons are passed down the electron transport chain, they lose their energy in small parcels (rather than in an immediate total loss), and in the final step, they reduce molecular oxygen to produce water. Part

of the energy released during the electron transport is conserved in the synthesis of ATP. Most of the cytochromes and other electron carrying proteins are tightly bound to the inner mitochondrial membrane. Cytochrome c is unique among these proteins in being easy to extract from mitochondria. When extracted, it is very stable in aqueous solutions. The biological function of cytochrome c is to pass electrons from cytochrome reductase to cytochrome oxidase within the electron transport chain. While transferring the electrons from cytochrome reductase to cytochrome oxidase, the iron atom located in the heme group of the cytochrome c molecule cycles between a reduced (Fe^{II}) and oxidized (Fe^{III}) state.

The respiratory chain of the bacterium *Micrococcus denitrificans* resembles the mammalian electron transport chain (Scholes and Smith, 1968). However, the bacterial electron transport chain can use either oxygen or nitrate as its terminal electron acceptor. A type c cytochrome can be extracted from bacterial cells, and this is presumably involved in the electron transport when oxygen is used as oxidant (Vernon, 1956). Despite having a net negative charge (Scholes *et al.*, 1971) (mammalian cytochromes possess a net positive charge) it can be oxidized by mammalian cytochrome oxidase. Furthermore, the bacterial oxidase oxidizes mammalian cytochrome c even faster than mammalian cytochrome oxidase does (Scholes *et al.*, 1971).

Pseudomonas aeruginosa cytochrome c_{551} is a component of a bacterial respiratory chain which is functionally analogous to the mammalian cytochrome c. Like the *V. denitrificans* respiratory chain, the *P. aeruginosa* electron transport chain can use oxygen or nitrate as a terminal electron acceptor (Yamanaka and Okunuki, 1963). The *Pseudomonas* cytochrome oxidase is biologically specific, i.e. it oxidizes *Pseudomonas* ferrocytochrome c, but it scarcely acts on reduced mammalian cytochrome c (Yamanaka and Okunuki, 1963).

1.2 Structure of cytochromes c

The purpose of this section is to briefly describe the structural features of mammalian and bacterial cytochromes c. The knowledge of the structure is important for understanding the functional role of cytochrome c in electron transport. The structure of cytochrome c has been studied by various physicochemical techniques. The following are the main features of mammalian, and in particular horse heart, cytochrome c.

Horse heart cytochrome c is a low molecular weight ($\sim 12,500$) heme protein shaped like a prolate spheroid with axes 30 A x 34 A x 34 A (Dickerson *et al.*, 1971a). The molecule consists of a single polypeptide chain of 104 amino acid residues and a covalently attached heme group.

The heme group is bound to the polypeptide chain by two thioether bridges to cysteine 14 and cysteine 17. The iron atom (located in the center of the porphyrin ring) is coordinated by six ligands in an octahedral arrangement. Four out of six ligands are porphyrin nitrogens. The fifth coordination site is occupied by the nitrogen of histidine 18 and the sixth by the sulphur of methionine 80. The amino acid analysis of horse heart cytochrome c shows that a cytochrome c molecule contains twenty-one basic residues (nineteen of them lysines) and twelve acidic amino acid residues producing a basic molecule with a high isoionic point at pH = 10.

The tertiary structures of crystalline horse and tuna ferricytochromes c (Dickerson *et al.*, 1971a; Swanson *et al.*, 1976) and tuna ferrocytochrome c (Takano *et al.*, 1973; Ashida *et al.*, 1971; Ashida *et al.*, 1973; Tanaka *et al.*, 1975; Takano *et al.*, 1976) have been determined by the x-ray diffraction technique. As revealed by x-ray crystallography, the folding of cytochrome c₂, extracted from the photosynthetic bacterium *R. rubrum* closely resembles the folding of reduced tuna cytochrome c (Salemme *et al.*, 1973). The x-ray model of cytochrome c indicates a very tight folding of the polypeptide chain around the heme group with the hydrophobic residues on the inside of the molecule, providing a proper environment for the hydrophobic heme group, and the charged residues on the

molecular surface. The heme group, located in a crevice with one edge exposed to the solvent, divides the polypeptide chain into two halves. The right half consists of residues 1 to 47 and the left one from 48 to 91, with the remainder of the polypeptide chain connecting the two tops of the halves like a strap. There are two short α -helical stretches from residues 1 to 11 and from 89 to 101.

Early reports (Dickerson *et al.*, 1971; Takano *et al.*, 1973) revealed large conformational differences between the tertiary structures of reduced and oxidized cytochrome c. Recent structure analysis of tuna ferricytochrome c (Swanson *et al.*, 1976) and tuna ferrocytochrome c (Takano *et al.*, 1976) at 2 Å resolution showed that this was an error, and now it is believed that the structures of reduced and oxidized cytochrome c are very similar.

Amino acid sequences have been determined for both *Micrococcus denitrificans* cytochrome c (Scholes *et al.*, 1971) and *Pseudomonas aeruginosa* cytochrome c (Ambler, 1963a; Ambler, 1963b). In contrast to mammalian cytochromes, both cM_d and cP_s are acidic having their isoelectric points less than pH 7. *M. denitrificans* cytochrome c has 135 amino acid residues and a molecular weight of 14,000. *P. aeruginosa* cytochrome c has only 82 amino acids and a molecular weight of approximately 9,000. The crystal structure of cM_d at 4 Å resolution has been reported by Timkovich and Dickerson (1973). The bacterial cytochrome c

shows the same "cytochrome fold" as observed in all other cytochromes (mammalian and photosynthetic). Dickerson (1971b) proposed a three-dimensional structure of cPs on the basis of the known structures of horse and tuna cytochromes.

1.3. Mechanism of electron transfer reactions

Because of its importance in oxidative phosphorylation, electron transfer by heme proteins has been the subject of many studies. Electron transfer by cytochrome c is essentially a chemical reaction. In this section the chemical basis of electron transfer pertinent to cytochrome c will be discussed. In addition, some general models of biological electron transfer and their application to electron transfer by cytochrome c will be presented.

1.3.1. Chemical basis of electron transfer

Oxidation-reduction reactions involve the exchange of one or more electrons between two reactants. One can distinguish two kinds of electron transfer reactions: inner sphere and outer sphere reactions (Halpern, 1961). Inner sphere electron transfer is characterized by the formation and rupture of a chemical bond between the two reactants. The electron is transferred via an activated complex which contains a group bonded to both reactants

(Taube and Myers, 1954). In the outer sphere electron transfer reactions, electrons are simply exchanged by collisions of freely moving molecules (Brownian motion) without the formation of chemical bonds. During the collision, a slight overlap of the pertinent orbitals occurs and allows the electron to be transferred from one molecule to the other. Outer sphere electron transfer reactions have been theoretically formulated by Marcus (1955; 1959; 1963). The theory is based on the Franck-Condon principle which states that the hydration atmospheres around an ion cannot rearrange in the time required for the electron transfer (Libby, 1952). The addition of an electron to the hydrated ion results in a formation of a hydrated ion in an incorrect solvent environment. The unfavorable configuration causes rearrangement of the hydration atmosphere which constitutes a potential barrier for the electron transport. The conservation of energy requires that before the electron transfer occurs, an activated complex is formed in which there exists a slight interaction (rearrangement) of electronic orbitals and the polarization of the surrounding medium of the two reacting molecules. By assuming weak electronic interaction, Marcus (1955; 1959; 1963) derived very simple equations for the rate of electron transfer.

These theoretical equations have been successfully applied to many inorganic electron transfer systems (Newton, 1968; Dulz and Sutin, 1963). The theory was also

applied to biological electron transfer involving cytochrome c. Excellent agreement was found between the calculated and experimental values for the reduction of ferricytochrome c by $\text{Ru}(\text{NH}_3)_6^{2+}$ (Ewall and Bennett, 1974) and for the oxidation of ferrocytochrome c by Tris(1,10-phenanthroline) cobalt(III) (McArdle *et al.*, 1974). However, when the same theory was applied to estimate the rate of electron transfer between iron hexacyanides and cytochrome c a large discrepancy between the measured and calculated values was obtained (Creutz and Sutin, 1974).

1.3.2. Electron transfer of heme proteins

By studying the electron transfer of the electron-carrying proteins one would like to answer the following questions: how does the electron get from one heme protein to another (in the respiratory chain, for example), what is mechanism by which the electron traverses its path from the surface of the molecule to the heme iron, what are the parameters affecting the electron transfer (the presence of ions, for example), and what are the interactions between two heme proteins when they exchange an electron?

Despite the great knowledge of physicochemical properties of many electron-carrying heme proteins, the mechanism of electron transfer of heme proteins is still largely unknown. There is ample evidence from e.g.

absorption spectra, ESR and NMR that the heme iron is the ultimate site of the electron but little is known of how the electron is transferred to and from the heme group. Below, some more general mechanisms of electron transfer pertinent to cytochromes are presented.

De Vault and Chance (1966) proposed quantum mechanical tunnelling as the mechanism of the electron transfer between two cytochromes in the photosynthetic bacterium *Chromatium*. According to this mechanism, an electron with less energy than the energy of the potential barrier, can be transferred across the barrier. Quantum mechanical tunnelling is a well known mechanism which has been used to explain many processes in physics and chemistry. Recent results by McElroy *et al.* (1974) are consistent with the hypothesis that electron transfer in photosynthetic bacteria can occur by tunnelling. The theoretical studies on electron transfer between biological molecules by thermally activated tunnelling have been recently discussed by Hopfield (1974).

On the basis of their model studies, Castro (Castro and Davis, 1969; Castro, 1971) proposed that electron transfer could take place via peripheral π -transfer. The process is essentially analogous to classic outer sphere electron transfer. As noted in Section 1.2 cytochrome c has part of its porphyrin ring exposed to the environment which would allow the peripheral attack of a reducing or

oxidizing reagent. According to this model, two cytochromes exchange an electron by slightly overlapping their exposed porphyrins.

In 1965 Winfield suggested that electron migration within the molecule could occur via a free radical pathway involving aromatic amino acid residues, such as tyrosine or tryptophan. This model was based on the experimental evidence that some peptides and amino acids can, under special conditions, easily form free radicals.

It was proposed by Dickerson (1974) that electron transfer between two molecules may involve more than one mechanism, for example, electron tunnelling for a certain distance followed by free radical electron flow.

1.3.3. Electron transfer of cytochrome c

The models of electron transfer discussed in the previous section have been applied to interpret electron transfer from cytochrome reductase to cytochrome c and from cytochrome c to cytochrome oxidase.

In this section the mechanism of electron transfer from cytochrome reductase to the iron atom of cytochrome c proposed by Takano *et al.* (1973) will be described. This mechanism is open to question, however, since it is based on previously reported structural differences of cytochrome c accompanying the change of oxidation state which, in fact,

do not occur (Swanson *et al.*, 1976; Takano *et al.*, 1976). It is expected that the authors (Takano *et al.*, 1973) will modify their mechanism appropriately to the new findings.

Takano *et al.* (1973) proposed a model whereby the electron is transferred through a channel of π -bonded aromatic amino acid residues within the molecule as suggested by Winfield (1965). In the first step the electron is transferred from cytochrome reductase to tyrosine 74 near the cytochrome c surface. From there the electron migrates via the electron cloud overlap to the nearby aromatic residue tryptophan 59. The excess negative charge on tryptophan 59 causes a second electron to be transferred from the adjacent tyrosine 67 (which is located parallel to the heme group at a distance of 4 Å) to the heme group. Both transfers are energetically allowed since the electron is always moved to a more delocalized system (larger aromatic rings). The positive and negative charges on the nearby residues probably cause the reorientation of tryptophan 59 and tyrosine 67 into positions so that the charges can neutralize each other via electron cloud overlap. Since the recent x-ray diffraction studies on the cytochrome c structure failed to disclose any reorientations of the aromatic amino acid residues this mechanism is probably not valid.

Two contrasting models for electron transfer *in vivo* have been proposed. One assumes that cytochrome c

interacts with cytochrome reductase and cytochrome oxidase at two widely separated binding sites. The other assumes that the electron enters and leaves the molecule at the same site, namely the exposed heme edge.

First, the evidence for separate binding sites will be discussed. Studies of electron transfer between cytochrome reductase and cytochrome c modified at tyrosine 74, tryptophan 59, tyrosine 67 and methionine 80 showed that the modified cytochrome c was defective in accepting the electrons from cytochrome reductase (Margoliash *et al.*, 1973). On the other hand, the oxidation of modified ferrocytochrome c with purified cytochrome oxidase was relatively unaffected. Cytochrome c modified at lysine 13 showed reduced activity with cytochrome oxidase, whereas the activity with cytochrome reductase was not affected at all (Margoliash *et al.*, 1973; Wada and Okunuki, 1969). Lysine 13 is located above the heme crevice on the front surface of the cytochrome c molecule. It is believed that modified lysine 13 physically blocks the interactions between cytochrome c and cytochrome oxidase.

Besides the chemical modification studies by Margoliash *et al.* (1973) and Wada and Okunuki (1969) there is further evidence that cytochrome c reacts with cytochrome oxidase and cytochrome reductase at two widely separated binding sites. Smith *et al.* (1973) isolated four different populations of rabbit antibodies against human cytochrome c,

two of which were found to specifically affect the electron transfer reactions of cytochrome c. One population specifically reduced electron transfer from ferrocytochrome c to cytochrome oxidase without affecting the reduction of ferricytochrome c by cytochrome reductase. The other blocked electron transfer from cytochrome reductase to cytochrome c, but did not affect the oxidation of ferrocytochrome c by cytochrome oxidase. Both chemical modification and antibody studies are consistent with the concept (Dickerson *et al.*, 1971) that the electron from the cytochrome reductase enters the cytochrome c molecule from left back and leaves it along the heme edge through the front surface. (The convention in defining the orientation of cytochrome c is to imagine an observer looking at the edge of the exposed heme with the N-terminal end at the top.)

Salemme *et al.* (1973a; 1973b) proposed that electron transfer in both directions (to and from the iron atom) occurs via the exposed heme edge. Support for this mechanism comes from NMR studies on ferricytochrome c by Redfield and Gupta (1971). They observed that the unpaired electron of ferricytochrome c spends more time on pyrole ring II which is located near cysteine 17 (close to the surface of the molecule) and on its diagonally opposite pyrole ring IV than on the other two pyrole rings. This observation suggests that it would be easier to add an electron to heme iron in the direction of pyrole II than

in any other direction (Redfield and Gupta, 1971). In addition, this pathway represents physically the shortest and therefore the most accessible link between the iron atom and the exterior of the molecule.

Another important question is whether or not the mechanism of electron transfer is the same when inorganic electron donors and acceptors are used, as in the intact mitochondria. Studies on the reduction of ferricytochrome c with inorganic reagents showed that there are at least two pathways by which the electron can reach the heme iron: adjacent attack (Sutin and Yandell, 1972) and remote attack (Hodges *et al.*, 1974). In adjacent attack, the reducing agent interacts with the polypeptide chain either rupturing the sulfur bond (Sutin and Yandell, 1972) or opening the crevice of the cytochrome c molecule (Yandell *et al.*, 1973) and then the reduction of heme iron occurs. Evidence for adjacent attack (Sutin, 1976) came from chromous ion binding studies by Grimes *et al.* (1974). They observed that after reduction of ferricytochrome c by chromous ion the chromium attaches to the cytochrome c molecule in the area of the heme crevice. In remote attack, the electron is transferred to the iron atom by an indirect route, probably by the exposed heme edge. Reductions of ferricytochrome c by $\text{Fe}(\text{EDTA})^{2-}$ (Hodges *et al.*, 1974) and by $\text{Ru}(\text{NH}_3)_6^{2+}$ (Ewall and Bennett, 1974) were suggested to occur via the exposed heme edge. McArdle *et al.* (1974) proposed that the

oxidation of ferricytochrome c by Tris(1,10-phenanthroline) cobalt(III) can also take place through the exposed heme edge.

1.4 Binding of ions to cytochrome c

The binding of ions to cytochrome c has been found to affect many physicochemical properties of the protein, including the rate of the electron transfer. Studies of the relationship between the binding of ions to the protein and electron transfer reactions are important for understanding the structural - functional properties of cytochrome c. The binding of ions to cytochrome c has been recently reviewed by Nicholls (1974).

Cytochrome c is a typical example of an oil drop model protein with both positively and negatively charged residues on its molecular surface. The charged groups on the surface of the molecule represent potential binding sites for small anions like phosphate, Cl^- , ATP, ADP, etc. and cations like K^+ , Na^+ , Mg^{++} , Ca^{++} ... etc. Numerous techniques have been applied to study the interactions between small ions and cytochrome c. Measurements of electrophoretic mobility (Barlow and Margoliash, 1966; Margoliash *et al.*, 1970), and of reduction potential (Margalit and Schejter, 1970; Schejter and Margalit, 1970; Margalit and Schejter, 1973a; Palcic, 1972), gel

filtration (Margalit and Schejter, 1973b), NMR studies (Stellwagen and Shulman, 1973a) and equilibrium dialysis measurements (Stellwagen and Cass, 1975) have all indicated binding of various ions to cytochrome c.

Electrophoretic measurements (Barlow and Margoliash, 1966) showed that the bound ions (Cl^- , for example) could not be removed by either ion-exchanging chromatography or gel filtration, but that electro dialysis of cytochrome c solutions was necessary to remove them completely.

Furthermore, it was observed that some ions bind with different affinity to the different forms of cytochrome c (Margoliash *et al.*, 1970); for example, phosphate ions bind equally tightly to both oxidation states, whereas chloride ions bind predominantly to the ferri- form of cytochrome c. Cacodylate and tris ions showed negligible effect on the electrophoretic mobility of cytochrome c. This and the fact that the isoelectric point of cytochrome c in tris-cacodylate buffer was found equal to the isoionic point, suggested that the mixture of tris base and cacodylic acid is a nonbinding buffer.

The presence of ions was shown to have an effect on reduction potential of cytochrome c when cytochrome c was titrated with potassium ferrocyanide (Margalit and Schejter, 1970; Schejter and Margalit, 1970; Margalit and Schejter, 1973a; Palcic, 1972). The results indicated that two more anions were bound to cytochrome c in the

oxidized state than in the reduced state. Modification of lysine residues of cytochrome c by guanidination or trinitrophenylation resulted in the removal of one binding site and it was suggested that modification of lysine 13 was responsible for the loss of one binding site (Palcic, 1972).

The binding of ions to cytochrome c was further demonstrated by gel filtration (Margalit and Schejter, 1973b). The binding of Cl^- and phosphate anions was found to be quite strong with a binding constant of the order of 10^4 M^{-1} .

Stellwagen and Shulman (1973a) observed interactions between Cl^- ions and reduced cytochrome c which were not detected by electrophoretic measurements. The NMR lines which they assigned to the amino proton of lysine 60 were shifted in the presence of Cl^- ions. Furthermore, they suggested that a phosphate ion was bound in vicinity of histidine 26 since it broadened the resonance line assigned to the imidazole amino proton of this histidine. The authors proposed that Cl^- ions perturbed the hydrogen bond between the amino hydrogen of lysine 60 and the carboxylate group of glutamic acid 62 and similarly, that phosphate ions perturbed the hydrogen bond between histidine 26 and the amide carbonyl of aspartic acid 31.

Stellwagen and Cass (1975) employed equilibrium dialysis to demonstrate the binding of iron hexacyanides

to cytochrome c. The experiments indicated that both forms of cytochrome c contained two non-equivalent binding sites for ferrocyanide. Two ferricyanide ions were found to bind to the ferricytochrome c molecule with approximately equal affinity.

Recently Ferguson-Miller *et al.* (1976) proposed that cytochrome c binds to cytochrome oxidase at two binding sites of different affinities. When cytochrome c is attached at the site of higher affinity it can be reduced by cytochrome reductase. Cytochrome c can be removed from this site, with a decrease in rate of electron transfer, if the concentration of ATP in the medium is increased to physiological levels. It was suggested that anions like ATP, ADP and P_i could have an important function in controlling the electron flow from cytochrome c to cytochrome oxidase by affecting the interactions of these two molecules.

1.5. Nature and scope of this work

One of the objectives of this work was to construct an instrument which could be used for studying the very fast reactions of cytochrome c in solution. Although commercial stopped-flow photometers are available, the following considerations led us to construct our own stopped-flow photometer (SFP):

- A. The kinetics of biological reactions are often complicated and their analysis very time consuming. Therefore, it would be convenient to analyze the kinetic runs by means of a computer. This means that the experimental data should be converted from analog to digital form, and then transferred to either paper or magnetic tape, to form a permanent record. The tape can then be fed into the computer for the data to be analyzed.
- B. The dead time of the SFP should be as short as possible. The best and of course the most expensive, SFP is produced by Durrum Co. and has a dead time of 3.6 ± 0.8 msec (Hammes and Haslam, 1968). The dead time can be shortened by reducing the diameter of the fluid delivery holes so as to increase the linear velocity of the flow in the apparatus.
- C. Many biological reactions are sensitive to traces of metals and therefore, the reactants should not come in contact with metal parts of the apparatus as they do in many commercial SFP.
- D. An arrangement for thermostating the entire system should be built into the stopped-flow unit.
- E. The apparatus should be easily adaptable for the fluorescence and light scattering measurements.

Once the stopped-flow photometer was constructed, its performance was extensively tested. The instrument and its

performance are described in detail in Appendix III.

In this work we undertook studies of the electron transfer between iron hexacyanides and cytochrome c. This system serves as a simple, well defined model for more complex electron transfer *in vivo*. Although some work has been reported on the electron transfer between cytochrome c and iron hexacyanides, many aspects, such as the effects of ions on reduction and oxidation of cytochrome c, the mechanism of reduction of ferricytochrome c, and the involvement of the charged groups on cytochrome c in electron transfer are still obscure. Information gained through this study will contribute to better understanding of the electron transfer properties of cytochromes of type c.

One of the essential steps in chemical kinetics is to determine the mechanism (order) of the reaction. This gives information on all the steps that occur simultaneously or consecutively in producing the observed reaction. Therefore, the first part of this study involved the determination of the reaction mechanisms (order) for both oxidation and reduction of cytochrome c by ferricyanide and ferrocyanide, respectively. The study of the mechanism of the electron transfer might shed some light on the mode (pathway) of the electron transfer.

Electrostatic interactions play a very important role in the process of the mitochondrial electron transport

(Smith and Minnaert, 1965). In order to study the involvement of protein charges in the electron transfer between iron hexacyanides and cytochrome c, two approaches were taken. The first involved the selection of three cytochromes c of different net charges and the comparison of their electron transfer properties. The second approach involved studies of the effect of the ionic strength on the kinetics of the electron transport. If electrostatic interactions are operative in electron transfer one would expect that the masking of protein charged groups with counter-ions from the medium will have a significant effect on the rate of electron transfer. Theoretical analysis of the ionic strength dependence of the rate of the electron transfer can yield information on the sign and the effective value of the charge on the protein operative in the electron transfer.

It has been shown by several techniques that various ions differentially interact with the two oxidative states of cytochrome c (Section 1.4.). The question emerges whether the binding of these ions affects the rate of electron transfer to and from cytochrome c when iron hexacyanides are used as reducing and oxidizing reagents. Therefore, in this work, we have examined the effects of various ions on the oxidation and reduction of cytochrome c. Since some of the ion binding sites have been identified one can speculate which parts of the

cytochrome c molecule are directly or indirectly involved in the electron transfer. This approach can yield some insight into the structure - function relationship of the cytochrome c molecule.

In the last part of this work, the lysine residues of native cytochrome c were converted by guanidination into homoarginine residues. This modification conserves the positive charge on the molecule. We have examined the electron transfer and ion binding properties of guanidinated cytochrome c and compared them with those of unmodified cytochrome c in an attempt to determine the importance of these residues in electron transfer reactions.

2. MATERIALS AND METHODS

2.1. Chemicals

Cacodylic acid purchased from Schwarz/Mann (Orangeburg, N.Y.) was passed through a Biorex 70 column (1.5 cm x 15 cm), dried, and then crystallized from a mixture of 95% ethanol and ethyl ether (2:1). Potassium ferrocyanide and potassium ferricyanide, both reagent grade, were obtained from BDH Chemicals LTD. (Poole, England) and J.T. Baker Chemical Co. (Phillipsburg, N.J.), respectively. Tris (Trizma base, Sigma Chemical Co., St. Louis, Mo.), reagent grade, was used without further purification. Distilled water deionized and redistilled in a glass still was used for all experiments. All other chemicals were reagent grade and were used without further purification.

2.2. Purification of cytochromes c

Horse heart cytochrome c was purchased from Sigma Chemical Co. (type VI, lot 82 C - 7700) and was further purified on a carboxymethyl cellulose (CMC) column (2.5 cm x 50 cm) equilibrated with 0.05 M Na_2HPO_4 - 0.05 M

NaH₂PO₄ buffer, pH 6.8 (Dixon and Thompson, 1968). All purification procedures were carried out at 4°C, unless otherwise stated. Two peaks were eluted from the column. The first peak which corresponded to ferrocytochrome c was discarded. The center of the second peak, corresponding to oxidized cytochrome c, was pooled and diluted 3-4 times with glass distilled water. Diluted cytochrome c solution was concentrated on a short CMC column (1.2 cm x 8 cm) equilibrated with 0.02 M sodium phosphate buffer, pH 7.2. Adsorbed cytochrome c was eluted from the column with 0.4 M sodium phosphate buffer and dialyzed in a rotating dialyzer (see Appendix I) against 0.05 M sodium phosphate buffer for 8-10 hours. The last purification step involved the electro dialysis of the cytochrome c solution which is described in section 2.3..

Micrococcus denitrificans and *Pseudomonas aeruginosa* cytochromes were gifts of Dr. R.A. Morton. Before use, *Micrococcus denitrificans* cytochrome c (cMd) was purified on a diethylaminoethyl (DEAE)-cellulose column, equilibrated with 0.01 M sodium acetate buffer, pH 6.0 (Scholes *et al.*, 1971). The adsorbed cMd was eluted from the column with a linear gradient from 0.1 M to 0.5 M sodium acetate buffer, pH 6.0. Since the amount of protein was not sufficient for electro dialysis, it was dialyzed for 24 hours against 0.05 M tris-cacodylate buffer, pH 7.0, and then for another 24 hours against

0.001 M tris-cacodylate buffer, pH 7.0. Reduced cMd was prepared by adding sodium dithionite to the solution of oxidized cMd. The unreacted reducing reagent was removed by filtering solution through a short column of Sephadex G-25 equilibrated with 0.001 M tris-cacodylate buffer, pH 7.0.

The lyophilized sample of *Pseudomonas aeruginosa* cytochrome c_{551} (cPs) was first dialyzed overnight against 0.001 M potassium phosphate buffer, pH 6.8, and then applied to a DEAE-cellulose column equilibrated with 0.001 M potassium phosphate buffer, pH 6.8 (Morton *et al.*, 1970). The elution was effected with a linear concentration gradient from 0.001 M to 0.1 M potassium phosphate buffer, pH 6.8. The eluted preparation was dialyzed (48 hours) against 0.001 M tris-cacodylate buffer, pH 7.0. *P. aeruginosa* ferrocycytochrome c was then prepared in the same manner as *M. denitrificans* ferrocycytochrome c.

2.3. Electrodialysis of horse heart cytochrome c

Horse heart cytochrome c chromatographed in 0.05 M sodium phosphate buffer was electrodialed in the electrodiaalysis apparatus described in Appendix II. The pH of the cytochrome c solution was adjusted to approximately pH 8 with solid tris. When ferrocycytochrome c was prepared, ferricytochrome c was first reduced with sodium dithionite.

The starting pH was kept close to the isoionic point ($\Delta \text{pH} < 3$), otherwise protein was adsorbed to the ion-exchange membranes. With a sample volume of 19 ml the applied voltage was 150 V, and 100 V when the volume was 12 ml. The course of the electro dialysis of cytochrome c solution can be seen in Figure 2.1. Towards the end of each run, when the current was low, the voltage was increased to between 200 V and 300 V, in order to remove all the remaining dialyzable ions. When the current stabilized, the solution was removed from the sample compartment, and the pH measured. The final pH value always reached the neighborhood of 10.05, the value of the isoionic point reported by Barlow and Margoliash (1966). After electro dialysis, the pH of cytochrome c solution was lowered to 7 by adding solid cacodylic acid, and finally dialyzed overnight against 0.001 M tris-cacodylate buffer, pH 7.0. The cytochrome c solution was stored at 4°C until used.

2.4. Preparation of ferrocytochrome c in D₂O.

Reduced horse heart ferrocytochrome c in D₂O was prepared by reduction of chromatographed cytochrome c with sodium dithionite and passing it through a short Sephadex G-25 column washed with deionized water. Reduced cytochrome c solution was lyophilized and the dry powder


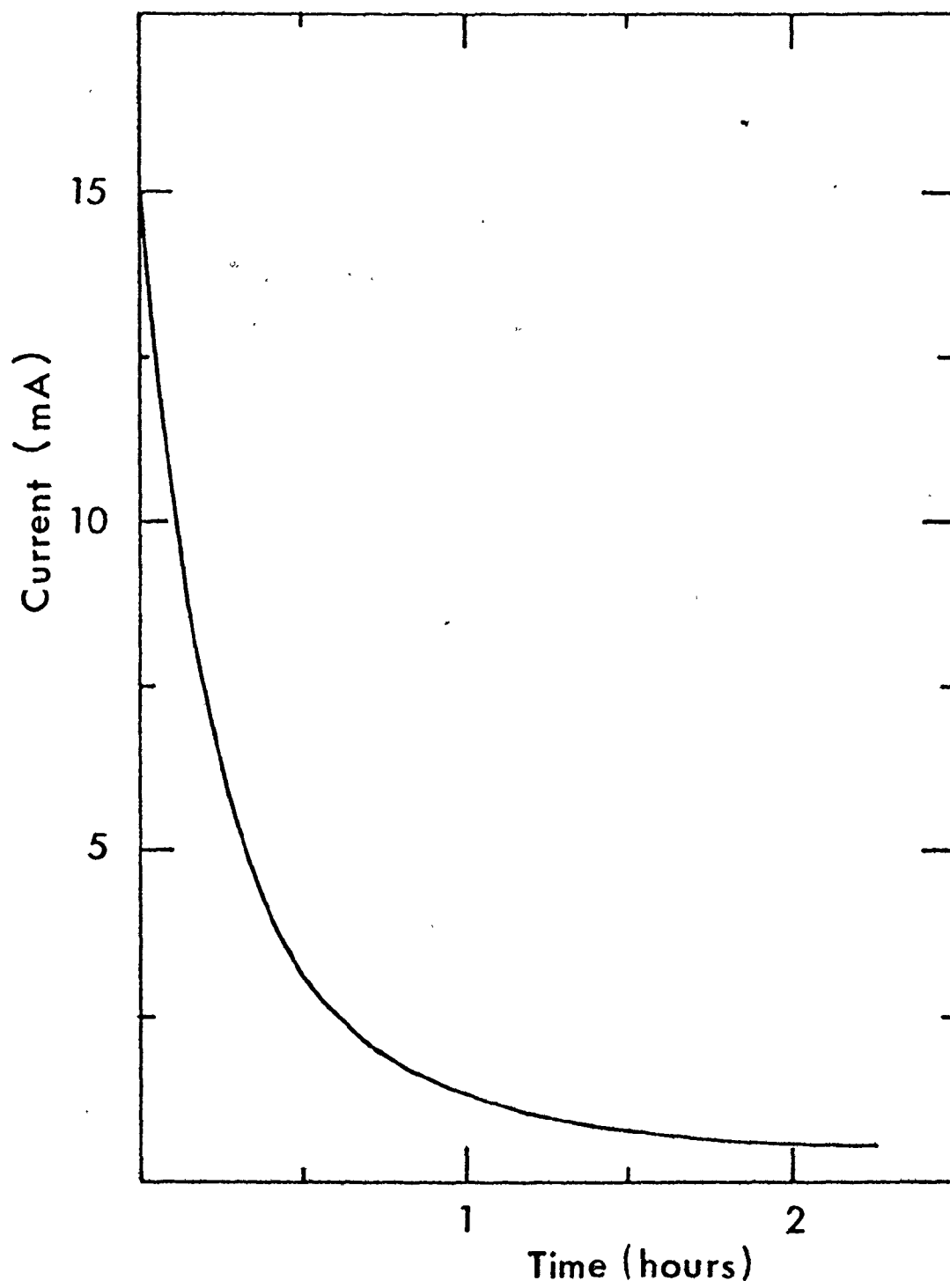


Figure 2.1. Electrodialysis of ferricytochrome c.

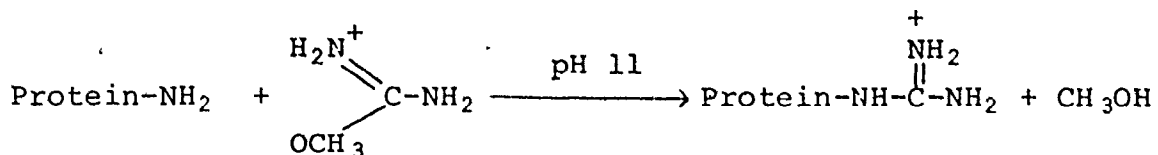
Applied voltage $U = 150$ V, temperature $T = 10^{\circ}\text{C}$, pH
after electrodialysis 10.05.



dissolved in D₂O. The last two procedures were then repeated two more times. The prepared ferrocytochrome c remained at least 90% reduced. Ionic strength and pD were adjusted by adding NaOD and DCl. The pH was determined by measuring the pH of the solution and assuming pD = pH + 0.4 (Lumry *et al.*, 1951).

2.5. Guanidination of horse heart cytochrome c

O-Methylisourea selectively reacts with ε-amino groups (Means and Feeney, 1971) converting lysine residues into homoarginine residues



The modification does not change the charge on the protein molecule.

Guanidination of horse heart cytochrome c was carried out following the procedure of Hettlinger and Harbury (1964). O-Methylisourea sulfate (Eastman Organic Chemicals, Rochester, N.Y.) was dissolved in distilled water at 4°C, to a final concentration of 0.5 M and the pH was adjusted to 8.5 with 4 N NaOH. Cytochrome c (1% final concentration) was added to this solution and the pH adjusted to 11 with 4 N NaOH. The reaction was allowed to proceed for 120 hours at 4°C. The resulting mixture was then dialyzed

in the rotating dialyzer against 0.02 M sodium phosphate buffer for 12 hours. Precipitated material was removed by centrifugation at 6000 rpm for 20 min. The modified protein was chromatographed on a CMC column equilibrated with 0.02 M sodium phosphate buffer and eluted with a linear concentration gradient from 0.02 M sodium phosphate buffer to the same buffer containing 0.5 M NaCl. The bulk of the guanidinated cytochrome c (gn-cytochrome c) came off the column as a single peak, which was collected, concentrated by ultrafiltration (Diaflo^R, Amicon Co., with UM-2 membrane) and dialyzed in the rotating dialyzer against 0.001 M tris-cacodylate buffer, pH 7.0, for 48 hours. The preparation was analyzed for lysine content according to the procedure described in section 2.6.. Since the electro dialysis of 0.3 mM gn-cytochrome c resulted in the precipitation of the protein, this purification step was omitted and only dialyzed cytochrome c was used for experiments. Gn-ferrocyclochrome c was prepared by reducing gn-ferricytochrome c with sodium dithionite and by passing it through a short Sephadex G-25 column.

2.6. Determination of lysine content of guanidinated cytochrome c

The lysine content of guanidinated cytochrome c was determined by the method of Kakade and Liener (1969).

The reagent 2,4,6-trinitrobenzene sulfonic acid (TNBS) reacts with primary amino group (Okuyama and Satake, 1960) yielding trinitrophenyl (TNP) derivatives which are coloured with an absorbancy peak at $\lambda = 345$ nm. In order to make the procedure specific for the ϵ -amino groups of lysine residues, Kakade and Liener included an ethyl ether extraction step which removes TNP N terminal amino acid and picric acid.

The procedure was carried out as follows. The pH of the guanidinated cytochrome c solution containing 4% NaHCO_3 was adjusted to 8.5 with 1 N NaOH. The concentration of cytochrome c was determined by measuring the absorbancy at the isobestic point of 526 nm with $\epsilon = 11,000 \text{ M}^{-1} \text{ cm}^{-1}$ (Fanger *et al.*, 1967). To 1 ml of the above solution, 1 ml of aqueous solution of 0.1% TNBS was added and the solution was placed for 1 hour in a shaking water bath with temperature regulated at 40°C . After this the peptide bonds of TNP-gn-cytochrome c were hydrolyzed by adding 3 ml of 12 N HCl and autoclaving it at 120°C (17 psi) for 1 hour. After cooling the hydrolyzate to room temperature, 5 ml of distilled water was added. Picric acid which is produced during the course of the hydrolysis was extracted from the hydrolysate with anhydrous ethyl ether. Extraction with ethyl ether was repeated until a constant absorbancy reading at $\lambda = 345$ nm was obtained. A blank was carried through the same procedure except that the addition of

3 ml 12 N HCl preceded addition of TNBS. To estimate the lysine content, the extinction coefficient $\epsilon_{345} = 1.46 \times 10^4 \text{ M}^{-1} \text{ cm}^{-1}$ was used (Kakade and Liener, 1969). The analysis of the procedure showed that out of 19 lysine residues in the cytochrome c molecule 0.4 lysine residues were not modified. Thus, within the experimental error of the technique (Kakade and Liener, 1969), all lysine residues appeared to be blocked against reaction with TNBS.

2.7. Preparation of buffers

Buffers of various ionic strengths containing binding and nonbinding ions were prepared as follows:

Potassium phosphate buffers covering the range of ionic strengths from 0.011 M to 0.5 M were prepared according to the nomogram published by Boyd (1965).

Nonbinding buffers of various ionic strengths were prepared by changing the concentrations of tris base and cacodylic acid keeping pH = 7.0. The concentration of tris ions (T^+) was calculated by taking into account the dissociation constant (K_a) of tris. At pH 7.0 (T^+) can be expressed:

$$(T^+) = \frac{(T)}{1 + (K_a)/(H^+)} \quad (2.7.1.)$$

where (T) is the molar concentration of added tris and (H^+) the concentration of hydrogen ions.

The dissociation constant, K_a , varies slightly with temperature and ionic strength and the values used were taken from the report published by Good *et al.* (1966). The concentration of cacodylate ions (C^-) was calculated using expression 2.7.2.:

$$(C^-) = \frac{(C)}{1 + (H^+)/K_a} \quad (2.7.2.)$$

where (C) is the molar concentration of added cacodylic acid. The value for pK_a ($pK_a = -\log K_a$) was taken as 6.2 (Keresztes-Nagy and Klotz, 1965). Measurements of the ionic strength dependence of pK_a showed that the deviations were too small to warrant considering. Once the concentrations of anions and cations were known, the ionic strength was calculated by equation 2.7.3.:

$$I = \frac{1}{2} \sum_i c_i z_i^2 \quad (2.7.3.)$$

where c_i is the molar concentration of i^{th} ion and z_i its charge. The summation extends over all ions present.

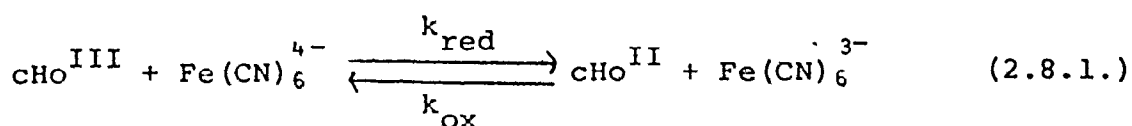
In order to study the effect of anions (Cl^- , phosphate, picrate) on the kinetics, the buffers were prepared so that the concentration of tris was kept constant, and partially neutralized (depending on the concentration of binding anion desired) with the acid containing the anion to be studied (HCl , H_3PO_4 , picric acid). Care was taken to maintain constant ionic strength throughout a

series of reactions if rate constants were to be compared. HCl and picric acid were assumed to be completely dissociated. The concentration of monovalent (H_2PO_4^-) and divalent (HPO_4^{--}) phosphate ions were calculated using the values of pK_a 's reported by Green (1933). The phosphate ion concentration given in the text is the sum of these two ionic concentrations. The pH was adjusted, if necessary, with cacodylic acid.

Buffers of various cations were similarly prepared. The concentration of cacodylic acid was kept constant and partially neutralized with the base (KOH) containing the cation to be studied. The pH was adjusted to 7.0 by adding tris.

2.8. Determination of apparent equilibrium constant.

The apparent equilibrium constant for the reaction between ferricytochrome c and potassium ferrocyanide (2.8.1.) can be determined spectrophotometrically. Since the



reduction potential of hexacyanoferrate system is known (Eaton *et al.*, 1967; Hanania *et al.*, 1967; Kolthoff and Tomsicek, 1935) one can, if desired, calculate the reduction

potential of the cytochrome c system relative to the standard hydrogen electrode. When reaction 2.8.1. is at equilibrium equation 2.8.2. results:

$$K_{eq} = \frac{k_{red}}{k_{ox}} = \frac{(cHo^{II}) (Fe(CN)_6^{3-})}{(cHo^{III}) (Fe(CN)_6^{4-})} \quad (2.8.2.)$$

The apparent equilibrium constant was determined by measuring the amount of the reduced cytochrome c after addition of known quantities of potassium ferrocyanide.

If one makes the correction due to the presence of reduced cytochrome c in the starting cytochrome c preparation (5-10%) one rewrites the equation 2.8.2. as equation 2.8.3..

$$K_{eq} = \frac{(A_1 - A_{ox}) (A_1 - A_o)}{\Delta\epsilon (A_{red} - A_1) \left[F_o - \left(\frac{A_1 - A_o}{\Delta\epsilon} \right) \right]} \quad (2.8.3.)$$

where the quantities A_o , A_1 , A_{red} , A_{ox} , F_o and $\Delta\epsilon$ have the following meanings: A_o and A_1 are the values of the absorbancy measured before and after the addition of potassium ferrocyanide, respectively, and F_o is the final concentration of potassium ferrocyanide. After the value of A_1 is determined, solid potassium ferricyanide is added to determine the absorbancy value of the completely oxidized cytochrome c solution (A_{ox}). Finally, a very small amount of sodium dithionite is added to determine the absorbancy of the completely reduced cytochrome c solution (A_{red}). $\Delta\epsilon$ is the difference in the molar

extinction coefficient between reduced and oxidized cytochrome c. The values of the extinction coefficients for oxidized and reduced cytochrome c reported by Margoliash and Frohwirt (1959) did not agree with our experimental data. It was noticed that their oxidized sample was not completely oxidized, but probably contained about 4.2% of reduced material. Under the assumption that their reduced sample was completely reduced a value for $\Delta\epsilon = \epsilon_{\text{red}}^{550} - \epsilon_{\text{ox}}^{550}$ of $19.5 \times 10^3 \text{ M}^{-1} \text{ cm}^{-1}$ was derived. All absorbancies were measured at 24°C in a 1 cm cuvette at 550 nm using UNICAM model 1800.

2.9. Stopped-flow measurements

The kinetics of the oxidation and reduction of cytochrome c was followed at $\lambda = 550 \text{ nm}$ with the stopped-flow photometer constructed in our laboratory (see Appendix III). The experimental runs were analyzed by a computer program (see Appendix IV) on a CDC-6400 computer.

The reacting mixtures for the stopped-flow measurements were prepared as follows. A small aliquot of the stock solution of oxidized or reduced cytochrome c in 0.001 M tris-cacodylate buffer was added to a buffer of defined composition. A small portion of this solution was used to determine the initial absorbancy (A_1 at $t = -TD$), see Appendix IV) and the concentration of cytochrome c.

The concentration was determined by measuring the absorbancy at 500 nm of oxidized cytochrome c (A_{ox}), after adding potassium ferricyanide, and the absorbancy of reduced cytochrome c (A_{red}), after adding sodium dithionite, by the formula:

$$C(\text{cyt } c) = \frac{A_{red} - A_{ox}}{\Delta \epsilon}$$

The following extinction coefficients were used: horse heart cytochrome c, gn-cytochrome c and *M. denitrificans* cytochrome c, $\Delta \epsilon_{550} = 19.5 \times 10^3 \text{ M}^{-1} \text{ cm}^{-1}$; *P. aeruginosa* cytochrome c, $\Delta \epsilon_{551} = 20.0 \times 10^3 \text{ M}^{-1} \text{ cm}^{-1}$ (Ambler, 1963a).

The concentration of potassium ferricyanide solution was determined by measuring the absorbancy at $\lambda = 420 \text{ nm}$, using the molar extinction coefficient of $\Delta \epsilon = 1000 \text{ M}^{-1} \text{ cm}^{-1}$ (Cassatt and Marini, 1974). Potassium ferrocyanide solutions were prepared by dissolving weighed amounts of solid potassium ferrocyanide in known volumes of buffer. Potassium ferro- and ferricyanide solutions were used within three hours of preparation.

The reacted solution was collected from the stopped-flow photometer and its absorbancy and pH measured. The value of the absorbancy so determined was used as the equilibrium value (A_{eq}).

3. EXPERIMENTAL RESULTS

3.1. Measurements of the apparent equilibrium constant

Measurements of the apparent equilibrium constant of the cytochrome c/iron hexacyanide reaction provides information on the ratio of the overall reduction and oxidation rate constants. Furthermore, the ionic strength dependence of the apparent equilibrium constant gives an insight into the variation of the redox potential of cytochrome c as the ionic strength of the medium is changed. The ionic strength dependence of the apparent equilibrium constant of the cytochrome c/iron hexacyanide system has been studied thus far by Margalit and Schejter (1970), Schejter and Margalit (1970), Margalit and Schejter (1973a) and Palcic (1972) in the range below $I < 0.01$ M. In this study, the range has been extended to an ionic strength of 0.5 M, using electro dialyzed cytochrome c.

In Figure 3.1 the negative logarithm of the apparent equilibrium constant is plotted against $f(I) = \frac{\sqrt{I}}{1 \pm 6\sqrt{I}}$, a function proposed by Schejter and Margalit (1970) (see also section 4.2.1.). This function was derived from extended Debye-Huckel theory assuming the

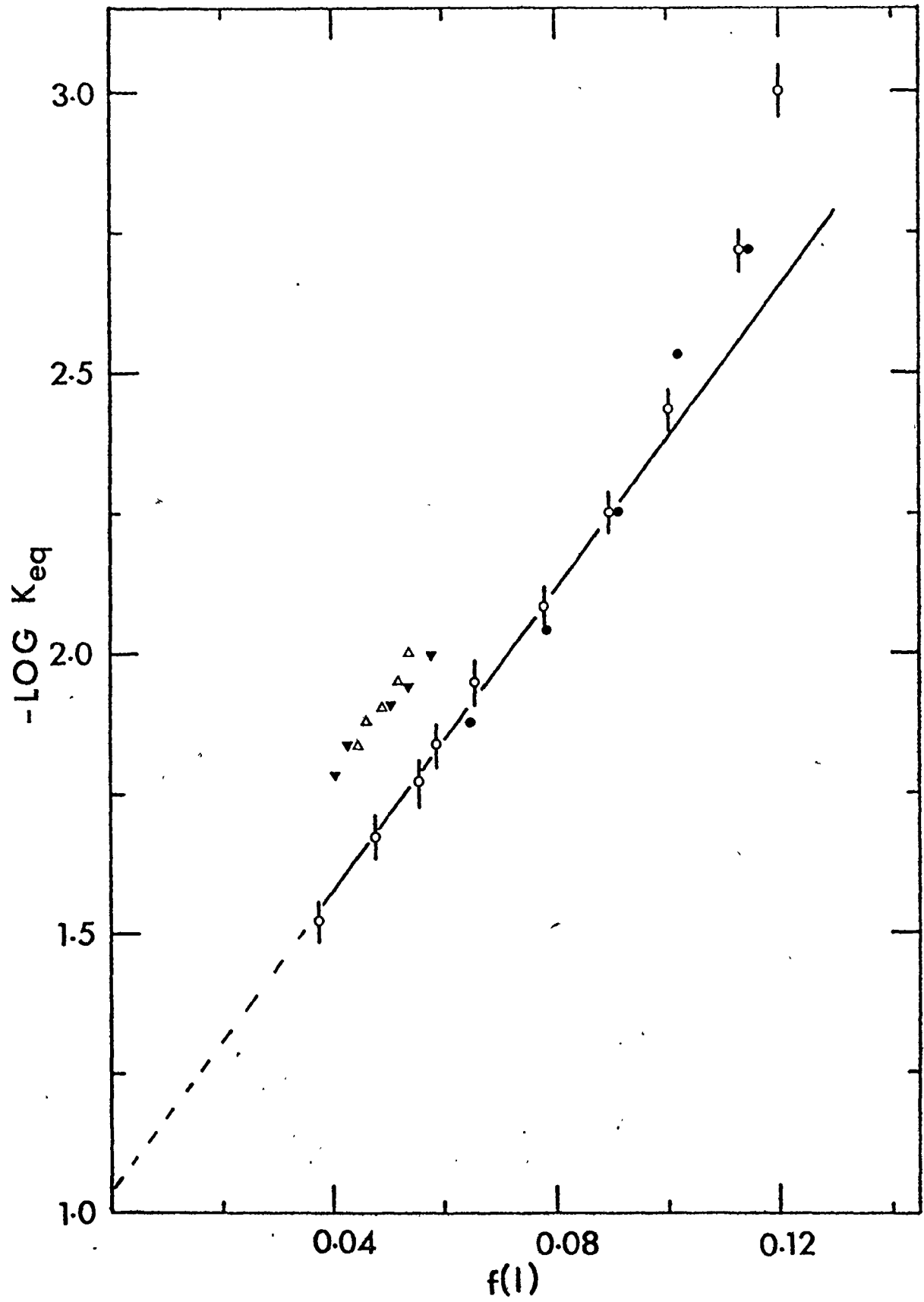
Figure 3.1: Variation of $-\log_{10} K_{eq}$ versus $f(I)$, where $f(I)$ is defined as $\sqrt{I} / (1 + 6\sqrt{I})$.

- (o) tris-cacodylate buffer, pH 7.0, temperature, 24°C;
- (●) potassium phosphate buffer, pH 7.0, temperature, 24°C.

The vertical bars represent the average absolute deviation from the mean values of 5-8 measurements.

For comparison, results reported by Schejter and Margalit (1970) (∇) and Palcic (1972) (Δ) are included.

Solutions of 10-30 μM of ferricytochrome c were titrated with potassium ferrocyanide to produce 50-70% reduction of ferricytochrome c.



mean value of the closest approach between cytochrome c and iron hexacyanide ion is 18.5 Å. The data points fit a straight line relationship up to an ionic strength of 0.05 M and then begin to deviate upwards. The apparent equilibrium constant was also measured in five concentrations of potassium phosphate buffer. The values of the apparent equilibrium constants in phosphate buffer agree, within experimental error, with the values for non-binding tris-cacodylate buffer. The extrapolation of the straight curve ($-\log K_{eq}$ vs $f(I)$) to zero ionic strength yielded an apparent reduction potential of 292 mV which is higher than the value reported by Schejter and Margalit (1970) (274 mV) and Palcic (1972) (285 mV). For comparison, in Figure 3.1 the values for the equilibrium constant reported by Schejter and Margalit (1970) and Palcic (1972) are included. There is a considerable disagreement between our results and previously reported data.

A possible explanation for this disagreement could be the preparation of cytochrome c. One usually prepares ferricytochrome c by adding a small amount of ferricyanide to the cytochrome c solution (Margoliash and Walasek, 1967; Palcic, 1972). In view of the recent observations by Stellwagen and Cass (1975) that iron hexacyanides bind to cytochrome c, the effect of potassium ferricyanide on the apparent equilibrium constant was examined. An electro dialyzed (mainly oxidized) cytochrome c

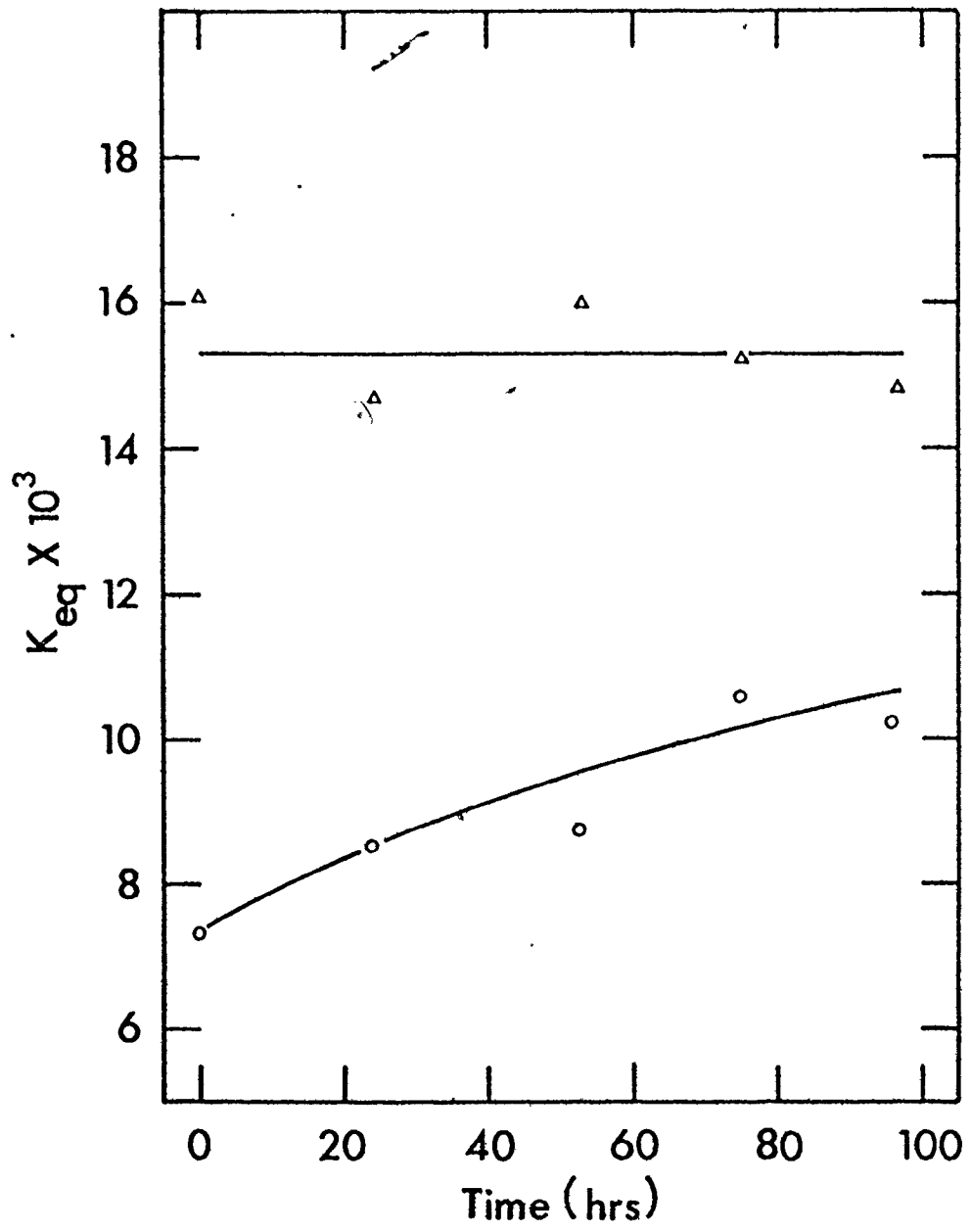
solution was dialyzed overnight against tris-cacodylate buffer I = 0.01 M, pH = 7.0. To this dialyzed cytochrome c solution (70 μ M in concentration) a small amount of potassium ferricyanide (35 μ M) was added. One half of this preparation was first electrodialed and then dialyzed for approximately 100 hours with four exchanges of 20 volumes of tris-cacodylate buffer I = 0.01 M, pH = 7.0. The other half was not electrodialed, but simply dialyzed in the same manner. At various times the apparent equilibrium constants of both cytochrome c preparations were measured. Figure 3.2 shows the results. The apparent equilibrium constant of electrodialed cytochrome c was constant (within 7%) throughout the course of dialysis (96 hours), whereas the apparent equilibrium constant of the dialyzed solution gradually increased but never reached (within 100 hours) the values determined with electrodialed preparation. Since the only difference between the solutions was electrodialed, we conclude that dialysis did not completely remove ferricyanide ions. This would explain why the previously reported values do not agree with our data.

3.2. Oxidation of ferrocytochrome c

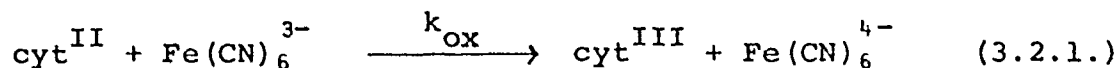
The oxidation of ferrocytochrome c with potassium ferricyanide involves the transfer of one electron from

Figure 3.2: Comparison between the apparent equilibrium constants measured with dialyzed cytochrome c and electrolyzed cytochrome c.

(Δ) electrolyzed cytochrome c; (o) dialyzed cytochrome c. Buffer, tris-cacodylate; ionic strength, 0.01 M; pH 7.0; temperature, 24°C. The solid lines were drawn by eye in order to indicate trends. The points represent the average values of 2-3 measurements.



ferrocytochrome c to ferricyanide and can be represented by expression 3.2.1.:



The oxidation of ferrocytochrome c by ferricyanide has been previously studied by Cassatt and Marini (1974) and Creutz and Sutin (1974). The experiments of both groups indicated that under pseudo-first order conditions (the concentration of potassium ferricyanide being at least five times greater than that of ferrocytochrome c) the observed first-order rate constant varied linearly with the concentration of potassium ferricyanide. Thus, Cassatt and Marini (1974) and Creutz and Sutin (1974) concluded that the oxidation of ferrocytochrome c by ferricyanide followed second order kinetics (equation 3.2.1.). Furthermore, it was observed by Morton *et al.* (1970) and Cassatt and Marini (1974) that the oxidation of ferrocytochrome c with potassium ferricyanide strongly depended on the ionic strength of the medium. The temperature dependence studies of the rate of oxidation (Morton *et al.*, 1970) indicated that the oxidation process was temperature independent. Later Cassatt and Marini (1974) showed that the rate of oxidation varied only slightly with temperature, and they reported a value of 1.7 kcal/mole for the energy of activation for the oxidation of ferrocytochrome c by ferricyanide.

3.2.1. Mechanism of oxidation of ferrocytochrome c

In order to determine the mechanism (order) of the reaction between ferrocytochrome c and potassium ferricyanide, the kinetics of the oxidation was studied under conditions where the concentrations of both reactants were approximately the same. In other words, the concentrations of reactants were far from satisfying pseudo-first-order conditions. The absorbancy changes due to the transition from the reduced to the oxidized form of cytochrome c (Figure 3.3) were followed with the stopped-flow photometer at 550 nm. All kinetic runs were done with both reactants prepared in non-binding tris-cacodylate buffer (pH 7.0, I = 0.195 M, T = 24°C), by independently varying the concentration of ferricyanide and ferrocytochrome c. Figure 3.4 shows a representative computer calculated averaged absorbancy differences ΔA (see equation IV.3) versus time for the reaction between ferrocytochrome c and potassium ferricyanide. Each kinetic run was analyzed as an irreversible second-order reaction. The reverse reaction (reduction of ferricytochrome c) was neglected since the equilibrium of the cytochrome c/iron hexacyanide system favors the oxidation of ferrocytochrome c (see Section 3.1.). Figure 3.5 displays the fitting of the experimental curve (seen in Figure 3.4) with a computer generated theoretical curve which is the solution of the differential equation

Figure 3.3. Absorption spectra of reduced and oxidized horse heart cytochrome c.

Cytochrome c was prepared in 0.1 M potassium phosphate buffer, pH 7.0, at 24°C. (—) reduced cytochrome c; (---) oxidized cytochrome c.

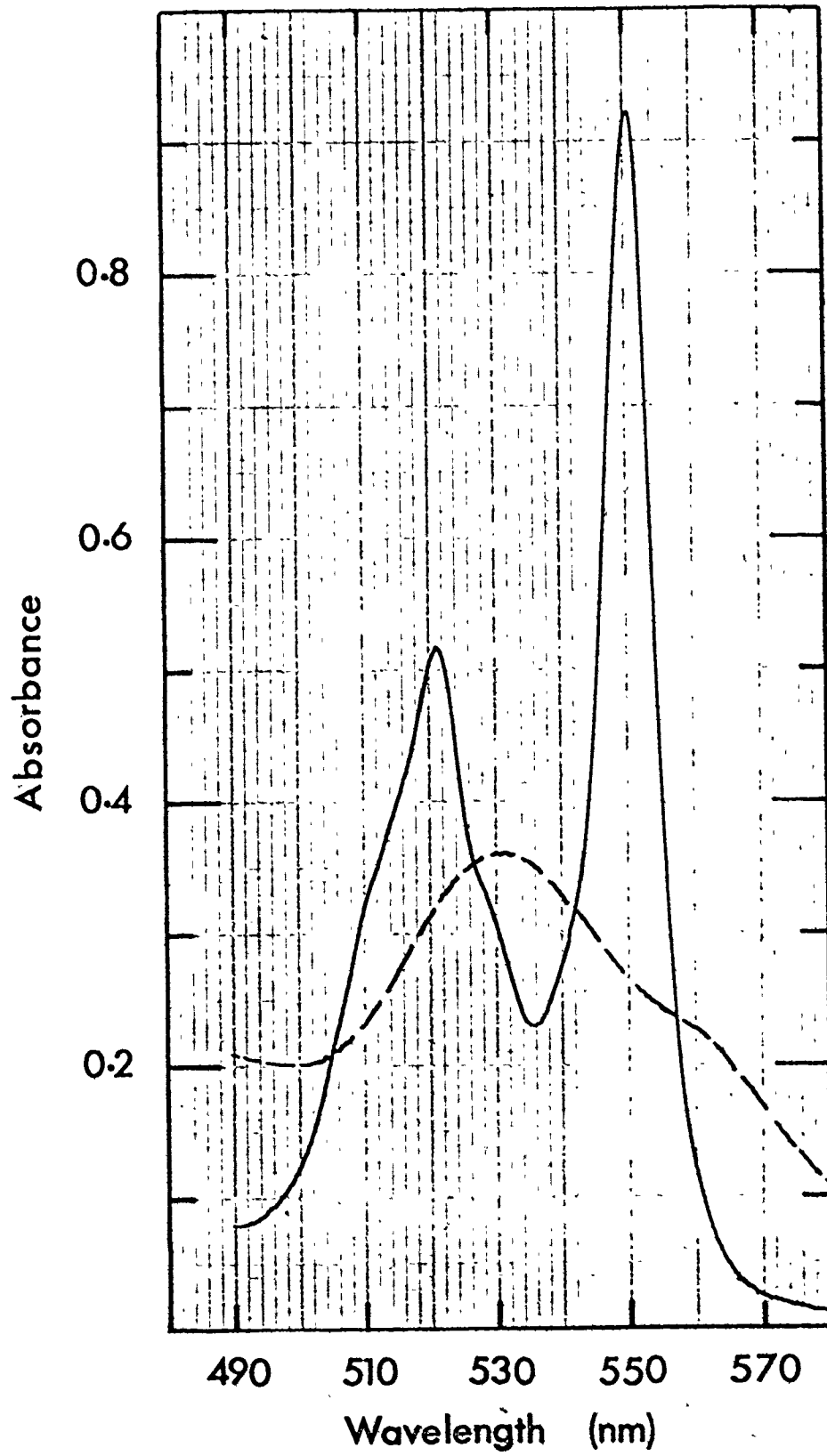


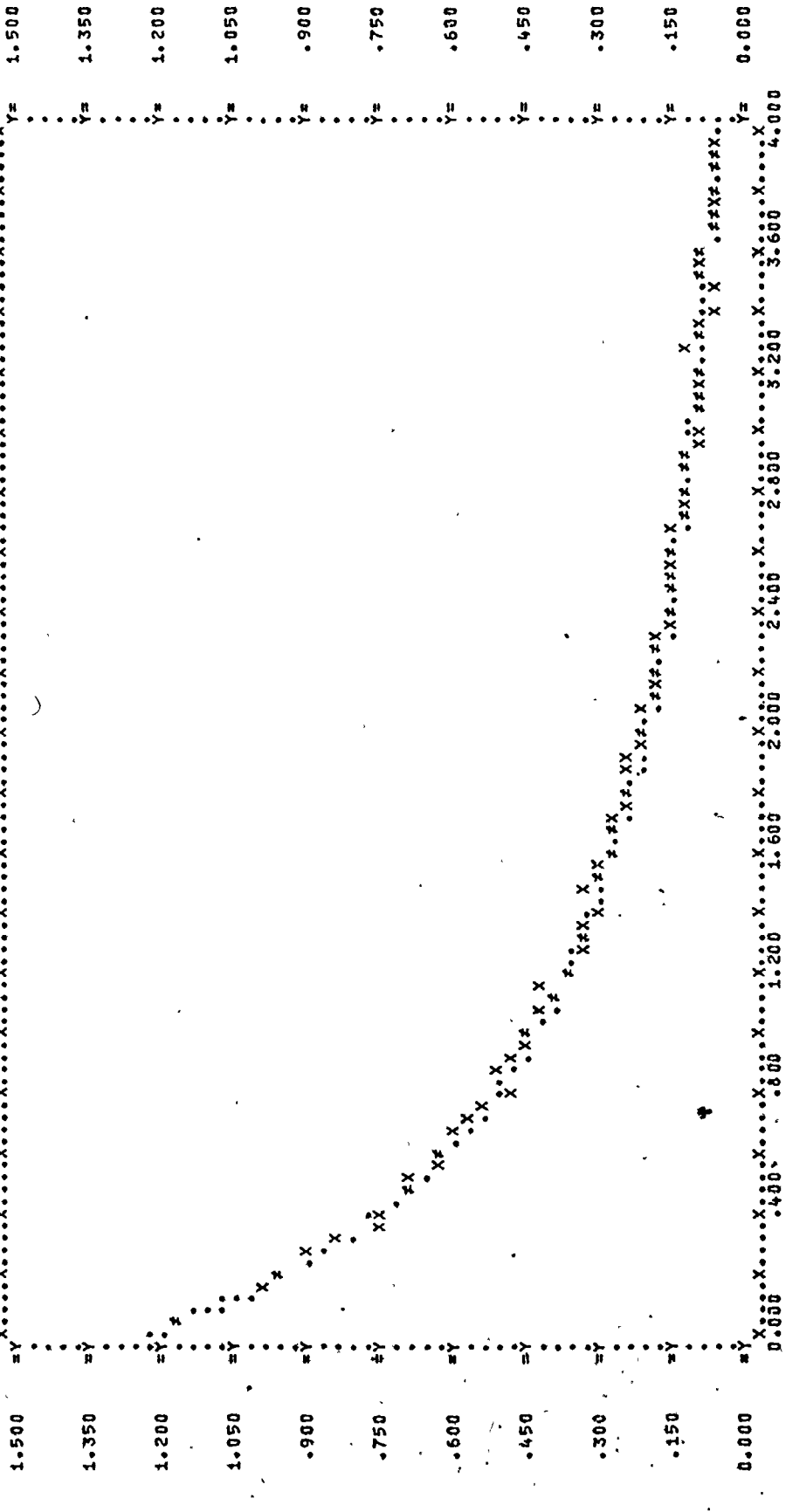
Figure 3.4. Computer-calculated averaged absorbancy differences as a function of time ($\Delta A(t)$ vs t) for the reaction between ferrocyanide and ferricyanide.

Oxidation of 6.48 μM (after mixing) ferrocyanide by 10.25 μM (after mixing) potassium ferricyanide. Buffer, tris-cacodylate; ionic strength, 0.194 M; pH 7.0; temperature, 24°C. Ordinate, absorbancy difference (ΔA); abscissa, time (t) in sec. (\neq denotes coincident points).

Figure 3.5. Computer fitting of the experimental $\Delta A(t)$ vs t curve.

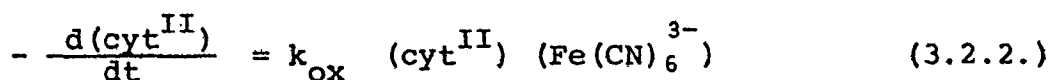
The computer calculated a theoretical curve (·) to fit the experimental points (x) which were also plotted in Figure 3.4. Reaction and conditions as stated in the caption of Figure 3.4. Parameters calculated for this run: (K1), $k_{ox} = 0.133 \times 10^{-8} \text{ M}^{-1} \text{ sec}^{-1}$; (K2), k_{red} set to 0.0; (TD), calculated dead time 1.396 msec.

SCALED LIMITS, XMIN= 0.0000 XMAX= 3.98963, YMIN= .05854 YMAX= 1.23594 164 POINTS PLOTTED (# DENOTES COINCIDENT POINTS)



ACT), THEORY (.), AND EXPERIMENT (X)
 AQ= .605E-05 BQ= 10.25E-04 CQ= 0. NRUN = 6 DD= 0 DELTE= -.1950E+05 (0.)
 AP= .12359 (.00194) IQ= 1.396 (.304) K1= .1330E+08 (.54E+06) K2= 0. (0.)

IV.6 (the rate for reverse reaction was assumed to be zero). Figure 3.6 illustrates the variation of the second order rate constant for the oxidation of ferrocytochrome c as a function of potassium ferricyanide concentration where the concentration of ferrocytochrome c was kept constant at 4.025 μM after mixing. In Figure 3.7, one can see the dependence of the second-order rate constant for oxidation of ferrocytochrome c where the concentration of ferrocytochrome c was varied and the concentration of ferricyanide was kept constant (10.24 μM). In both cases, the second-order rate constant was found to be independent of the concentration of the varying reactant. The average values for both sets of experiments are in good agreement, and the value of $(13.3 \pm 0.6) \times 10^6 \text{ M}^{-1} \text{ sec}^{-1}$ (the error represents the average absolute deviation from the mean value) for the second-order rate constant was determined for the oxidation of ferrocytochrome c at ionic strength of $I = 0.194 \text{ M}$, pH 7.0, and temperature of 24°C . These experiments show that, within the range of the reactants employed, the oxidation of reduced heart cytochrome c is second-order with negligible rate of the reverse reaction. This can be summarized by a rate expression 3.2.2.:



with $k_{\text{ox}} = 13.3 \times 10^6 \text{ M}^{-1} \text{ sec}^{-1}$ ($I = 0.194 \text{ M}$, pH 7.0 and temperature of 24°C). The same rate law was assumed to

Figure 3.6. Variation of the second-order rate constant for the oxidation of ferrocytochrome c as a function of ferricyanide concentration.

The concentration of ferricyanide was varied from 5.8 μM to 21.8 μM ; concentration of ferrocytochrome c was kept constant at 4.03 μM . Buffer, tris-cacodylate; ionic strength, 0.194 M; pH 7.0; temperature, 24 $^{\circ}\text{C}$. The error bars represent statistical uncertainties of the fit as discussed in Appendix IV.

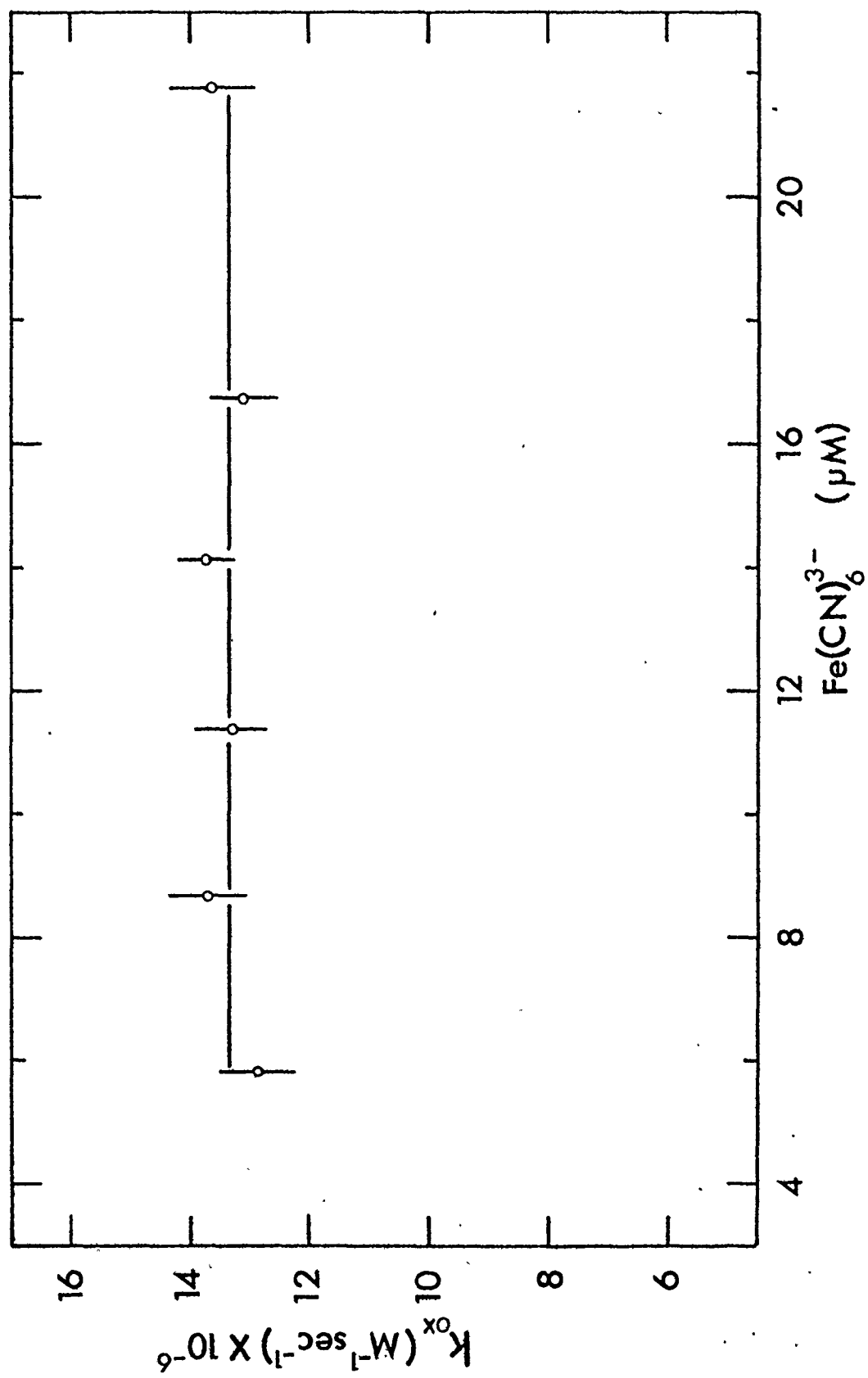
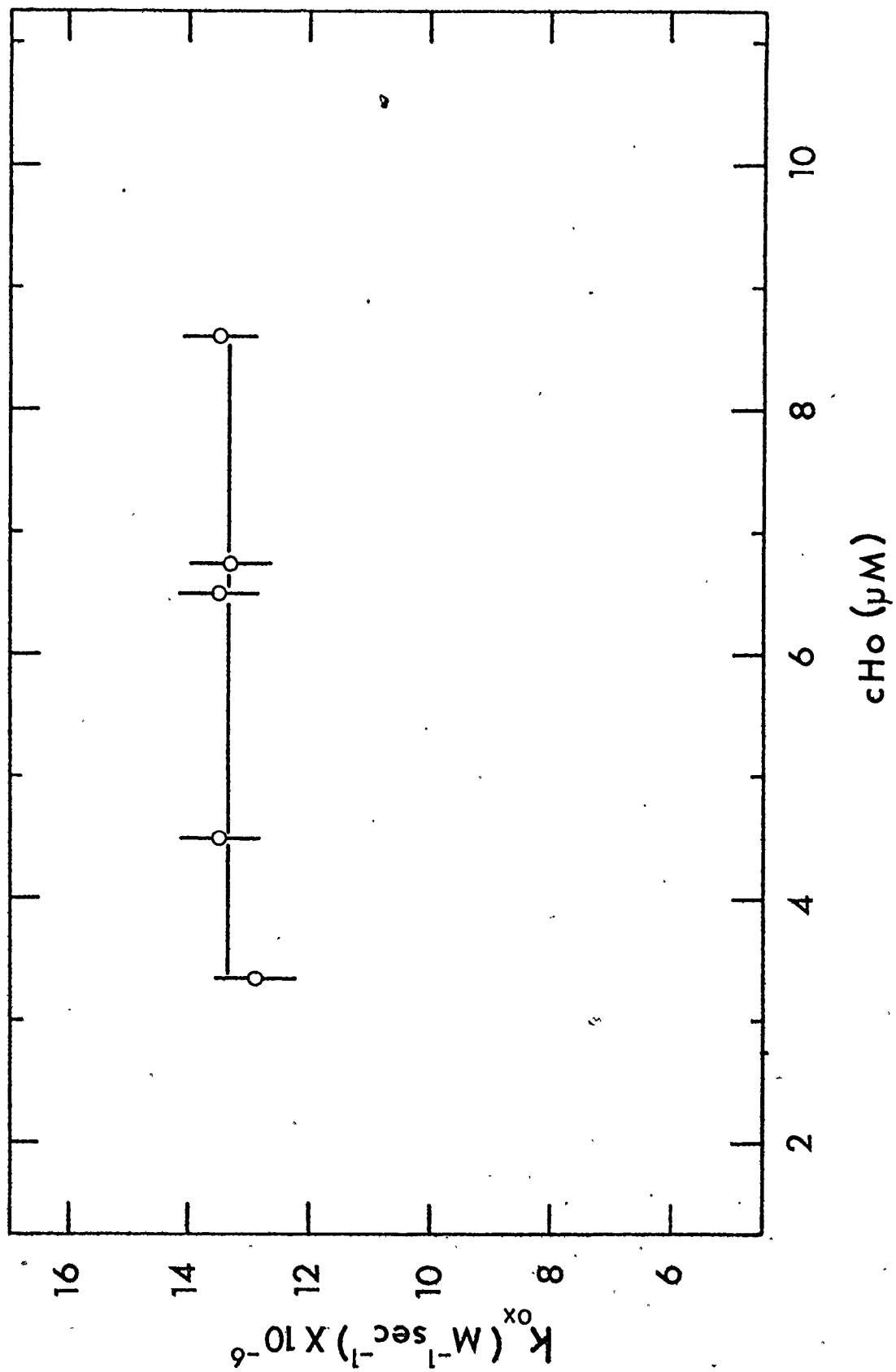


Figure 3.7. Variation of the second-order rate constant for the oxidation of ferrocytochrome c as a function of ferrocytochrome c concentration.

Concentration of ferrocytochrome c was varied from 3.35 μM to 8.6 μM , concentration of ferricyanide was kept constant at 10.24 μM . Buffer, tris-cacodylate; ionic strength, 0.194 M; pH 7.0; temperature, 24°C. The error bars represent the statistical uncertainties of the fit as discussed in Appendix IV.



hold for different ionic strengths and for the other cytochromes used in this study.

3.2.2. The effect of ionic strength on the oxidation of ferrocyanide

Ferricyanide and ferrocyanide are highly charged molecules and so one would expect that reactions involving these molecules would be sensitive to the ionic strength of the medium. The ionic strength determines the electrostatic field surrounding the charged molecule and, therefore, the electrostatic interactions between the reacting molecules. According to the Debye-Hückel theory, at low ionic strengths the logarithm of the rate constant should vary linearly with the square root of the ionic strength (Frost and Pearson, 1961a). Furthermore, the theory predicts that the ionic strength will have a different effect on the reaction between two similarly charged ions than on the reaction involving two oppositely charged ions.

Cytochromes c of three different species (horse heart, *Micrococcus denitrificans* and *Pseudomonas aeruginosa*) were chosen to study the effect of charges on the molecule and ionic strength of the medium on the oxidation process. Horse heart cytochrome c has a net positive charge of about +9 at pH 7.0, whereas *Micrococcus denitrificans* and

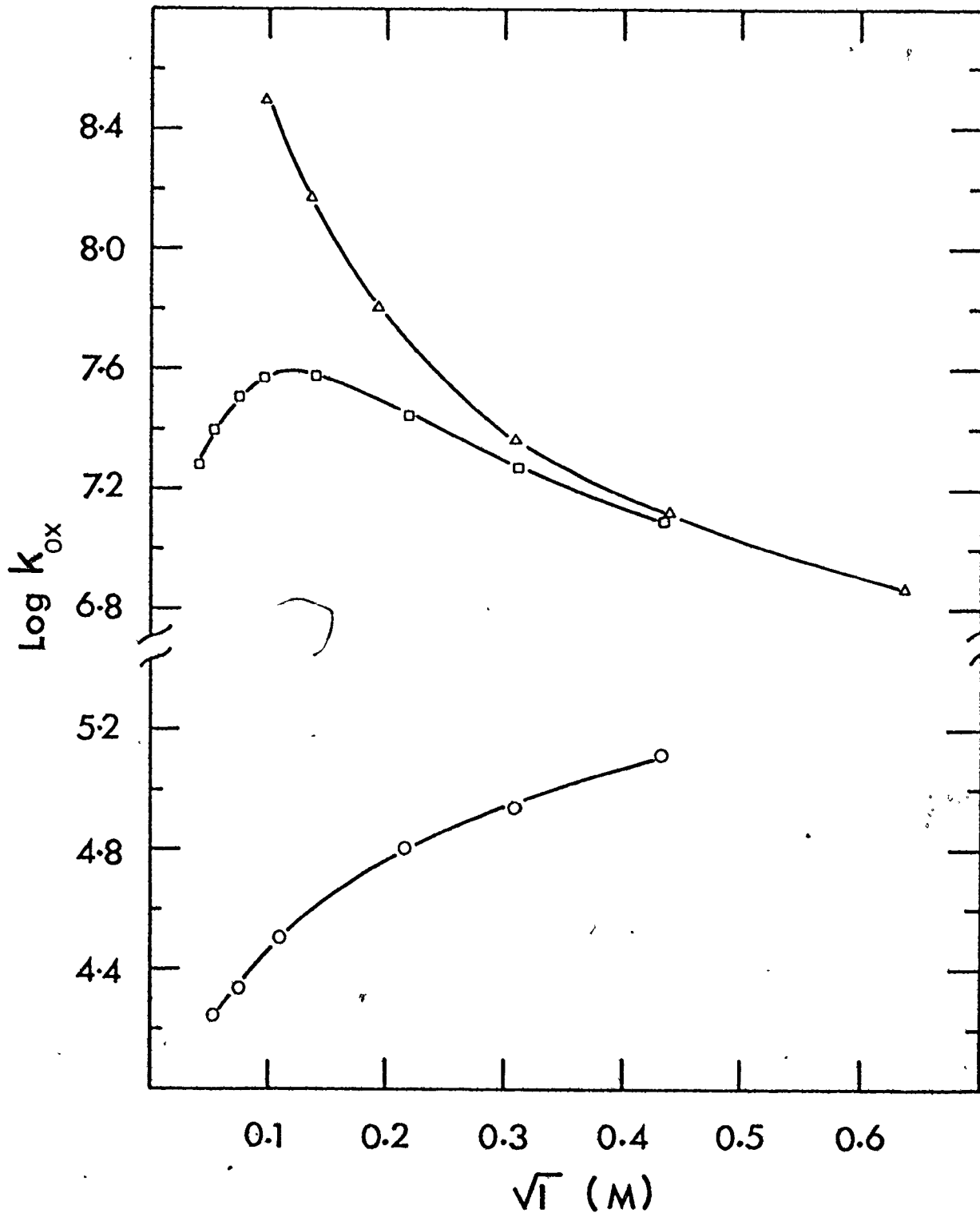
Pseudomonas aeruginosa cytochromes both have a net negative charge at pH 7.0. Figure 3.8 shows the logarithm of the second-order rate constant for the oxidation of horse heart, *M. denitrificans* and *P. aeruginosa* cytochromes plotted against the square root of the ionic strength.

It can be seen in Figure 3.8 that the rate constant for the oxidation of horse heart ferrocytochrome c was a function of the ionic strength. With increasing ionic strength, the rate of oxidation decreased which is expected for a reaction between two oppositely charged molecules. Below an ionic strength of about 0.01 M, the oxidation of reduced horse heart cytochrome c occurred so rapidly that the reaction was completed within the dead time of the experiment. The fastest second-order rate constant that could still be measured was $3 \times 10^8 \text{ M}^{-1} \text{ sec}^{-1}$ at the ionic strength of 0.01 M (tris-cacodylate) pH 7.0, $T = 24^\circ\text{C}$. The presented curve in Figure 3.8 was measured with electro dialyzed horse heart ferrocytochrome c. It should be added that when gel filtration was used to remove excess sodium dithionite we obtained the same results except that the rate constants were more scattered.

The oxidation of cPs^{II} occurred much more slowly (one-hundred times, at $I = 0.2 \text{ M}$) than the oxidation of cHo^{II} . The rate of oxidation of cPs^{II} increased with increasing ionic strength, an observation that can be accounted for by the similar charge on the two reacting

Figure 3.8. Effect of the ionic strength on the rate
of oxidation (log k_{ox} vs \sqrt{I}) for
cytochromes: (Δ) cHo^{II} ; (\square) cMn^{II} ; (\circ)
 cPs^{II} .

All experiments were done in tris-cacodylate buffers of various strengths, pH 7.0, 24°C. The solid lines were drawn by eye to indicate trends. Each point represents an average value of 3-4 experiments.



molecules. Below ionic strength 0.01 M, the logarithm of the rate of oxidation seems roughly proportional to the square root of the ionic strength, but the curve deviates from the straight line at higher ionic strengths.

The behaviour of the ionic strength dependence of the oxidation of cMn^{II} was somewhat surprising. At low ionic strengths, the rate of oxidation increased with ionic strength (as would be expected for a reaction of two ions of similar charge), then it reached a broad maximum at approximately $I = 0.015 \text{ M}$ ($\sqrt{I} = 0.122$) and finally decreased with higher ionic strength.

3.2.3. Specific anion effects on the oxidation of ferrocyanide

3.2.3.1. The oxidation of the ferrocyanide in potassium phosphate buffer.

Evidence for phosphate and potassium binding to ferrocyanide first came from electrophoretic measurements by Barlow and Margoliash (1966) and Margoliash *et al.* (1970). They observed that the presence of either phosphate or potassium affected the electrophoretic mobility of horse heart ferrocyanide. The NMR studies by Stellwagen and Shulman (1973) suggested that phosphate bound to ferrocyanide in vicinity of

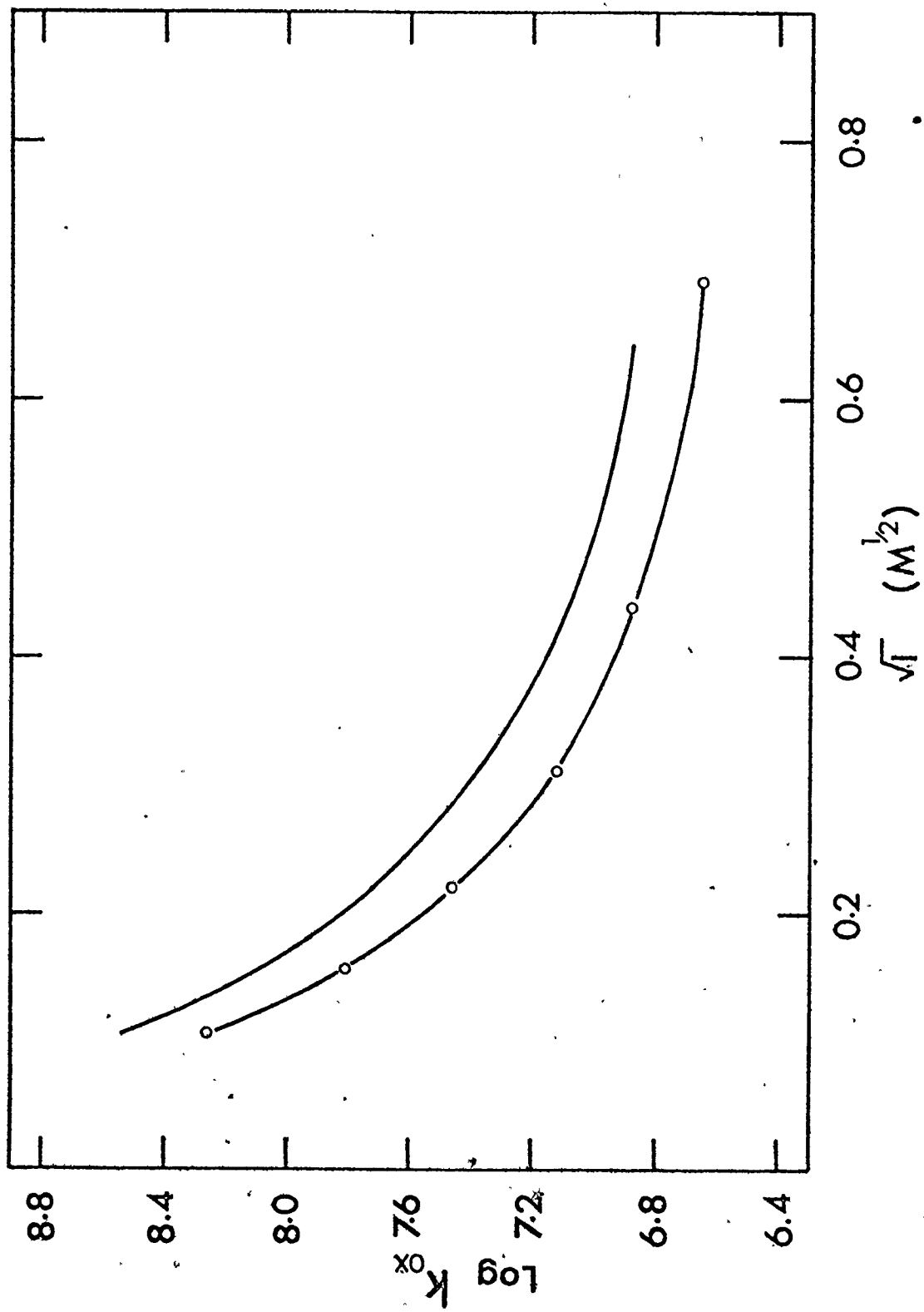
histidine 26. The question arises whether the interaction of phosphate and potassium affects the rate at which the electron leaves the molecule. Furthermore, one would like to know how the ionic effects vary with the total ionic strength of the medium.

In order to examine the difference between the binding buffer, potassium phosphate, and the non-binding buffer, tris-cacodylate, the rate of oxidation of horse heart ferrocyclochrome c was measured in both over the ionic strength range from 0.011 M to 0.5 M. Figure 3.9 shows the logarithm of the rate constant for the oxidation of ferrocyclochrome c as a function of the square root of the ionic strength. Oxidation in potassium phosphate buffer occurred at about half the rate of the non-binding, tris-cacodylate buffer. Morton *et al.* (1970) and Cassatt and Marini (1974) measured the ionic strength dependence of the rate of oxidation in potassium phosphate buffers in which the ionic strength was varied by adding KCl. The oxidation rate constants measured here in potassium phosphate buffer coincide with the values reported by Morton *et al.* (1970). At the lower ionic strengths, there is about an 8-fold disagreement between our values and the values reported by Cassatt and Marini (1974).

The measurements of the rate constants for the oxidation of horse heart ferrocyclochrome c in potassium phosphate buffer showed that these ions do interact with

Figure 3.9. Comparison of $\log k_{ox}$ vs \sqrt{I} in tris-cacodylate and potassium phosphate buffer.

(—) tris-cacodylate buffer, pH 7.0, temperature 24°C (redrawn from Figure 3.8); (o) potassium phosphate buffer, pH 7.0, temperature 24°C. The solid line was drawn by eye to indicate the trend. Each point represents an average value of 2-3 experiments.



ferrocytochrome c, slowing down the oxidation process. It should be emphasized that these experiments (Figure 3.9) do not separate the effect of potassium from phosphate. If one compares the curves ($\log k_{\text{ox}}$ vs \sqrt{I}) measured in binding and non-binding buffer, one can observe that the effect was present at all ionic strengths measured.

3.2.3.2. The effect of phosphate and chloride anions on the oxidation of ferrocytochrome c

Since the binding sites for chloride and phosphate on ferrocytochrome c have been tentatively identified (Stellwagen and Shulman, 1973) the mechanism and the strength by which a single anion (Cl^- , or phosphate) affects (if at all) the oxidation of horse heart ferrocytochrome c should be examined.

As indicated in section 2.3.3., the oxidation of ferrocytochrome c strongly depends on the ionic strength of the medium. Keeping this in mind, one can design experiments that will test the effect of an anion on the rate of oxidation. Measurements of the rate of oxidation of ferrocytochrome c in buffers of constant ionic strength, constant temperature and constant pH, and with a progressively higher portion of the non-binding anion (cacodylate) replaced with a binding anion (Cl^- , or phosphate) indicated that the rate of oxidation becomes slower as

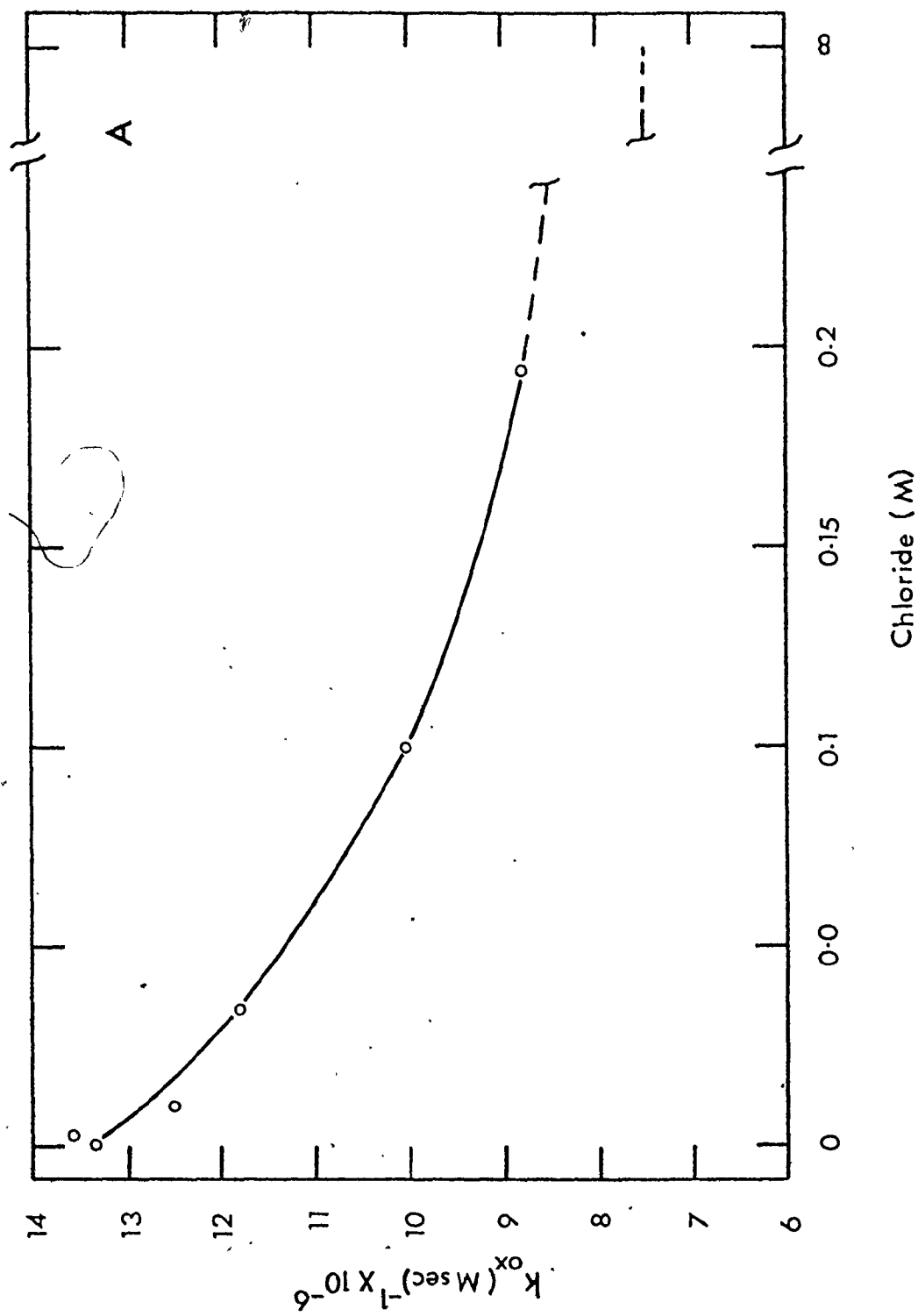
the concentration of binding anion increases (Figure 3.10A and B). This decrease in rate was not large, the rate constant being decreased by $\sim 40\%$ at the highest anion concentration compared to the value in non-binding buffer alone.

3.2.3.3. The effect of picrate on the oxidation of ferrocytochrome c

To test whether the shape of the binding anion plays a role in its interaction with cytochrome c, picrate (trinitrophenolate, a tyrosine analogue), an aromatic ion was chosen. Since picrate uncouples oxidative phosphorylation (Hanstein and Hatefi, 1974) the effect of this anion is of special interest. Furthermore, it was observed by Wada and Okunuki (1969) that trinitrobenzenesulfonate, which is structurally very similar to picrate, shows high reactivity with lysine 13, a residue which may be involved in anion binding. The experiments were performed at a relatively low ionic strength, $I = 0.05 \text{ M}$, because of the low solubility of picric acid. At the highest picrate concentrations (Figure 3.11) the rate of oxidation was decreased to $1/6$ the value in the non-binding buffer. The effect of picrate on the oxidation of ferrocytochrome c was compared to the effect of chloride under the same conditions. As can be seen from Figure 3.11

Figure 3.10 A and B. Effect of chloride (A) and phosphate (B) on the rate of oxidation of horse heart ferrocyanochrome c.

Conditions for both sets of experiments: ionic strength, 0.194 M; pH = 7.0; 24°C; initial conditions: ferrocyanochrome c 4 μ M, ferricyanide 12.2 μ M. The solid line represents the curve calculated using the equation 4.3.8 and parameters given in Table 3 (see section 4.3.1.). The broken line shows the extrapolation to $A \rightarrow \infty$ (see section 4.3.1.). Each point represents a single measurement.



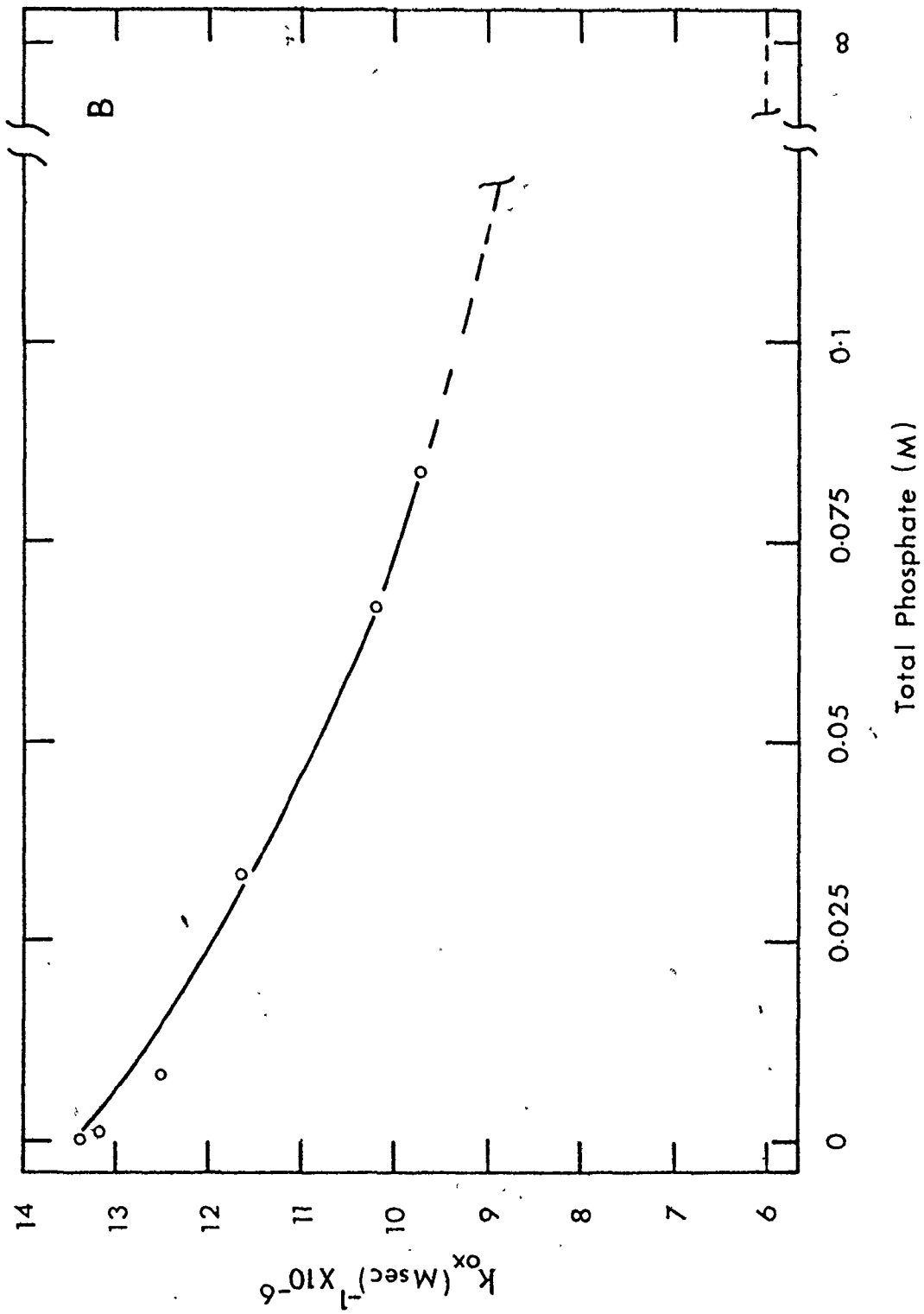
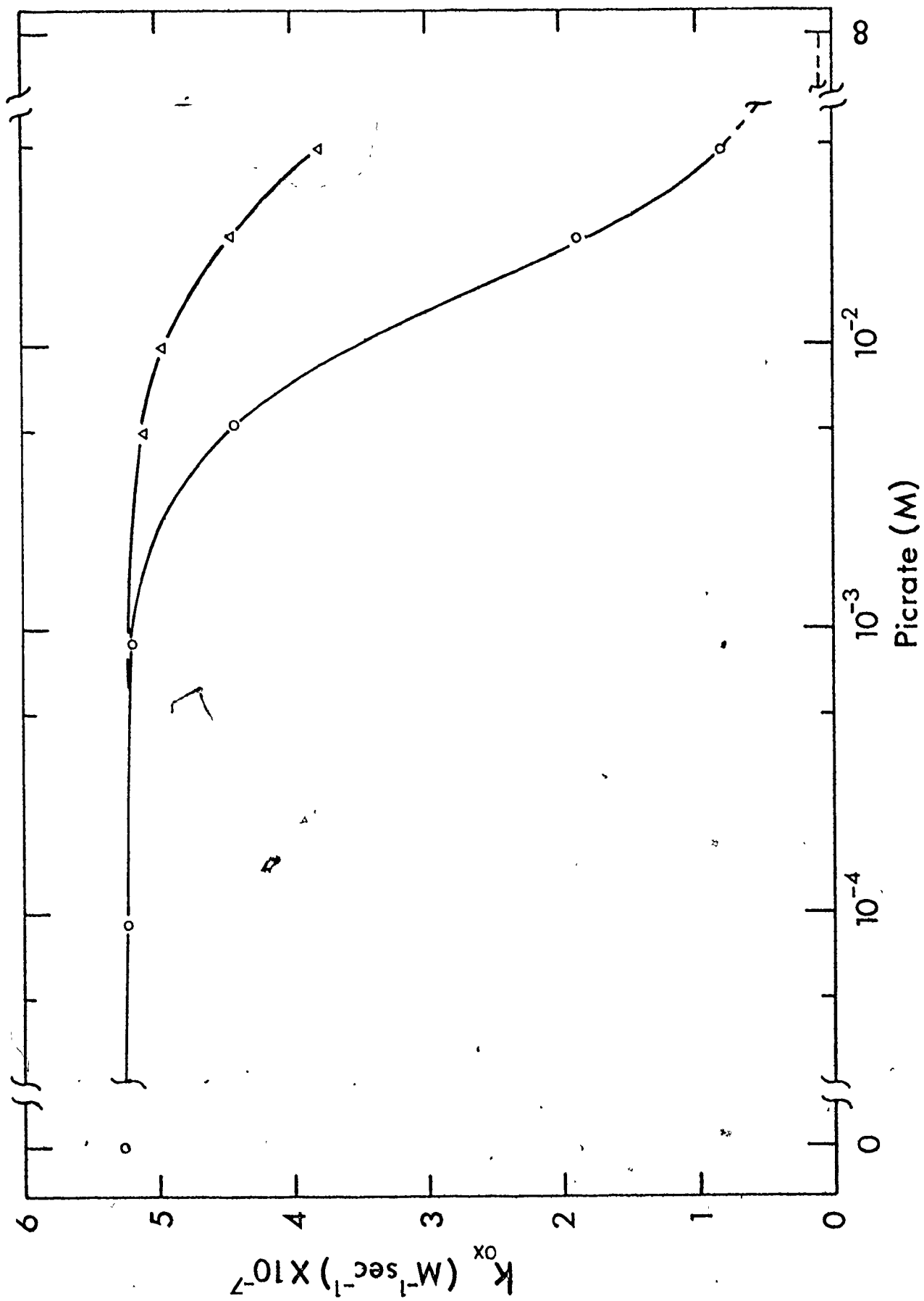


Figure 3.11. Effect of picrate (o) on oxidation of ferrocyanochrome c.

Also shown for comparison is the effect of chloride (Δ) on the oxidation of ferrocyanochrome c. The conditions in both sets of experiments were the same: ionic strength, 0.0485 M; pH 7.0; 24°C. Initial concentration of ferrocyanochrome c was 2.7 μ M, initial concentration of ferricyanide was 4.4 μ M. The solid line is the curve calculated using equation 4.3.8 and parameters given in Table 3; the broken line the extrapolation to $A \rightarrow \infty$ (see section 4.3.1.). Each point represents a single measurement.



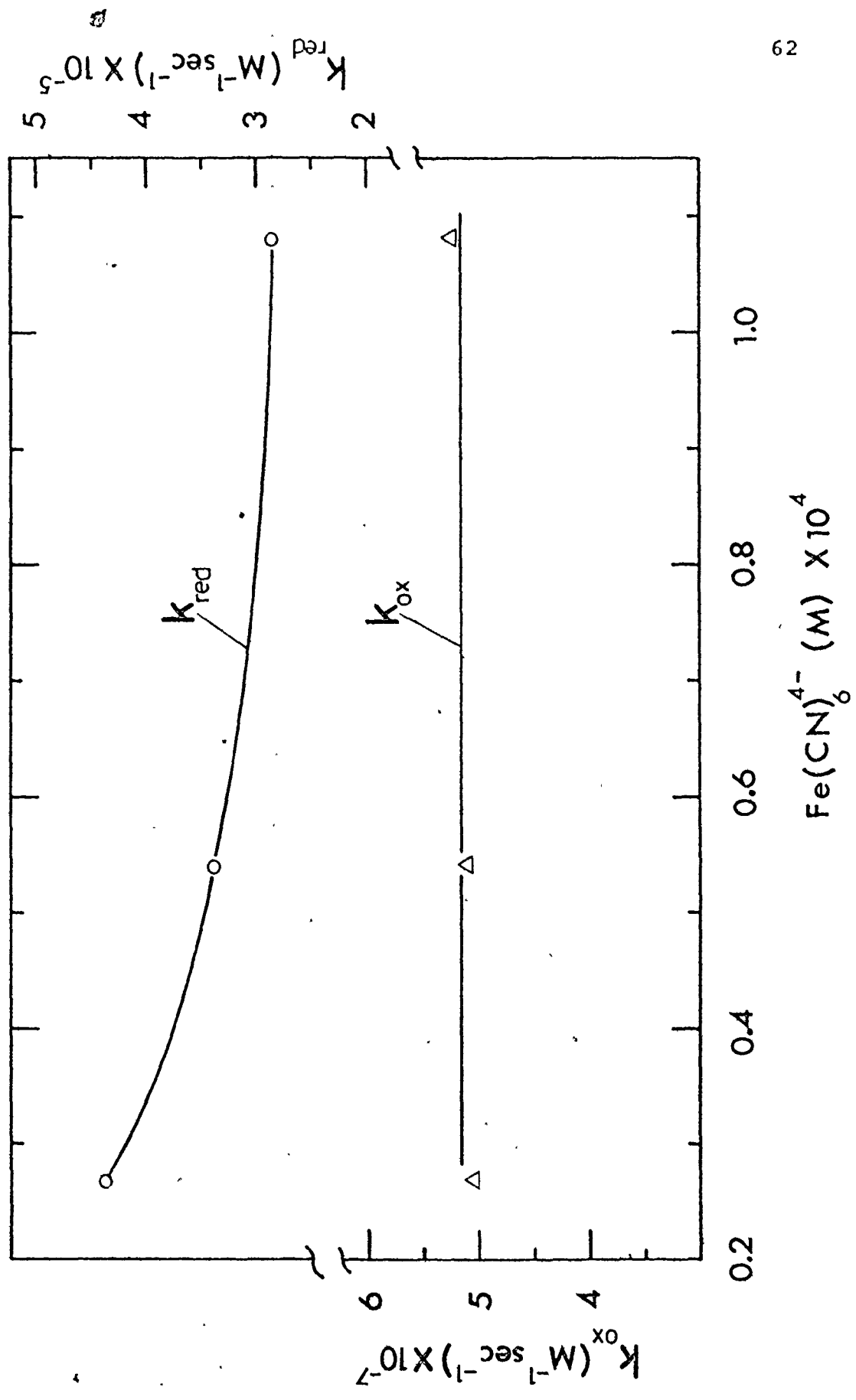
picrate affects the oxidation reaction much more than chloride.

3.2.3.4. The effect of ferrocyanide on the oxidation of ferrocytochrome c.

Measurements of the equilibrium constant of cytochrome c/iron hexacyanide system (Section 3.1.) indicated that the reaction strongly favors the oxidized form of cytochrome c. If a small amount of ferrocyanide is added to the ferrocytochrome c solution, the oxidation of ferrocytochrome c will still take place. Stellwagen and Cass (1975) carried out equilibrium dialysis studies of ferrocyanide binding to ferrocytochrome c and observed that ferrocytochrome c contains two non-equivalent sites for ferrocyanide. We studied the effect of ferrocyanide on oxidation rate of ferrocytochrome c. Various amounts of potassium ferrocyanide were added to the ferrocytochrome c solution and the oxidation of ferrocytochrome c was studied at constant ionic strength, pH and temperature (Figure 3.12). The experimental runs were analyzed as reversible second-order kinetics (see Appendix IV). This kind of analysis yields two rate constants: a constant for the forward reaction (k_{ox}) and a constant for the reverse reaction which occurs due to the presence of ferrocyanide (k_{red}). The experiments showed that there was no effect on the rate of oxidation

Figure 3.12. Effect of potassium ferrocyanide on the rate of oxidation and on the rate of reduction as measured by the oxidation of ferrocytochrome c.

Left ordinate, rate of oxidation (Δ); right ordinate, rate of reduction (o). Ionic strength, 0.05 M; initial concentrations: ferrocytochrome c, 3 μ M; ferricyanide, 4.1 μ M. Each pair of points is the average of two experiments.



but the rate of reduction decreased by approximately 40%.

3.2.4. Specific cation effects on the oxidation of ferrocytochrome c

3.2.4.1. The effect of potassium on the oxidation of ferrocytochrome c.

The electrophoretic measurements of Margoliash *et al.* (1970) revealed that cations like K^+ , Na^+ , Ca^{2+} , Mg^{2+} bound to ferro-form of cytochrome c, but did not affect the electrophoretic mobility of ferri-form. We have chosen K^+ as a representative cation to evaluate the effect of a cation on the oxidation of ferrocytochrome c by ferricyanide.

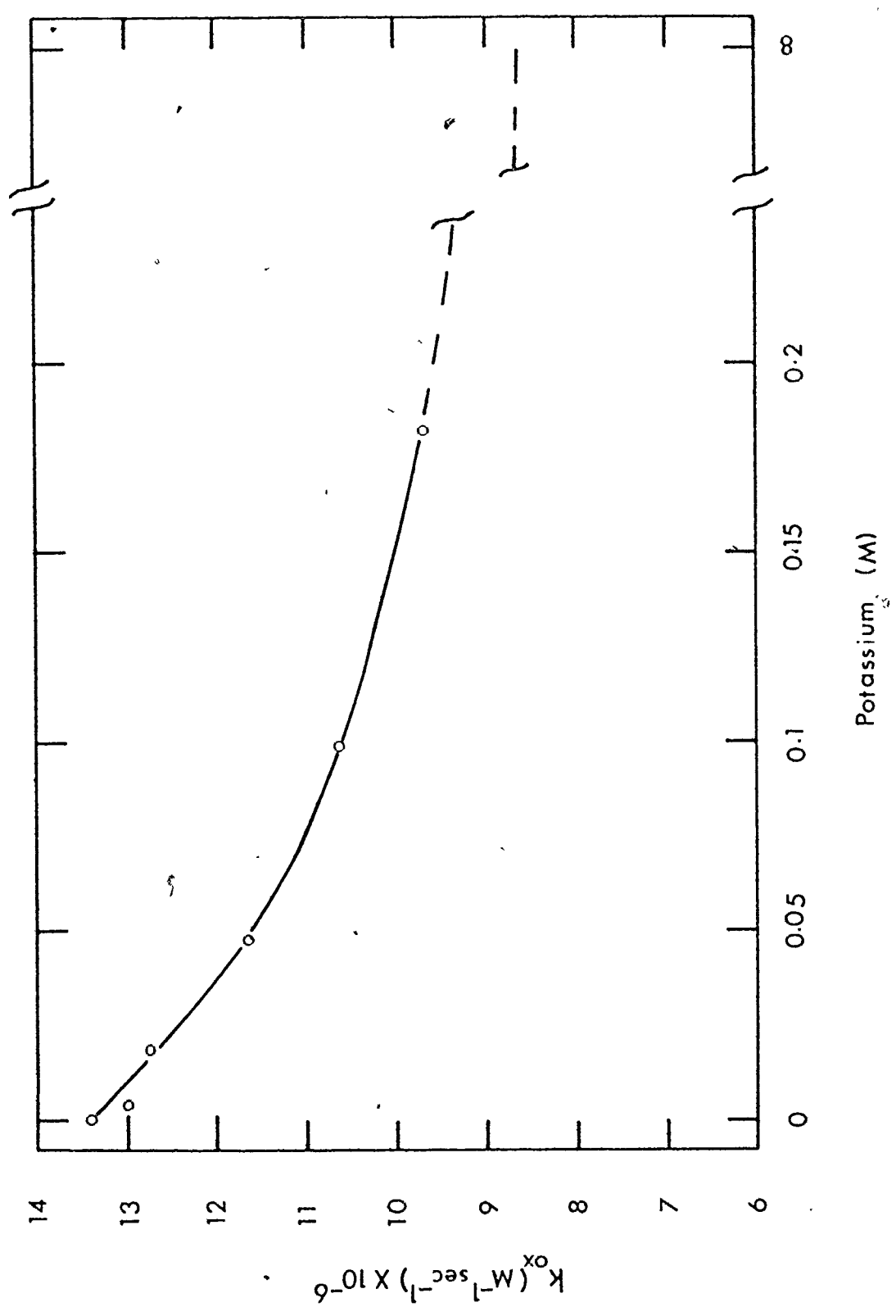
Figure 3.13 shows the effect of K^+ on the oxidation of cHo^{II} . The buffer was tris-cacodylate with tris cation replaced by various concentrations of K^+ . Like chloride and phosphate, K^+ decreased the rate of oxidation of cHo^{II} by ferricyanide.

3.2.5. Effect of D_2O on the oxidation of ferrocytochrome c

To examine the effect of solvent on the rate of electron transfer, the oxidation of ferrocytochrome c by ferricyanide in D_2O was measured. The replacement of H_2O

Figure 3.13. Effect of potassium ion on the rate of oxidation of ferrocytochrome c.

Ionic strength, 0.194 M; pH 7.0; 24°C. Initial concentration of ferrocytochrome c was 4 μ M, initial concentration of ferricyanide was 12.2 μ M. The solid line is the curve calculated using equation 4.3.8 and parameters in Table 3; the broken line the extrapolation to $A \rightarrow \infty$ (see section 4.3.1.). Each point in the figure represents a single measurement.



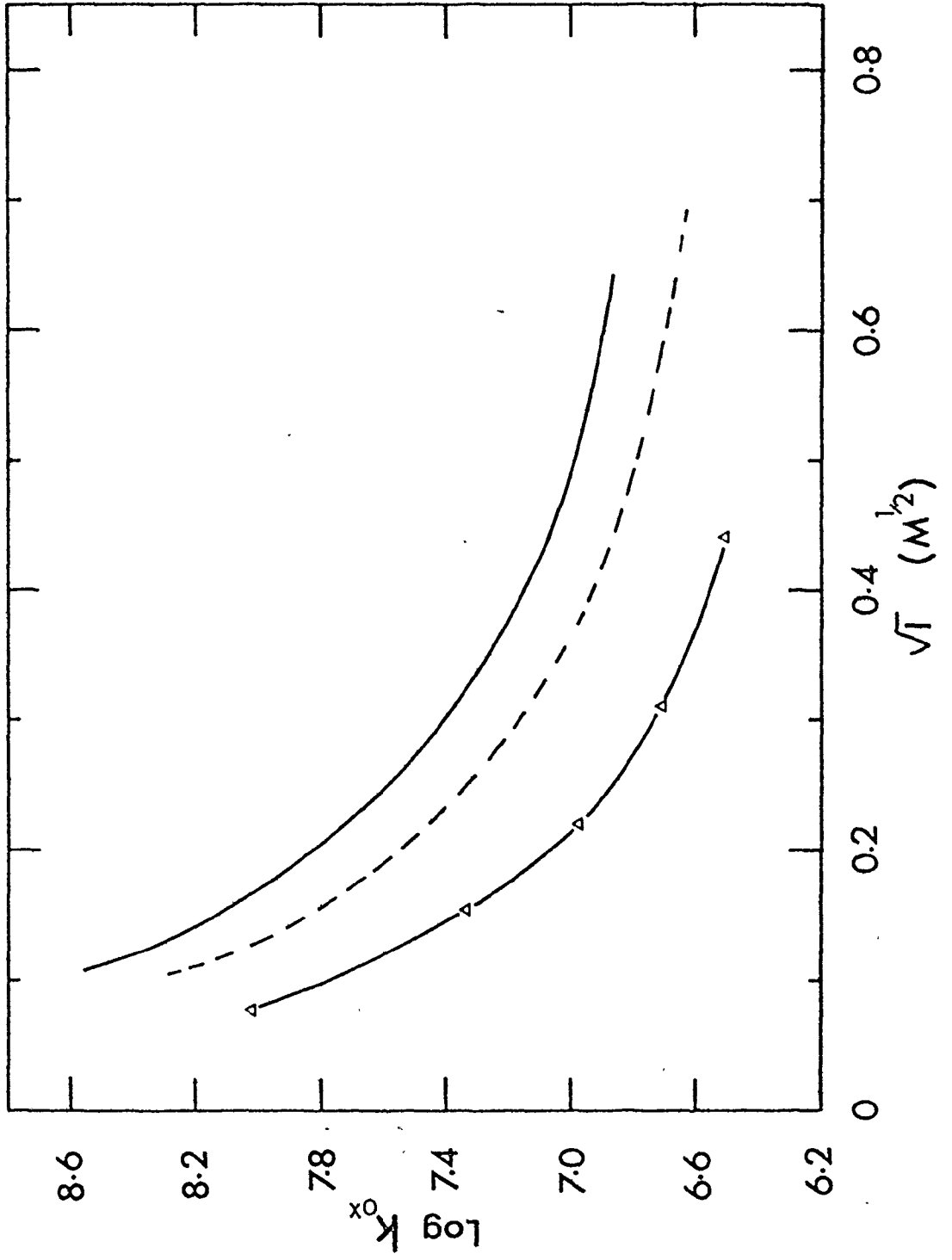
by D_2O will affect properties associated with the hydration shell of the protein. This will be further discussed in Section 4.3.1.. Figure 3.14 shows the ionic strength dependence of the rate constant for the oxidation of CHo^{II} in D_2O at $24^{\circ}C$ and $pD = 7.4$. The ionic strength was varied by changing the concentration of $NaCl$. For comparison the ionic strength dependences of the rate constant for oxidation in non-binding (tris-cacodylate) buffer and in binding (potassium phosphate) buffer are shown.

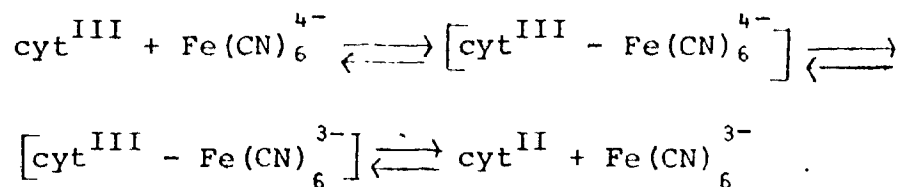
3.3. Reduction of ferricytochrome c with potassium ferrocyanide

The kinetics of the reduction of ferricytochrome c by potassium ferrocyanide have been studied by the temperature jump technique (Havsteen, 1965; Brandt *et al.*, 1966; Zabinski *et al.*, 1974) and by NMR spectroscopy (Stellwagen and Shulman, 1973b). On the basis of their experiments, Brandt *et al.* (1966) concluded that the reduction of ferricytochrome c by potassium ferrocyanide follows reversible second-order kinetics. Later, Stellwagen and Shulman (1973b) proposed a more complex mechanism of the reduction process which besides a reduction reaction, included a reversible binding and a dissociation step:

Figure 3.14. Ionic strength dependence of the rate constant for oxidation of CHO^{11} in D_2O .

Temperature, 24°C ; pD 7.4. The data for tris-cacodylate (—) (redrawn from Figure 3.8) and potassium phosphate (---) (redrawn from Figure 3.9) are also shown. The points represent the average of 2-3 experiments.





While the present work was in progress, Miller and Cusanovich (1975) and Wood and Cusanovich (1975) reported stopped-flow measurements of the reduction of ferricytochrome c by ferrocyanide. They concluded that their results were in agreement with the mechanism proposed by Stellwagen and Shulman (1973b) although some of the steps of the above mechanism could not be detected (Miller and Cusanovich, 1975).

3.3.1. Mechanism of reduction of ferricytochrome c

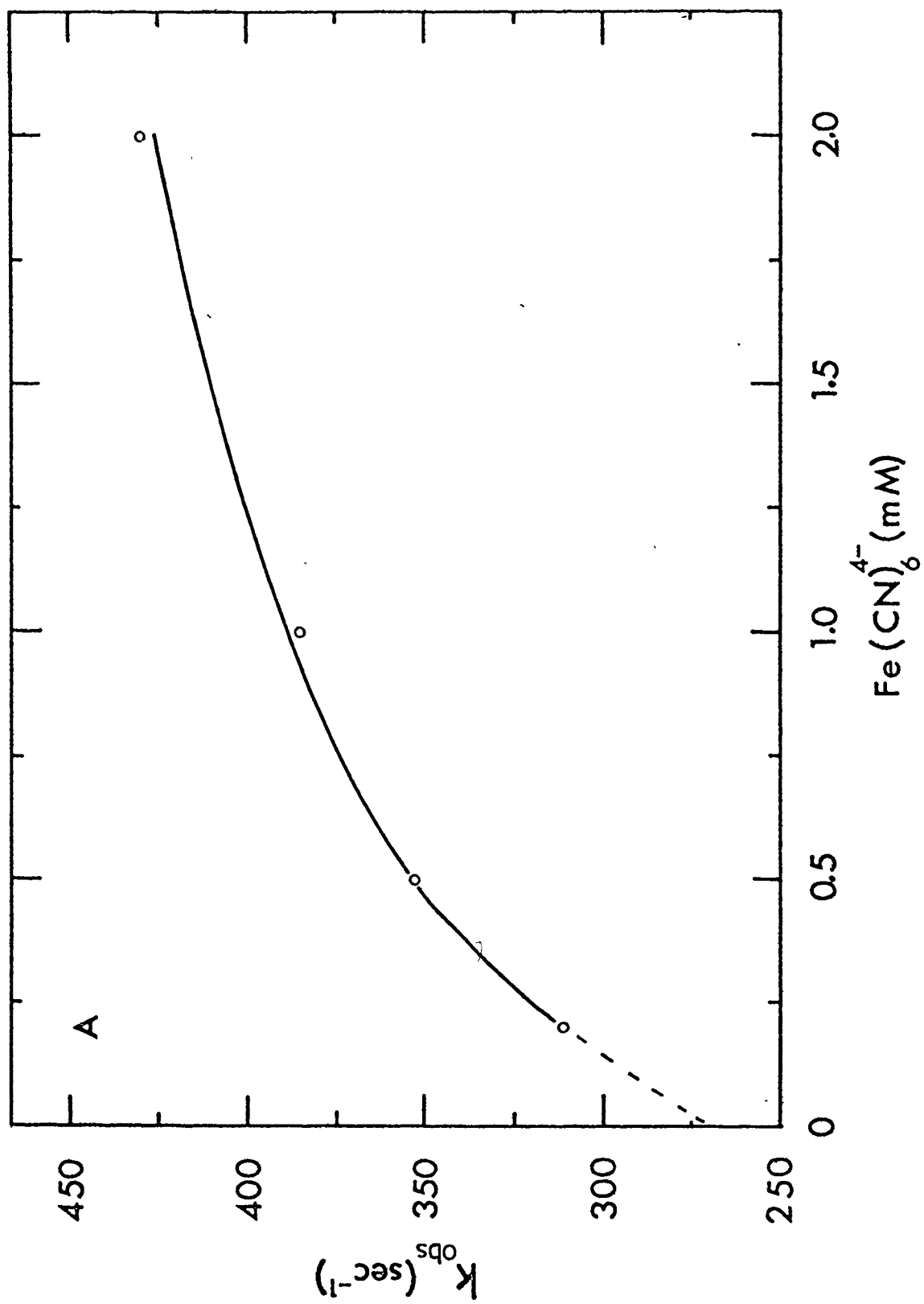
The reduction of ferricytochrome c by potassium ferrocyanide was followed by measuring the rapid increase in absorbancy at the α band (550 nm). Since the opposite reaction (oxidation) is much faster than the reduction of ferricytochrome c, large concentrations of potassium ferrocyanide (10-100 fold excess over ferricytochrome c) were necessary to produce measurable changes in absorbancy. Under these conditions the reaction is very rapid. The plots relating the logarithm of the changes in the absorbancy to time were to a good approximation straight lines as was observed by Miller and Cusanovich (1975) and

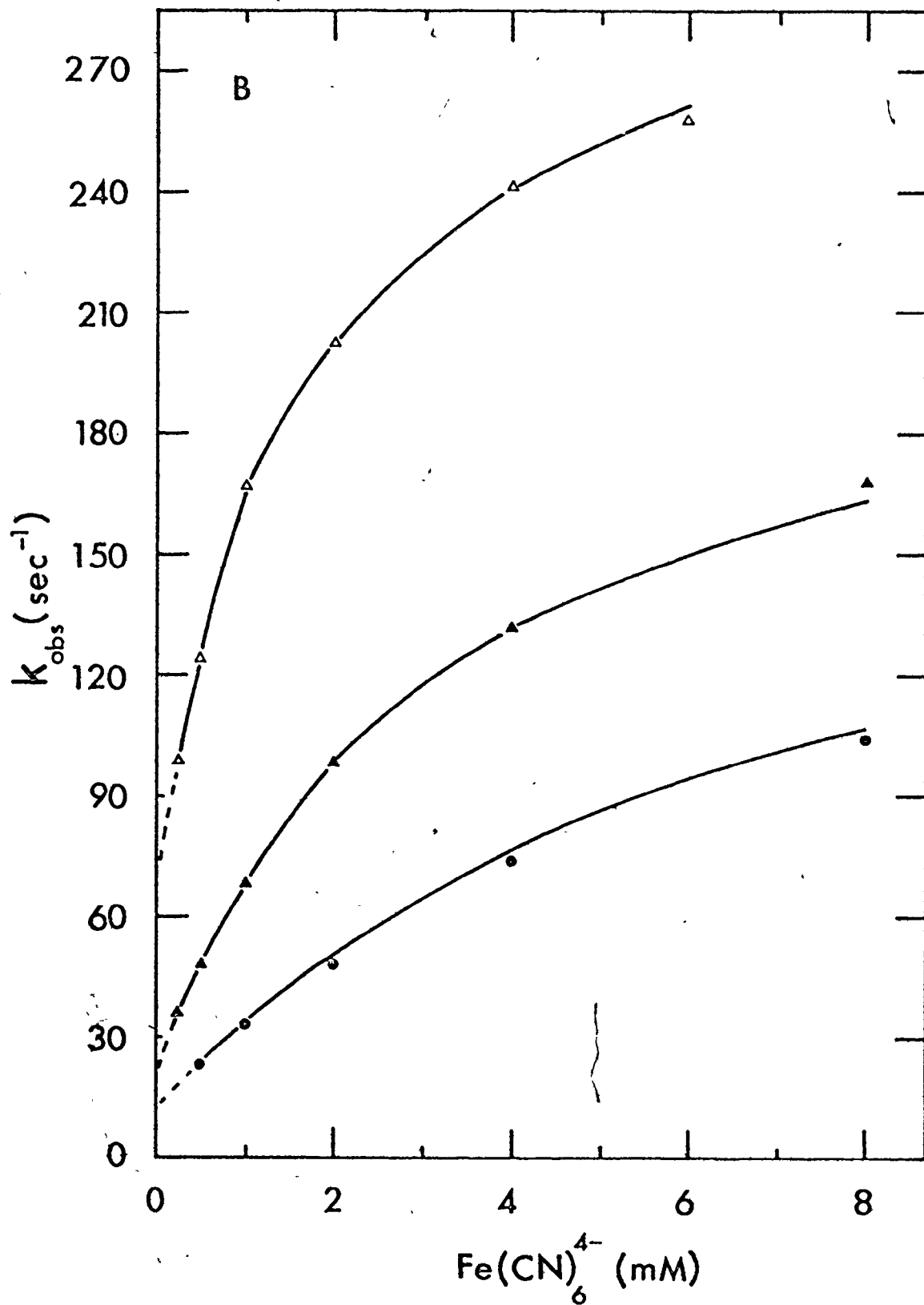
therefore an apparent first order rate constant could be calculated for the reaction.

To determine the mechanism of the reduction process, the rate of reduction was measured at various concentrations of potassium ferrocyanide, while the concentrations of cytochrome c was kept constant. Since it was observed that the ionic strength had a noticeable effect on the reduction process, the ionic strength was also held constant. The points in Figure 3.15 A and B show the relationships between the observed first-order rate constant for reduction of ferricytochrome c and the potassium ferrocyanide concentrations at several ionic strengths. For a reversible second-order reaction (when pseudo-first-order conditions are satisfied), one expects plots of the observed first-order rate constant against the concentration of ferrocyanide to be straight lines intersecting the ordinate at points different from zero (Strickland *et al.*, 1975). Particularly at the lower ionic strength the curvature in the plots of k_{obs} vs $\text{Fe}(\text{CN})_6^{4-}$ was noticeable. Furthermore, it can be seen from Figures 3.15A and B that the extrapolated values ($\text{K}_4\text{Fe}(\text{CN})_6 \longrightarrow 0$ or $\longrightarrow \infty$) were strongly dependent on the ionic strength of the medium. The hyperbolic shape of the curves k_{obs} vs $\text{Fe}(\text{CN})_6^{4-}$ (Figures 3.15A and B) suggests the formation of one or more complexes between the reactants (Strickland *et al.*, 1975). Strickland *et al.* (1975) analyzed the kinetics of

Figure 3.15 A and B. Relationship between the observed first-order rate constant for reduction of ferricytochrome c and the concentration of potassium ferrocyanide at several ionic strengths.

Conditions of the experiments: pH 7.0; temperature, 24°C; buffers, tris-cacodylate; ionic strengths, (o) 0.027 M (Figure A), (Δ) 0.1 M (Figure B), (\blacktriangle) 0.235 M (Figure B), (\bullet) 0.5 M (Figure B). The concentration of cytochrome c was the same for all four ionic strengths (10.6 μ M after mixing). The solid lines represent curves calculated by equation 3.3.3 using the kinetic parameters in Table 1. The broken lines represent extrapolations to $\text{Fe}(\text{CN})_6^{4-} \rightarrow 0$.





the following reaction:



They showed that under the conditions where C is in the steady state, and $B_0 \gg A_0$ (B_0 and A_0 are the initial concentrations of the reactants B and A, respectively), the product (D) appeared at an exponential rate, i.e. $\log \Delta A(t)$ was linear with time t . By assuming $k_2 \gg k_3$ they derived an expression for the variation of the observed first-order rate constant as a function of substrate concentration B (equation 3.3.2).

$$k_{\text{obs}} = k_1 k_3 B / (k_1 B + k_2) + k_4 \quad (3.3.2)$$

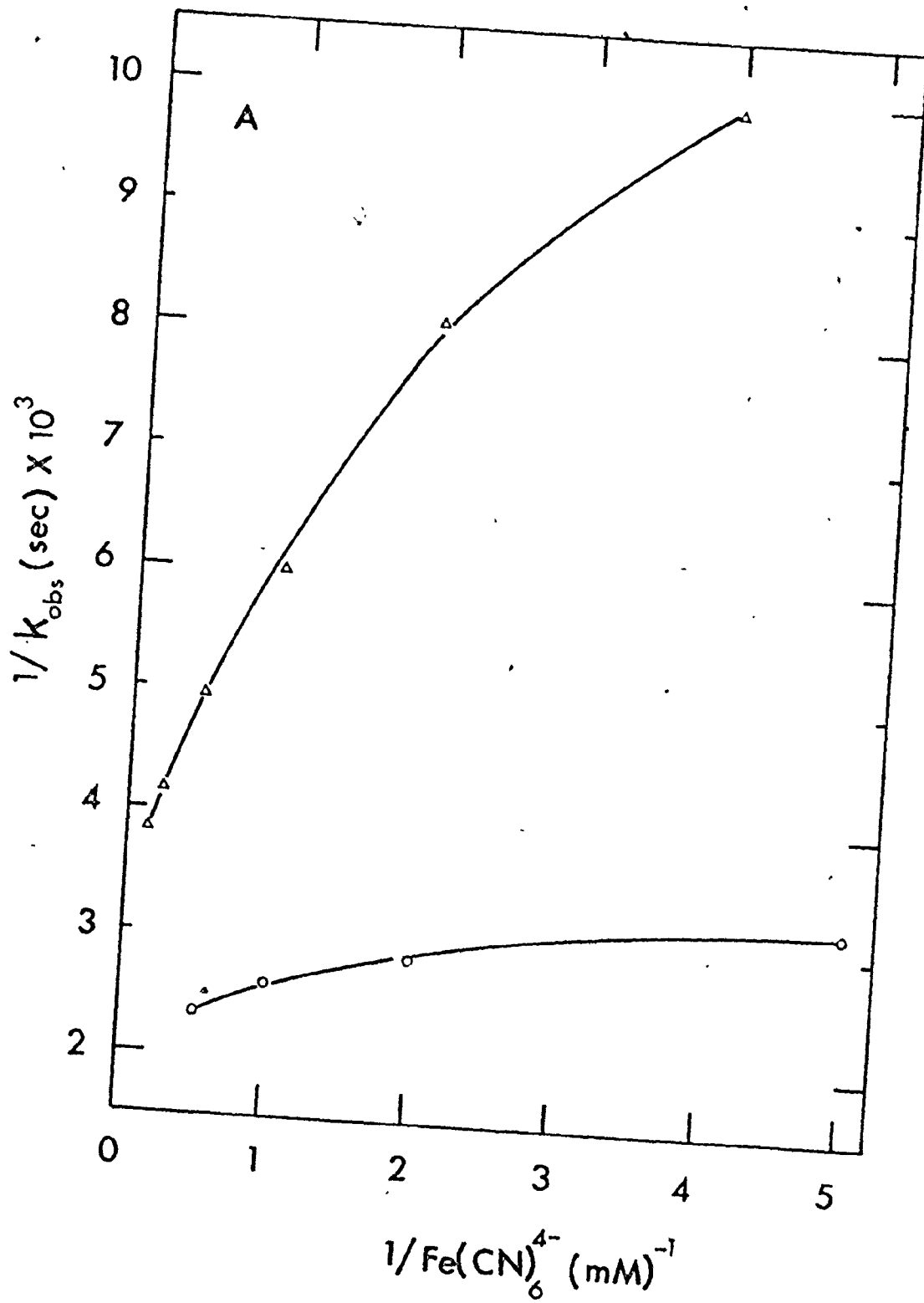
If one defines the dissociation constant as $K_d = k_2/k_1$, equation 3.3.2 can be re-written as equation 3.3.3:

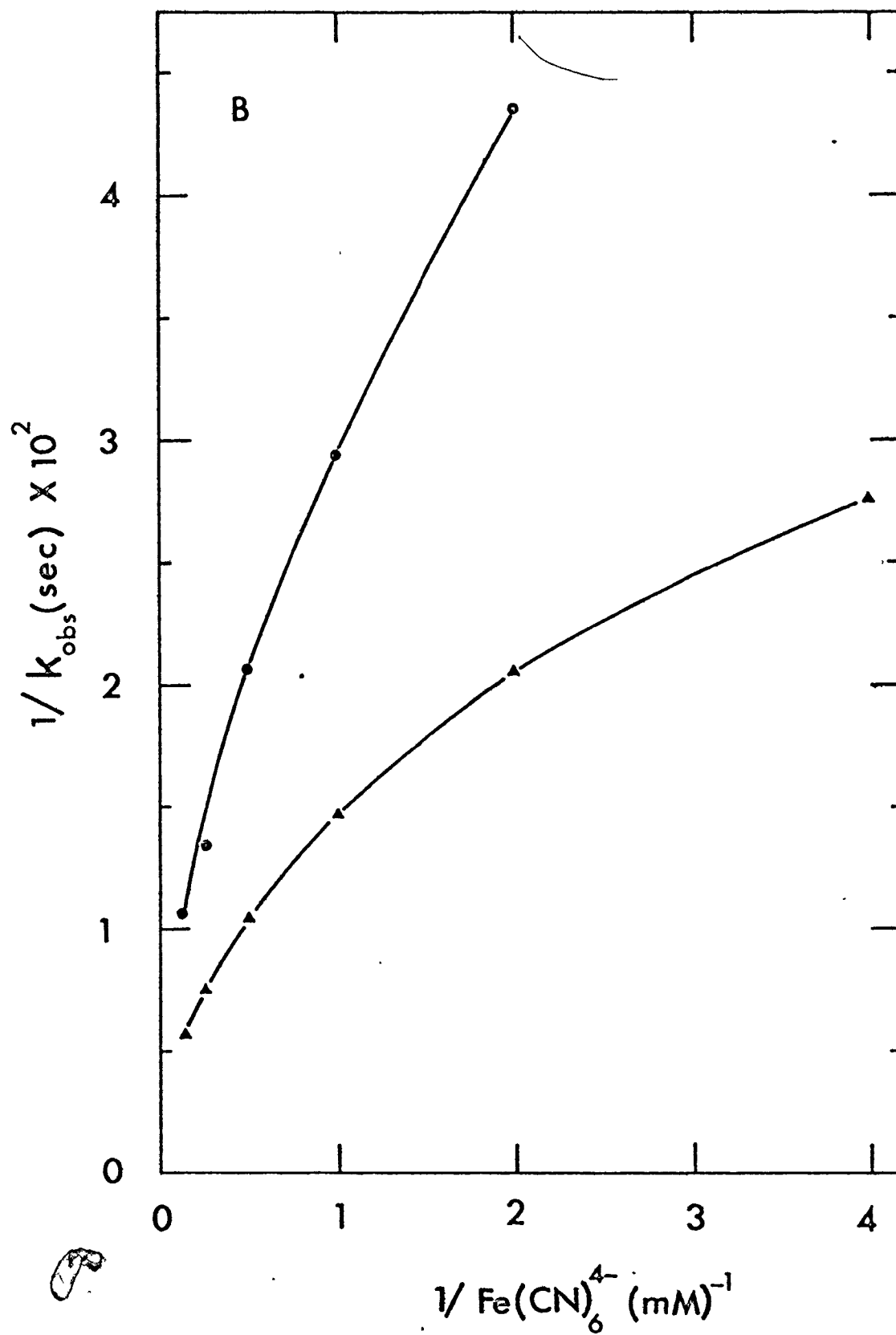
$$k_{\text{obs}} = k_3 / (K_d/B + 1) + k_4 \quad (3.3.3)$$

If the reverse reaction of the second step in mechanism 3.3.1 is negligible ($k_4 = 0$) it can easily be shown that a plot of $1/k_{\text{obs}}$ vs $1/B$ should be a straight line. To test whether this holds in our case the curves in Figures 3.15A and B were replotted as double reciprocal plots in Figures 3.16A and B. As can be seen, the double reciprocal plots are nonlinear, indicating that the rate constant k_4 is not zero. From equation 3.3.3 one can derive equation 3.3.4:

Figure 3.16 A and B. Double reciprocal plots of the observed first-order rate constant and the concentration of potassium ferrocyanide ($1/k_{\text{obs}}$ vs $1/\text{potassium ferrocyanide}$).

Conditions: pH 7.0; temperature 24°C ; ionic strengths: (o) 0.027 M (Figure A), (Δ) 0.1 M (Figure A), (\blacktriangle) 0.235 M (Figure B), (\bullet) 0.5 M (Figure B).





$$1 / (k_{\text{obs}} - k_4) = 1 / k_3 + K_d / k_3 B \quad (3.3.4)$$

which states that if k_4 is finite a plot of $(1 / (k_{\text{obs}} - k_4))$ vs $1/B$ gives a straight line. In the next step values for the rate constant k_4 were obtained from the extrapolation of the k_{obs} vs $\text{Fe}(\text{CN})_6^{4-}$ curves (Figures 3.15A and B) to zero concentration of ferrocyanide and the experimental data of Figures 3.15A and B were replotted as the reciprocal of the concentration of potassium ferrocyanide. As can be seen from Figure 3.17 the plots $1 / (k_{\text{obs}} - k_4)$ vs $1 / \text{Fe}(\text{CN})_6^{4-}$ yield straight lines which would be expected if the appearance of ferrocyanide c (when ferricytochrome c is reduced with ferrocyanide) follows the mechanism 3.3.1 with all four constants different from zero. From the intercepts and the slopes of the straight lines the values for k_3 and K_d can be determined. The values for the constants K_d , k_3 , k_4 are given in Table 1. To verify the consistency of the analysis, the parameters in Table 1 were used in equation 3.3.3 to calculate the solid curves of k_{obs} vs $\text{Fe}(\text{CN})_6^{4-}$ shown in Figures 3.15A and B. There is good agreement between the experimental points and calculated curves. Our experimental data are, therefore, consistent with the following reaction scheme:

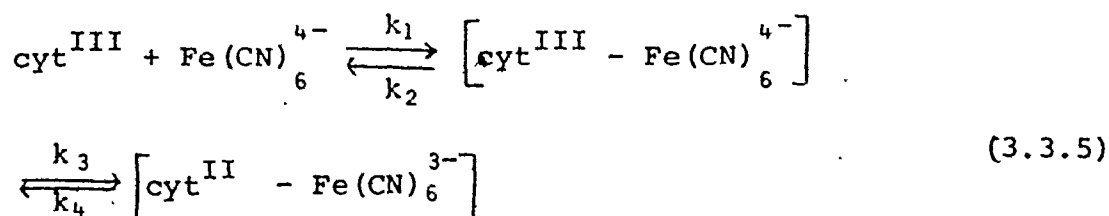


Figure 3.17. The plots of $1/(k_{\text{obs}} - k_4)$ vs $1/(\text{Fe}(\text{CN})_6^{4-})$ at several different ionic strengths.

Conditions as stated in Figure 3.15 A and B.

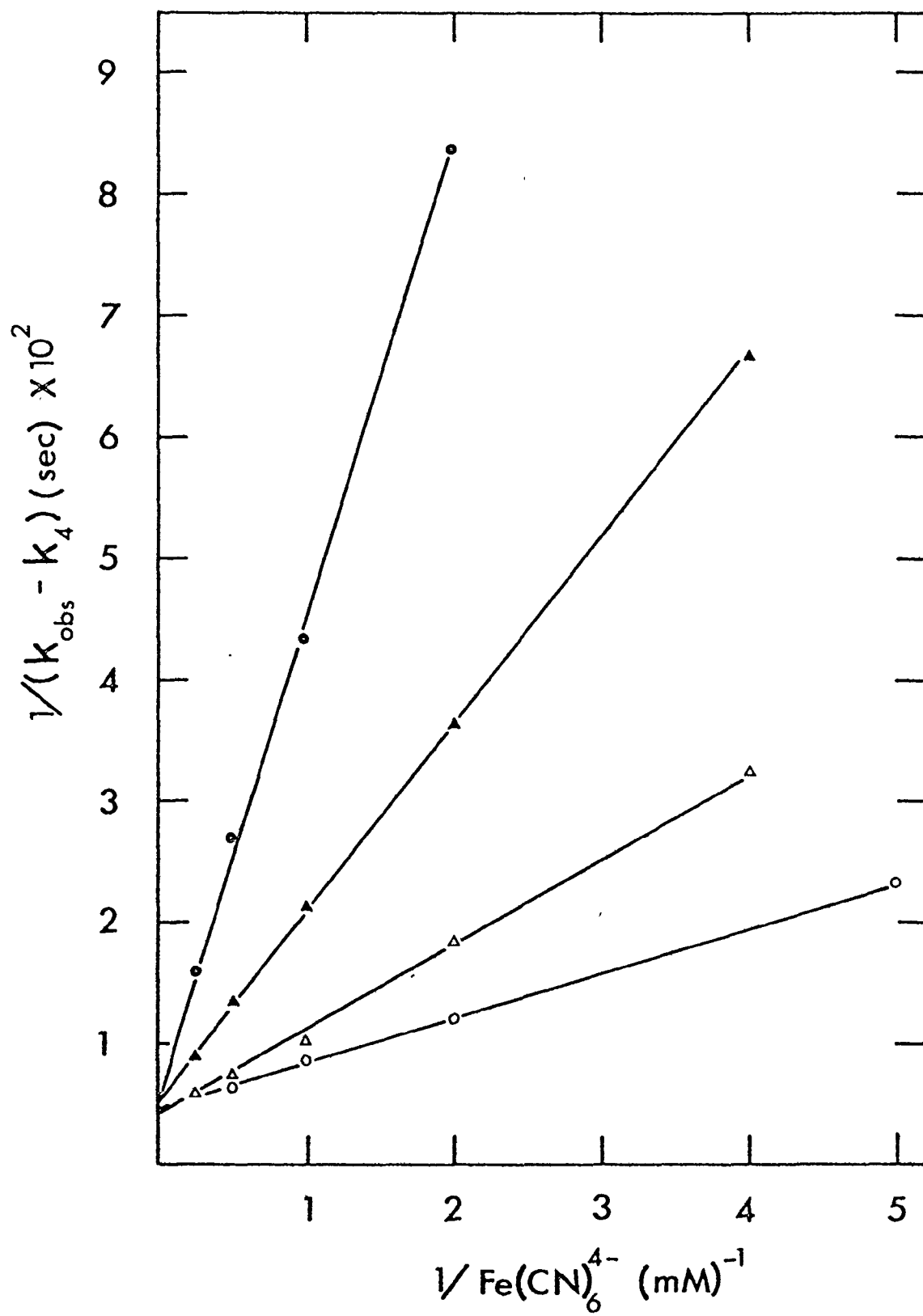
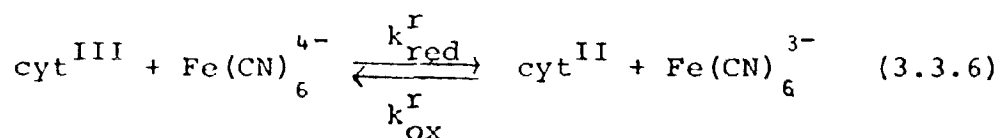


Table 1

Kinetic Parameters K_d , k_3 and k_4 at Different
Ionic Strengths

Ionic strength (M)	K_d (M)	k_3	k_4
0.5	7.1×10^{-3}	182	11
0.235	2.9×10^{-3}	190	21
0.1	1.8×10^{-3}	250	70
0.027	7.5×10^{-4}	208	270

Although it could not be detected in our experiments, the ferrocyanochrome c -ferricyanide complex (see equation 3.3.5) dissociates into free ferrocyanochrome c and ferricyanide (Stellwagen and Shulman, 1973b). If we include the dissociation step the reduction of ferricytochrome c by ferrocyanide can be represented by an overall reversible second-order reaction 3.3.6:



where $k_{\text{red}}^{\text{r}}$ and k_{ox}^{r} are second-order rate constants which may depend on ferrocyanide concentration. In some cases (e.g., when the steady state concentrations of the intermediate complexes are negligible compared to the concentration of other species, see Morton *et al.*, 1970), the formation of intermediate does not affect the overall second-order rate constant. We, therefore, examined the effect of the potassium ferrocyanide concentration on the overall second-order rate constants. Kinetic runs whose first order rate constants are reported in Figures 3.15 A and B were fitted to a reversible second order reaction. Good fitting of the experimental curves was obtained. This can be accounted for by the small total absorbancy changes of the kinetic runs (from 0.03 to 0.08) which make the differences between exponential and hyperbolic decay negligible. The analysis of the reaction runs in this way yields two reaction constants:

a second-order rate constant for the reduction (forward) reaction ($k_{\text{red}}^{\text{r}}$), and a second-order rate constant for the oxidation (reverse) reaction (k_{ox}^{r}). The superscript r designates that the rate constant was determined by studying the reduction of ferricytochrome c. The ratio of these two rate constants ($k_{\text{red}}^{\text{r}}/k_{\text{ox}}^{\text{r}}$) corresponds to the apparent equilibrium constant discussed in section 3.1.. The variations of the overall reduction and oxidation rate constants with the concentration of potassium ferrocyanide at several ionic strengths are presented in Figures 3.18A and B, respectively. These plots are not straight lines, as would be expected if the reactions followed reversible second-order kinetics, the deviation being most pronounced at lower ionic strengths. At the highest ionic strength ($I = 0.5 \text{ M}$), both rate constants (k_{ox}^{r} and $k_{\text{red}}^{\text{r}}$) seem to be almost independent of the potassium ferrocyanide concentration.

At ionic strengths below 0.1 M the values of k_{ox}^{r} were always much lower than the values for k_{ox} (at the same ionic strength) determined by measuring oxidation of ferrocytochrome c. The difference between these two quantities depended on the ionic strength and the concentration of ferrocyanide. A possible reason for this discrepancy will be discussed in section 4.1.2..

Figure 3.18 A. Variation of the overall second-order rate constant for reduction (k_{red}^r) of ferricytochrome c as a function of potassium ferrocyanide concentration.

Buffer, tris-cacodylate; pH 7.0; temperature, 24°C; ionic strengths, (Δ) 0.1 M, (\blacktriangle) 0.235 M, (\bullet) 0.5 M. The solid lines were drawn by eye to indicate the trends.

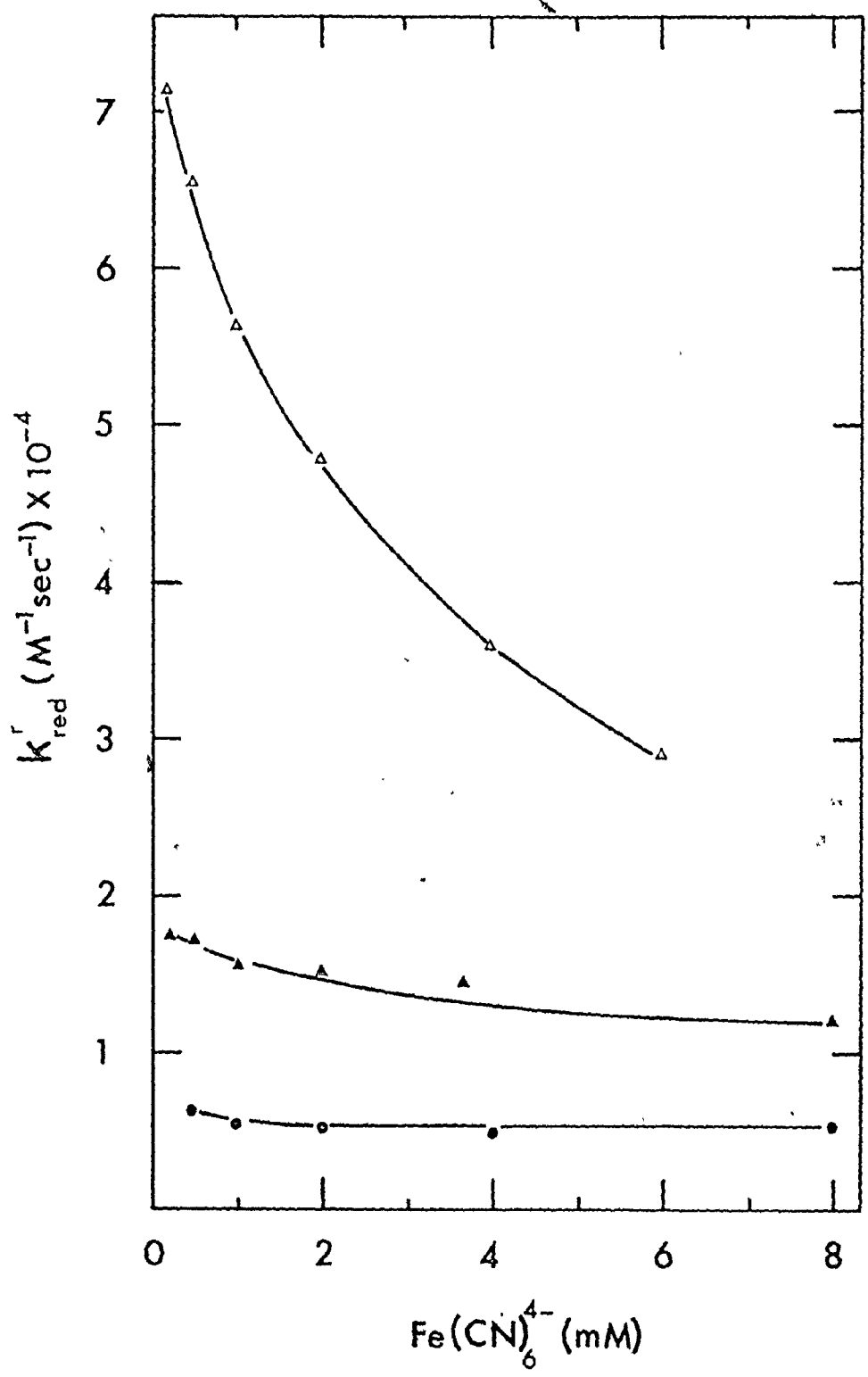
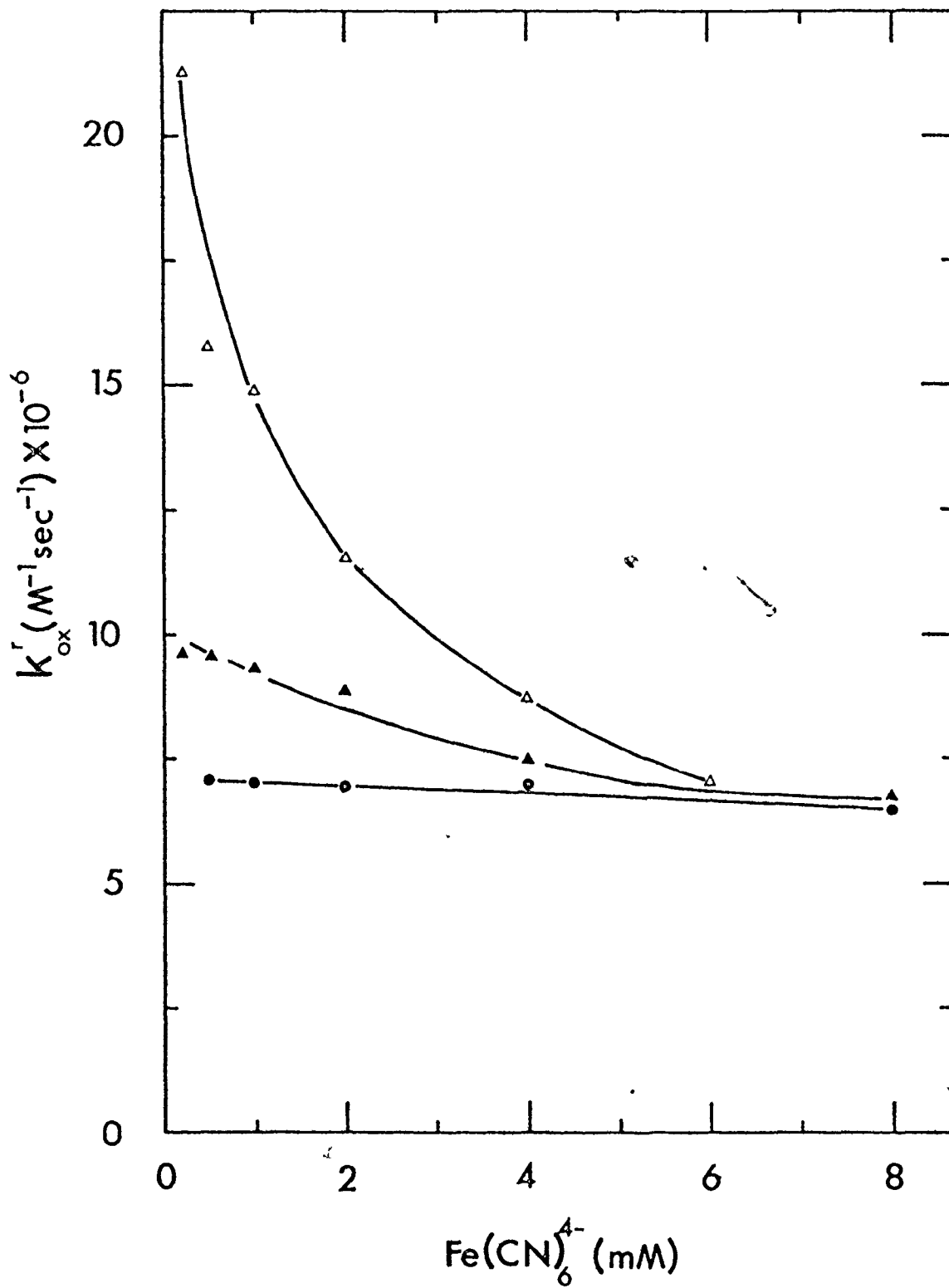


Figure 3.18 B. Variation of the overall second-order rate constant for oxidation (k_{OX}^r) as a function of potassium ferrocyanide concentration.

Buffer, tris-cacodylate; pH 7.0, temperature, 24°C; ionic strengths, (Δ) 0.1 M, (\blacktriangle) 0.235 M, (\bullet) 0.5 M. The solid lines were drawn by eye to indicate trends.



3.3.2. The effect of the ionic strength on the reduction of ferricytochrome c

The results reported in section 3.3.1. showed that ionic strength has a large effect on the reduction of the ferricytochrome c. Figure 3.19 shows the relationship of the logarithm of the observed first-order rate constant to the square root of the ionic strength at several concentrations of potassium ferrocyanide. At lower ionic strength, the rate of reduction of ferricytochrome c is increased as expected for a reaction between two oppositely charged molecules. The curves $\log k_{\text{obs}} \sqrt{I}$ become more linear at lower ionic strengths.

3.3.3. Specific anion effects on the reduction of ferricytochrome c

3.3.3.1 The effect of Cl^- and phosphate on the reduction of ferricytochrome c

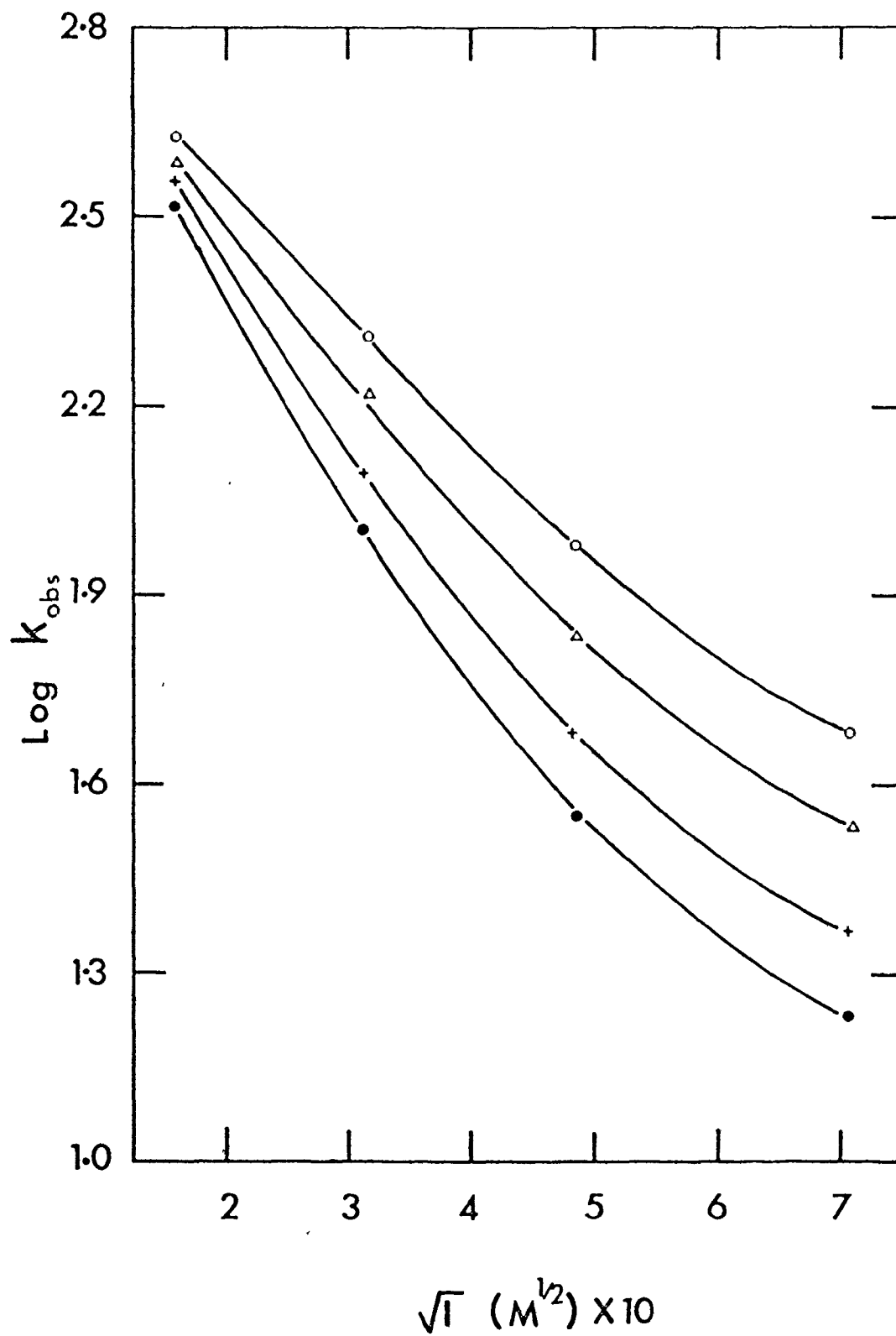
The binding of ions to cytochrome c is intimately related to the function of cytochrome c. Schejter and Margalit (1970), Palcic (1972) and Margalit and Schejter (1973a) observed that the presence of chloride ion changes the reduction potential of cytochrome c. The following study was undertaken to decide which reaction, oxidation

Figure 3.19. Ionic strength dependence of the observed first-order rate constant for reduction of ferricytochrome c at different concentrations of potassium ferrocyanide.

Buffer, tris-cacodylate of various ionic strengths: pH 7.0; temperature 24°C. Concentrations of potassium ferrocyanide: (o) 2 mM, (Δ) 1 mM, (+) 0.5 mM, (\bullet) 0.25 mM. The solid lines were drawn by eye to indicate trends.

2

2



or reduction, is the one affected by the presence of chloride ions. In addition, it attempted to resolve the apparent discrepancy that phosphate does interact with both forms of cytochrome c (Margoliash *et al.*, 1970; Margalit and Schejter, 1973b), but does not change the reduction potential (see section 3.1.).

As discussed in section 3.3.1. when the reduction of ferricytochrome c is analyzed in terms of a reversible second order reaction, overall rate constants for both reduction and oxidation could be derived. The ratio of the two constants is related to the reduction potential of cytochrome c (E_{cyt}°) by equation 3.3.7:

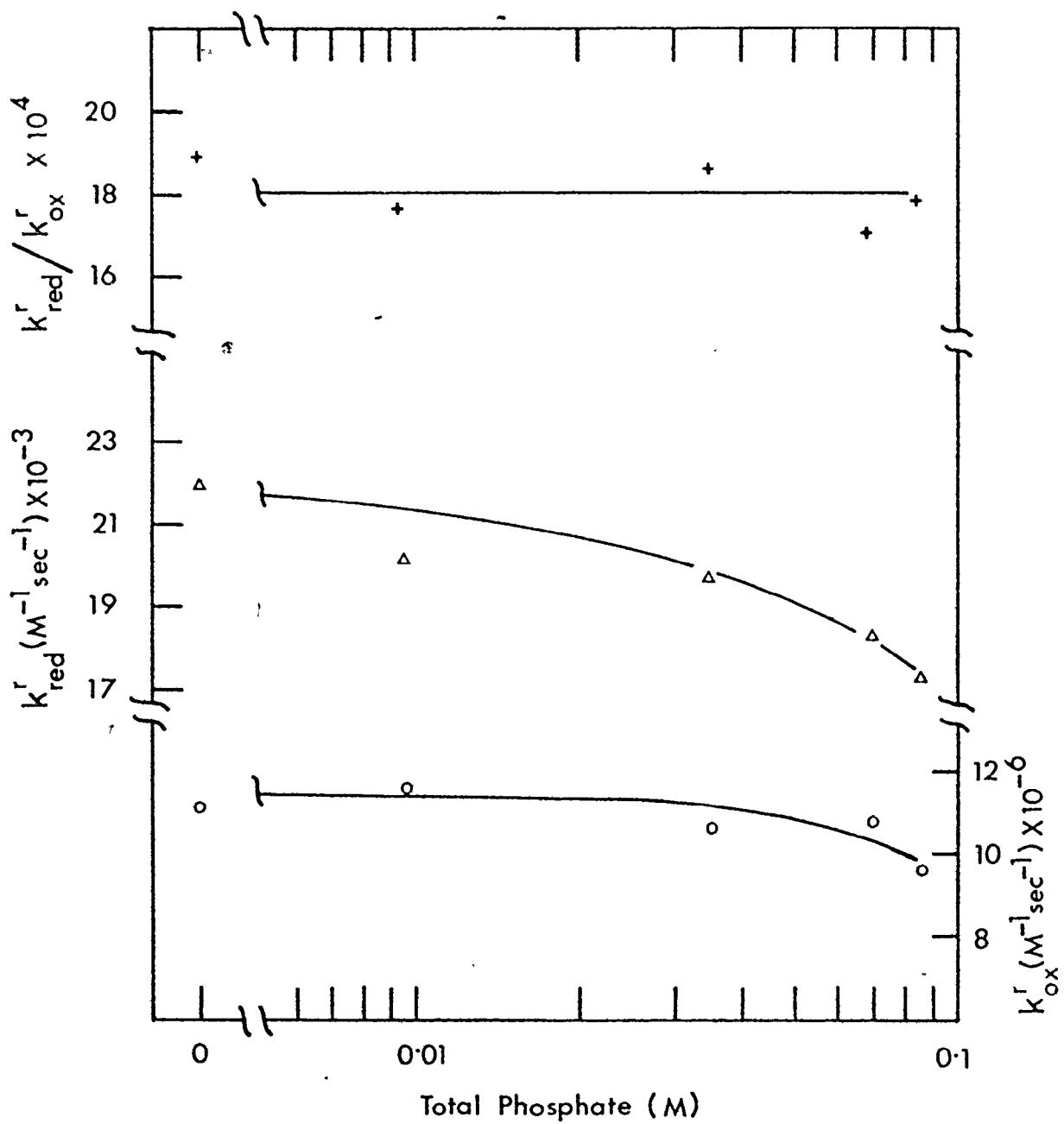
$$E_{\text{cyt}}^{\circ} = E_{\text{Fe}}^{\circ} + \frac{RT}{nF} \ln(k_{\text{red}}^r/k_{\text{ox}}^r) \quad (3.3.7)$$

where E_{Fe}° is the reduction potential of the ferri/ferrocyanide couple, R the gas constant, T the absolute temperature, F the Faraday constant and n the number of electrons transferred. By studying the reduction of ferricytochrome in the presence of various binding buffers one can determine the effect of ion binding on the rate of reduction and oxidation. Furthermore, one can estimate the effect of the binding of the ions on the reduction potential by equation 3.3.7.

Chloride and phosphate had very different effects on the reduction of ferricytochrome c. Phosphate decreased both oxidation and reduction rates equally (Figure 3.20)

Figure 3.20. Effect of phosphate on the reduction of ferricytochrome c.

The effect on the overall rate constants for reduction (Δ) (left ordinate), and for oxidation (o) (right ordinate). The ratio of the rate constants is plotted as well (+) (left ordinate). Ionic strength, 0.196 M; pH 7.0; temperature, 24°C. The initial concentration of ferricytochrome c was 10.35 μ M, that of ferrocyanide was 1 mM. The solid lines were drawn by eye to indicate trends.



leaving the ratio of the overall rate constants unchanged within the experimental error of 10%. Since the reduction potential is proportional to the logarithm of the ratio of the two constants, $(k_{\text{red}}^r/k_{\text{ox}}^r)$, we conclude that the redox potential was not significantly affected by the increased concentration of phosphate.

On the other hand, chloride decreased the overall rate constant of reduction much more than that of oxidation (Figure 3.21) lowering the ratio of the two constants. As a result, the redox potential of cytochrome was decreased by approximately 4-5% at the highest chloride concentration.

3.3.3.2. The effect of picrate on the reduction of ferricytochrome c

Figure 3.22 shows the effect of picrate on the overall second-order rate constants for reduction and oxidation as derived from reduction kinetics of ferricytochrome c. The experiments were performed at a lower ionic strength of $I = 0.0485 \text{ M}$, (pH 7.0), and the kinetics runs analyzed as reversible second-order reactions. At the highest picrate concentration (0.0485 M), there is a marked decrease (fifty fold) in the rate of reduction of ferricytochrome c, whereas the rate of oxidation remained almost unaffected. The decrease in the reduction rate corresponds to the drop in the redox potential by

Figure 3.21. Effect of chloride on the reduction of ferricytochrome c.

The effect of chloride on the overall rate constants for reduction (Δ) (left ordinate) and oxidation (o) (right ordinate). The effect of chloride on the ratio of the two constants (+) (left ordinate) is presented as well. Ionic strengths, 0.196 M; pH 7.0; temperature, 24°C. Initial concentration of ferricytochrome was 10.55 M, that of ferrocyanide was 1 mM. The solid lines were drawn by eye to indicate trends.

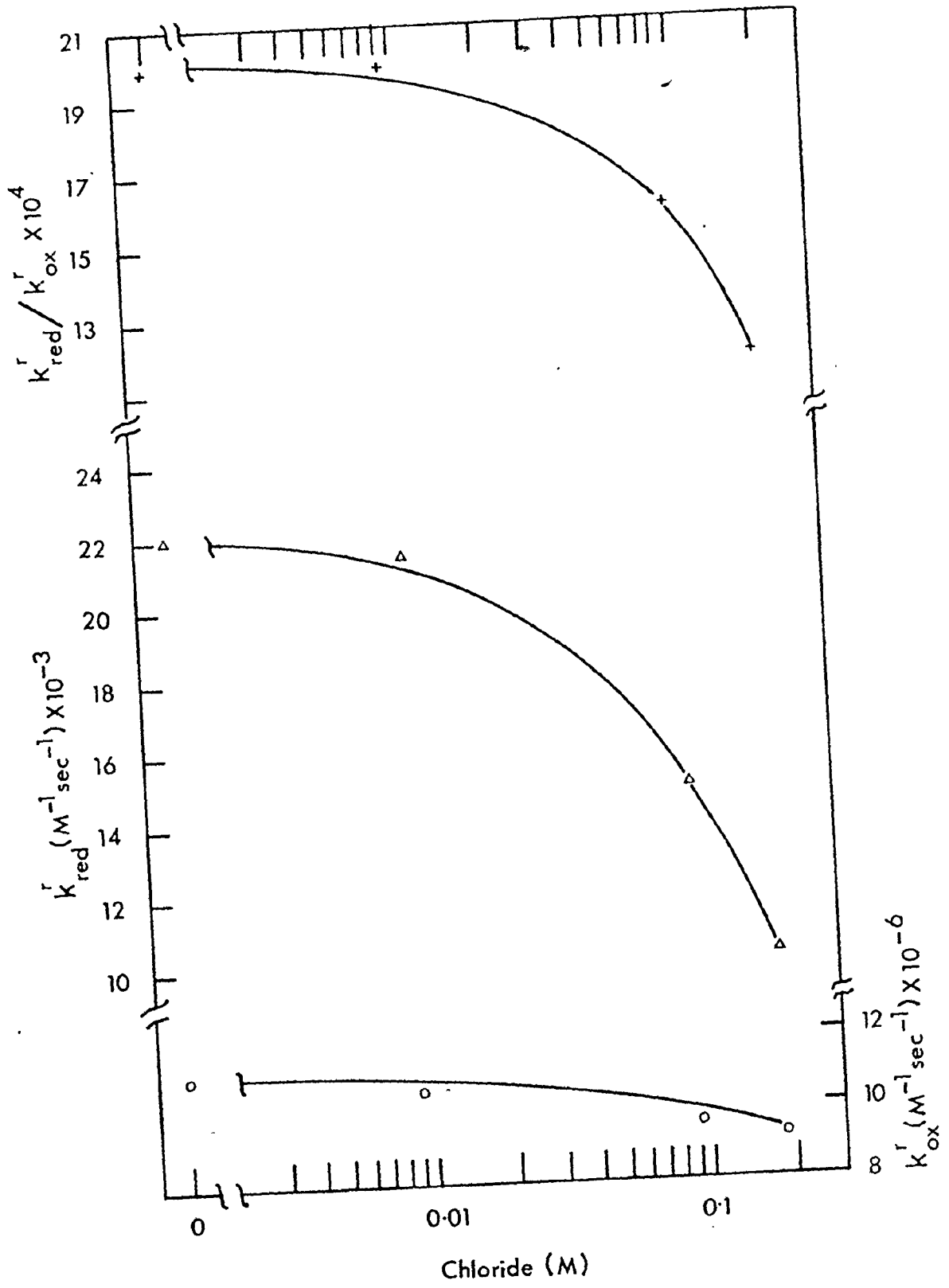
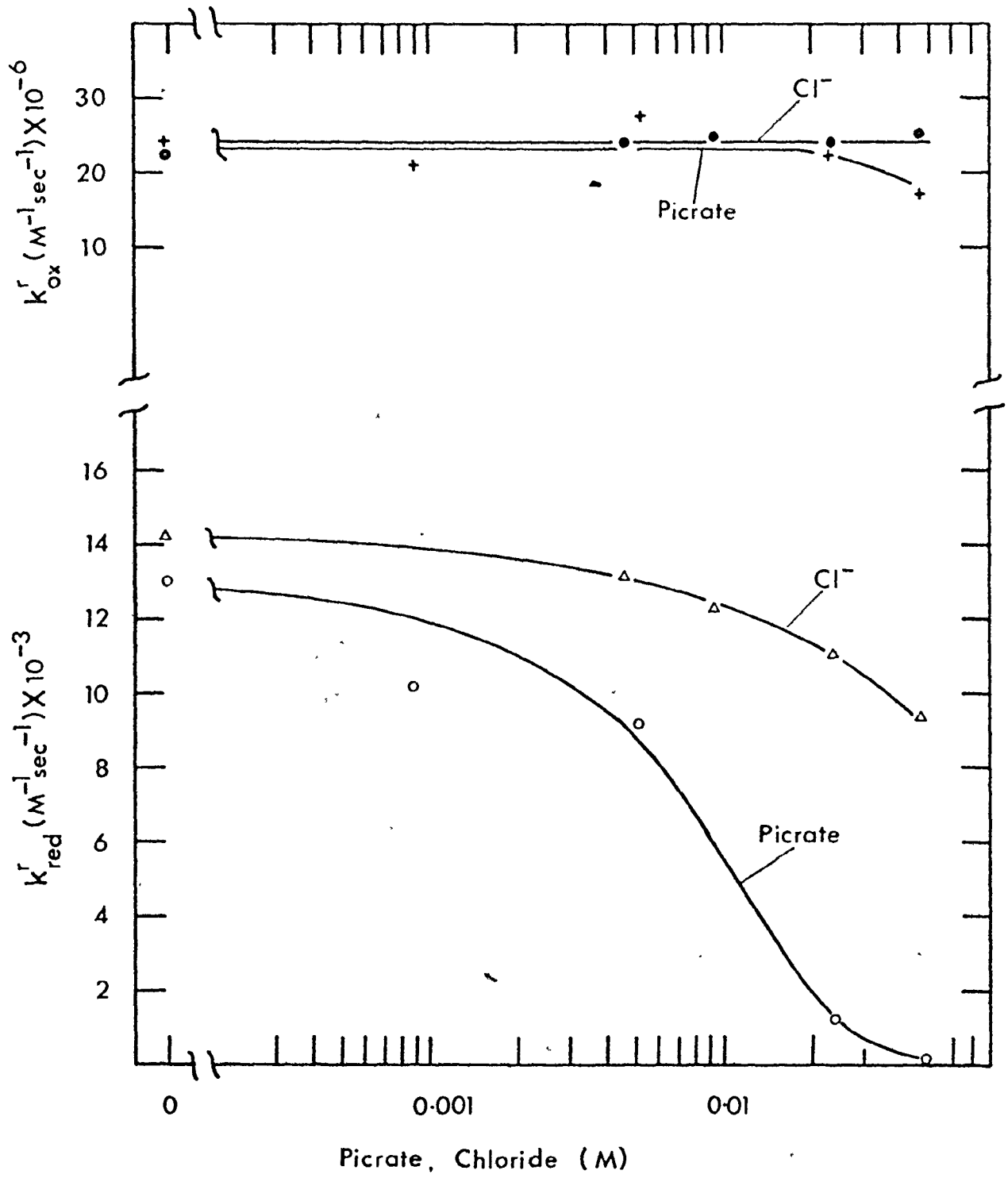


Figure 3.22. Effect of picrate and chloride on the overall rate constants for reduction (o,Δ) and oxidation (+,●).

Picrate (o,+) and chloride (Δ,●) were compared at $I = 0.0485 \text{ M}$, $\text{pH } 7.0$, 24°C . The initial concentration of ferricytochrome c was $11.2 \mu\text{M}$, that of ferrocyanide was 1 mM . The solid lines were drawn by eye to indicate trends.



approximately 30%. Again a comparison was made between the effect of picrate and chloride under the same conditions. The presence of Cl^- ions decreased the rate of reduction by some 30-40% (at $\text{Cl}^- = 0.0485 \text{ M}$), but did not significantly affect the rate of oxidation. The limiting values ($(\text{Cl}^-) \longrightarrow 0$, (picrate) $\longrightarrow 0$) for both curves agreed within experimental errors (8-10%).

3.4. Guanidinated cytochrome c

3.4.1. Oxidation of guanidinated ferrocytochrome c

The rate law determined for the oxidation of unmodified ferrocytochrome c (section 3.2.1.) was assumed to hold for the oxidation of gn-ferrocytochrome c. In other words, it was assumed that the oxidation of reduced gn-cytochrome c followed irreversible second-order kinetics. Figure 3.23 shows the logarithm of the second order rate constant for oxidation of gn-ferrocytochrome c plotted against the square root of the ionic strength. The results obtained with this modified cytochrome c are compared with those obtained with unmodified (Figure 3.23). The oxidation of gn-ferrocytochrome c was about 20% more rapid than the oxidation of native ferrocytochrome c. The difference is not large, but it is believed to be outside the experimental errors of 5-10%.

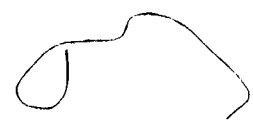
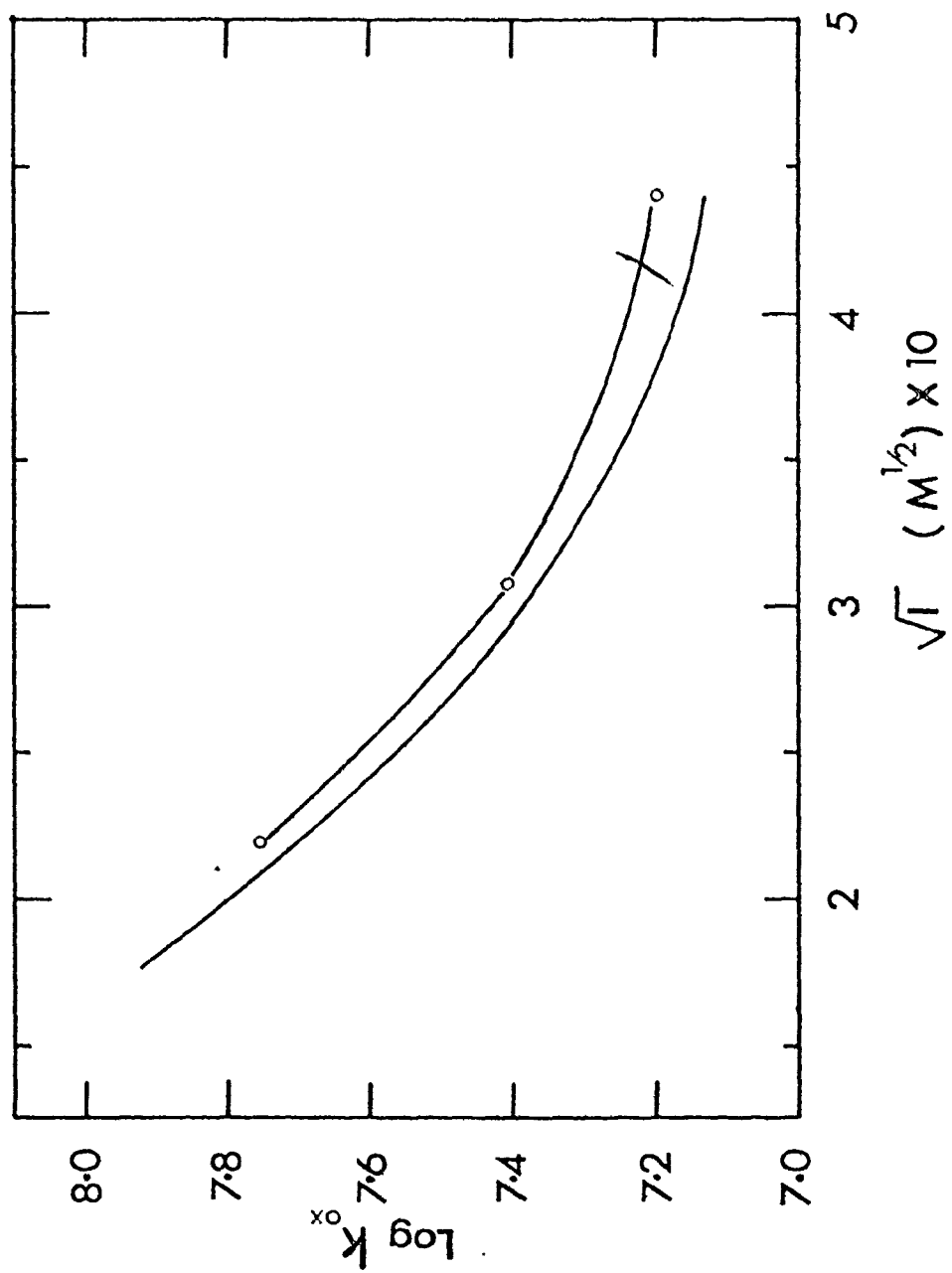


Figure 3.23. Comparison of the ionic strength dependence of the oxidation rate constant between modified and unmodified ferrocytochrome c.

(o) guanidinated ferrocytochrome c, solid line unmodified ferrocytochrome c, from Figure 3.8. Buffer, tris-cacodylate of various strengths; pH 7.0; temperature, 24°C. The solid lines were drawn by eye to indicate trends. The points represent average values of 2-3 experiments.



3.4.2. Reduction of guanidinated ferricytochrome c

In contrast to the oxidation of gn-ferrocytochrome c the reduction of gn-ferricytochrome c occurs more slowly than the reduction of unmodified ferricytochrome c. This is illustrated in Figure 3.24. Both sets of experiments (unmodified, modified) were done under the same conditions of ionic strength, pH, and temperature. In the range of the potassium ferrocyanide concentrations used (0.25 mM to 6 mM) the observed first-order rate constants for reduction of gn-ferricytochrome c were found to average 20% lower than the values for the unmodified cytochrome c.

As for unmodified ferricytochrome c the reduction was analyzed as a reversible second-order reaction. The second-order rate constants for overall oxidation and reduction of gn-cytochrome c are compared in Figure 3.25 with corresponding rate constants for unmodified cytochrome c. The modification of cytochrome c did not affect the general shape of the curves relating the second-order rate constants to the concentration of potassium ferrocyanide. However, the values of reduction rate constants were lower and the values of oxidation rate constants were higher for guanidinated cytochrome c protein than the corresponding rate constants for unmodified cytochrome c. The average ratio of the two rate constants ($k_{\text{red}}^{\text{r}}/k_{\text{ox}}^{\text{r}}$) for guanidinated cytochrome c was calculated to be approximately 60% lower

Figure 3.24. Observed first-order rate constant for reduction of unmodified and modified ferricytochrome c as a function of potassium ferrocyanide concentration.

(Δ) unmodified ferricytochrome c; (+) guanidinated cytochrome c. Buffer, tris-cacodylate; ionic strength, 0.1 M; pH 7.0; temperature, 24°C. The solid lines were calculated using equation 3.3.3 and kinetic parameters in Table 4.

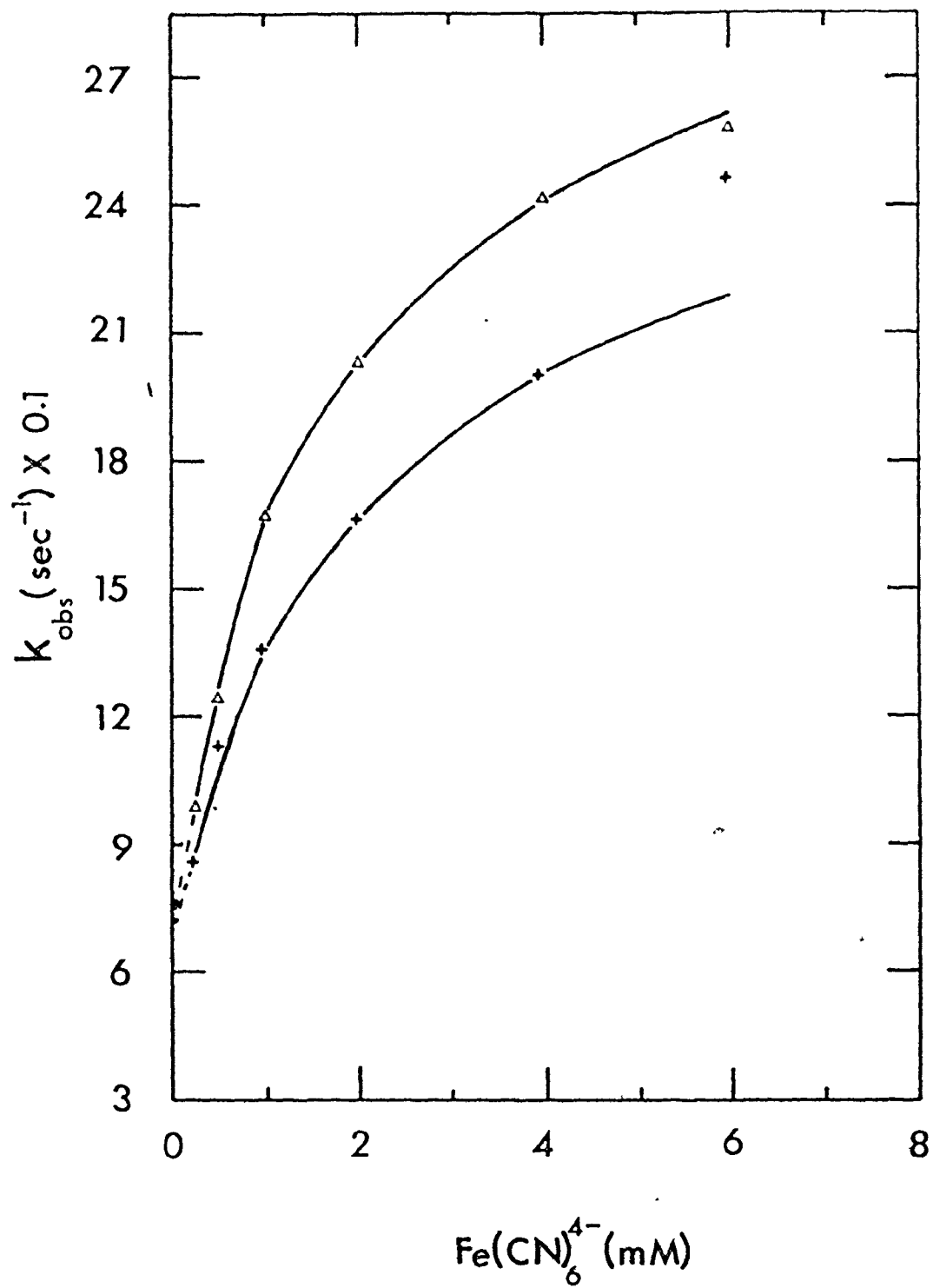
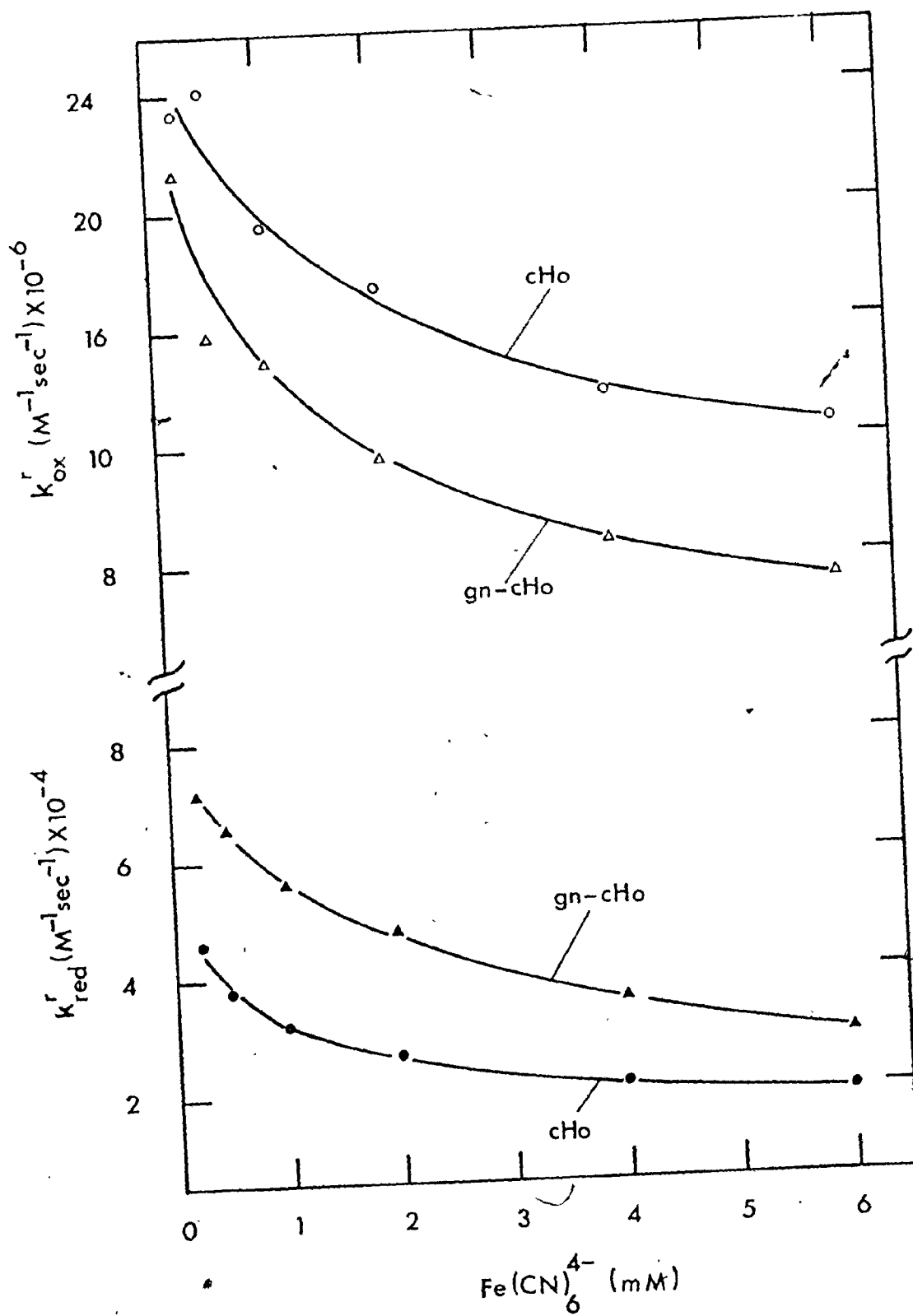


Figure 3.25. Variation of the overall forward and reverse rate constants derived from reduction kinetics of modified ferricytochrome c as a function of potassium ferrocyanide concentration.

(●) the overall rate constant for reduction; (○) the overall rate constant for oxidation. Also included for comparison are k_{red}^r (▲) and k_{ox}^r (Δ) for unmodified cytochrome c. Buffer, tris-cacodylate; ionic strength 0.1 M; pH 7.0; temperature, 24°C. The solid lines were drawn by eye to indicate trends.



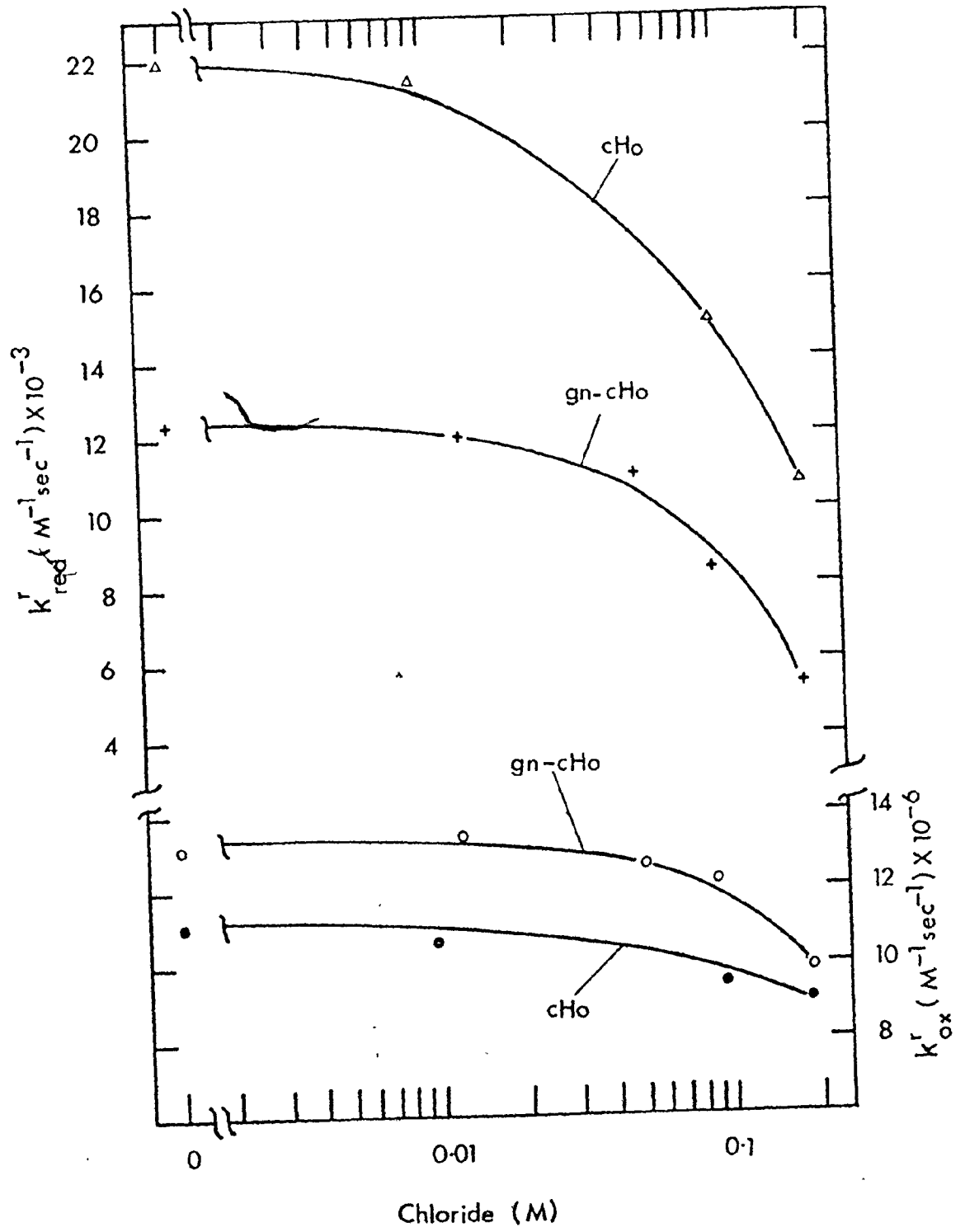
than the value for unmodified cytochrome c. It was estimated that guanidination lowered the redox potential of the cytochrome c system at $I = 0.1 \text{ M}$, pH 7.0 by about 10%.

3.4.3. The effect of Cl^- on the reduction of guanidinated cytochrome c

To examine the effect of the modification on the binding of chloride ions, similar experiments to those described in section 3.3.2.1. were performed with gn-cytochrome c. In Figures 3.26A and B the effect of chloride on the overall rate of reduction and oxidation of modified cytochrome c is compared to the effect on the corresponding rate constants of unmodified cytochrome c. All four curves show similar trends, i.e. with increasing chloride concentration all four rate constants become lower. Furthermore, in both cases the presence of chloride affects the rate of reduction more than it does the rate of oxidation.

Figure 3.26. Effect of chloride on the reduction of guanidinated ferricytochrome c.

(+) the rate constant for overall reduction (left ordinate),
(o) the rate constant for overall oxidation (right ordinate).
Also included is the effect of chloride on reduction of
unmodified ferricytochrome c. (Δ) $k_{\text{red}}^{\text{r}}$ (left ordinate),
(\bullet) k_{ox}^{r} (right ordinate). Ionic strength, 0.196 M; pH 7.0;
temperature, 24°C. Initial concentration of gn-ferricytochrome
c was 10.5 μM , initial concentration of ferrocyanide was 1 mM.
The solid lines were drawn by eye to indicate trends.



4. ANALYSIS OF EXPERIMENTAL RESULTS AND DISCUSSION

4.1. Mechanism of electron transfer

4.1.1. Oxidation of ferrocyanochrome c

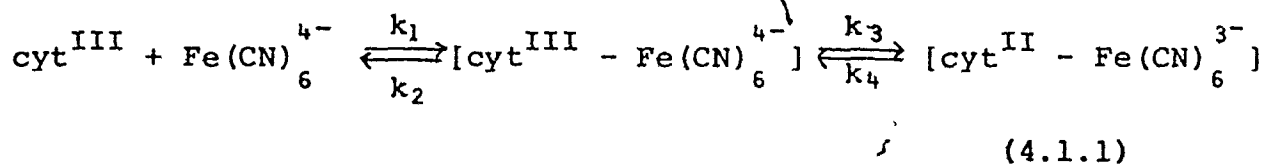
Our studies of the mechanism of the oxidation of ferrocyanochrome c by ferricyanide (section 3.2.) confirmed the previously reported results that the oxidation process follows second-order kinetics (Creutz and Sutin, 1974; Casatt and Marini, 1974). Creutz and Sutin (1974) reported a value of $1.2 \times 10^7 \text{ M}^{-1} \text{ sec}^{-1}$ for the oxidation of ferrocyanochrome c with potassium ferricyanide (phosphate buffer and sodium chloride; ionic strength 0.1 M, pH 7.2) which agrees quite well with our value of $1.3 \times 10^7 \text{ M}^{-1} \text{ sec}^{-1}$ in potassium phosphate buffer, ionic strength 0.1 M, pH 7.0.

Analysis of the ionic strength dependence of the second-order rate constant for the oxidation of ferrocyanochrome c in non-binding (tris-cacodylate) buffer (see section 4.2.1.) suggests that the oxidation of ferrocyanochrome c with ferricyanide is a diffusion-controlled reaction. This result together with the lack of any observed intermediate indicate that the reactants

exchange the electron on collision. This in turn implies that the electron on the heme iron must be easily accessible to the ferricyanide ion at the surface of the cytochrome c molecule. Inspection of the x-ray model of the cytochrome c molecule suggests the exposed heme edge as a possible electron path. This path has been previously proposed by Redfield and Gupta (1971) and was supported by the chemical modification experiments of Margoliash *et al.* (1973) and by Wada and Okunuki (1969). Further support for this pathway comes from our estimation of the area of the reaction site of ferrocytochrome c which was calculated to be 170 Å² (see section 4.2.1.). This is close to the area of 120 Å² estimated for the heme cleft by Dickerson (1968). Thus, it seems reasonable to propose that when ferricyanide is used as an electron acceptor the electron leaves the heme iron via the exposed heme edge.

4.1.2. Reduction of ferricytochrome c

Analysis of the dependence of the observed first-order rate constant for the reduction of ferricytochrome c on the concentration of ferrocyanide (section 3.3.1.) indicated that the appearance of reduced cytochrome c follows the mechanism given by expression 4.1.1:



Miller and Cusanovich (1975) proposed a similar mechanism for reduction of horse heart ferricytochrome c by ferrocyanide except that they neglected the reverse reaction in the second step (k_4 in equation 4.1.1 was assumed to be zero). In Table 2 our values¹ for K_d and k_3 are compared with values reported by Miller and Cusanovich (1975). As can be seen, the values for k_3 agree quite well and in both cases seem to be independent of the ionic strength. There are larger differences in the values for K_d . This may not be surprising because of differences in buffers and temperatures. It should be pointed out that our data indicate an increase in the dissociation constant with increasing ionic strength (consistent with Stellwagen and Cass, 1975) whereas the data of Miller and Cusanovich shows first an increase and then a decrease.

The mechanism 4.1.1 is also consistent with the reaction scheme suggested by Stellwagen and Shulman (1973b) except that they included the dissociation step of the $[\text{cyt}^{\text{II}} - \text{Fe}(\text{CN})_6^{3-}]$ complex which could not be measured in our experiments. The values for the dissociation constant K_d and for the rate constants k_3 and k_4 reported by Stellwagen and Shulman (1973b) are also included in Table 2. As can be seen our values for K_d and k_3 agree better with the results of Stellwagen and Shulman than with those of

¹ It should be emphasized that the assumption $k_2 \gg k_3$ might not be valid and the data could probably be fitted equally well assuming $k_2 \approx k_3$ or $k_3 \gg k_2$. In the case when $k_3 \gg k_2$ the following mechanism could be operative: $A + B \rightleftharpoons C \rightleftharpoons D + E$. Assumption $k_2 \gg k_3$ has as a consequence that k_1 must be larger or of the order as $10^6 \text{ M}^{-1} \text{ sec}^{-1}$.

Table 2

Kinetic Parameters ($K_d = k_2/k_1$, k_3 , k_4 , $K_d' = k_5/k_6$ and K_{eq}) for Reduction of Ferricytochrome c at Several Ionic Strengths

Ionic strength (M)	$K_d \times 10^3$ (M)	k_3 (sec ⁻¹)	k_4 (sec ⁻¹)	$K_d' \times 10^7$ (M ⁻¹)	$K_{eq} \times 10^3$
0.027 ^a	0.75	203	270	86	8.77
0.10 ^a	1.8	250	70	19.6	3.9
0.235 ^a	2.9	190	21	5.6	1.77
0.5 ^a	7.1	182	11	3.33	0.77
0.035 ^b	0.14	133	-	-	-
0.242 ^b	0.625	154	-	-	-
0.321 ^b	0.42	167	-	-	-
0.40 ^b	0.29	133	-	-	-
- ^c	2.5	208	-	-	-
- ^d	1.04	-	-	-	-
- ^d	3.2	-	-	-	-

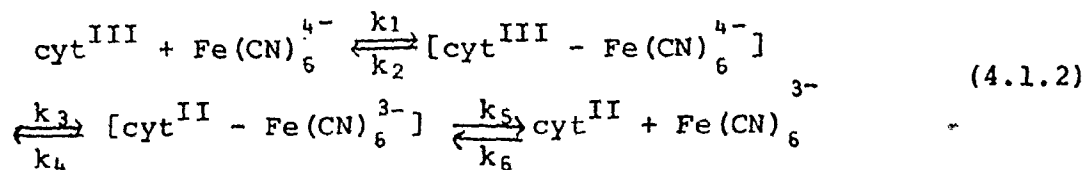
- a This work. Buffer, tris-cacodylate; pH 7.0, temperature, 24°C.
- b Miller and Cusanovich (1975). Buffer, 0.02 M potassium phosphate supplemented with NaCl; pH 7.0; 20°C.
- c Stellwagen and Shulman (1973b). Ionic strength not reported; temperature, 25°C.
- d Stellwagen and Cass (1975). Ionic strength not reported; pH 7.0, temperature, 25°C

The authors reported two different binding sites.

Miller and Cusanovich. However, there is a large disagreement between our value for the rate constant k_3 and the value determined by Stellwagen and Shulman. The latter determined the rate constant k_4 by measuring the effect of ferricyanide on the broadening of the NMR line due to ferrocytochrome c (in presence of excess ferrocyanide to keep cytochrome c reduced). Thus, the value for k_4 was determined by studying the reverse reaction, i.e. the oxidation of ferrocytochrome c. The discrepancy can, therefore, be resolved by assuming different pathways for the oxidation and reduction of cytochrome c by iron hexacyanides (see below).

Further support for the complexing of ferrocyanide by ferricytochrome c came from the equilibrium dialysis studies by Stellwagen and Cass (1975). It was observed that horse heart ferricytochrome c bound ferrocyanide ions at two non-equivalent binding sites (see Table 2). The values determined by the equilibrium dialysis measurements are comparable to the values determined by NMR (Stellwagen and Shulman, 1973b) and by stopped-flow measurements.

If one combines the measurements of the apparent equilibrium constant (section 3.1) with the stopped-flow measurements one can determine the dissociation constant ($K_d = k_5/k_6$) for the $[\text{cyt}^{\text{II}} - \text{Fe}(\text{CN})_6^{3-}]$ complex in the mechanism:



The apparent equilibrium constant for the above mechanism is:

$$K_{eq} = (k_1 k_3 k_5) / (k_2 k_4 k_6) \quad (4.1.3)$$

Since the ratios k_1/k_2 , k_3/k_4 and K_{eq} are known (Table 2) one can calculate $K_d^1 = k_5/k_6$ (Table 2). The low values we obtain for K_d^1 indicate that the equilibrium of this step strongly favors the formation of the ferricyanide-ferrocyanochrome c complex. Thus, in the reduction of ferricytochrome c the last step (dissociation of the ferricyanide-ferrocyanochrome c complex) is unfavorable. This is consistent with our neglecting the last step in the analysis of k_{obs} vs $Fe(CN)_6^{4-}$ (section 3.3.1.).

Our results on the reduction of ferricytochrome c by ferrocyanide indicate that the mechanism of reduction markedly differs from the mechanism observed for the oxidation of ferrocyanochrome c by ferricyanide. This difference can be resolved by assuming different pathways for the electron in reduction and oxidation. The following observations support this hypothesis.

First, the second-order rate constant for oxidation of ferrocyanochrome c was unaffected when ferrocyanide was present in the reaction mixture (section 3.2.3.4.). On the other hand, the reverse reaction (reduction of ferricytochrome c) was slowed by increasing concentrations of ferrocyanide (section 3.3.2.). Thus the effect of

ferrocyanide on the second-order rate constant for reduction indicated complex formation, while the data for oxidation did not. Since the bound ferrocyanide ion does not interfere with the oxidation of ferrocytochrome c, but does interfere with the reduction of ferricytochrome c, different paths for the electron may exist.

Second, if the electron transfer to and from the heme iron takes place along the same path (the heme edge, for example) one should be able to predict the reaction rates using the theory developed by Marcus (Creutz and Sutin, 1974). According to this (Marcus, 1955; 1959; 1963), the rate for oxidation of ferrocytochrome c can be expressed:

$$k_{\text{ox}} = (k_{11} k_{22} K_{\text{eq}})^{\frac{1}{2}} \quad (4.1.4)$$

where k_{11} is the self-exchange rate constant for ferri-cytochrome-ferrocycytochrome c, k_{22} the self-exchange rate constant for ferricyanide-ferrocyanide and K_{eq} the equilibrium constant for the iron hexacyanide-cytochrome c system. With $k_{11} = 0.5 \times 10^3 \text{ M}^{-1} \text{ sec}^{-1}$ (Gupta *et al.*, 1972), $k_{22} = 9.6 \times 10^3 \text{ M}^{-1} \text{ sec}^{-1}$ (Campion *et al.*, 1967) and $K_{\text{eq}} = 316$ ($I = 0.1 \text{ M}$) estimated from the present equilibrium measurements, the calculated value for k_{ox} is $3.9 \times 10^4 \text{ M}^{-1} \text{ sec}^{-1}$. This is 500 times smaller than the measured value of $2.3 \times 10^7 \text{ M}^{-1} \text{ sec}^{-1}$. Creutz and Sutin (1974) proposed that specific anion effects could enhance the rate of electron transfer. As shown in the experimental section

the effects of anions on both reduction and oxidation of cytochrome c are not very large and furthermore, we observed that the presence of ions slows down the electron transfer rather than enhances it. The discrepancy between the experimental and calculated values could, however, be accounted for by assuming two different electron pathways for reduction and oxidation.

Third, with the aim of elucidating the hexacyanide binding sites, Stellwagen and Cass (1975) carried out combined equilibrium dialysis and chemical modification studies of the binding of hexacyanides to cytochrome c. On the basis of their results they proposed that lysine 79 and nearby lysines 13 and 27 (and perhaps lysine 25) form a binding site for hexacyanides. This would place iron hexacyanides near the exposed heme edge and as a result the electron would probably reach the heme iron through the thioether bridge of cysteine 17. However, Power *et al.* (1975) found this hypothesis inconsistent with the role of the lysine 79 residue in the alkaline isomerization. The alkaline conformational transition of cytochrome c involves the replacement of the heme ligand methionine 80 with lysine 79 at alkaline pH ($pK_a \sim 9$) (Wilgus and Stellwagen, 1974). If the binding of iron hexacyanides were to occur at lysine 79, they should shift the pK_a of the transition at least one pH unit higher and this was not observed (Power *et al.*, 1975). As concluded by Power

et al. (1975) the identification of the hexacyanide binding sites is still uncertain, but it seems that the binding might not occur in the vicinity of the heme edge where we have postulated electron flow.

4.2. Involvement of electric charges on cytochrome in electron transfer

4.2.1. Effect of ionic strength on oxidation

The effect of the ionic strength on the reaction rate can be theoretically treated in terms of Debye-Huckel theory. Debye and Huckel proposed the following semi-empirical equation to describe the relation between the activity coefficient of an ion (γ_i) and the ionic strength (I) (Frost and Pearson, 1961a).

$$-\log \gamma_i = \frac{z_i^2 A \sqrt{I}}{1 + B a_i \sqrt{I}} \quad (4.2.1)$$

where z_i is the charge of the i -th ion, a_i is the distance of the closest approach of an ion to the i -th ion (in cm) and A and B are two constants with values (at 25°C for aqueous solution); $A = 0.509 \text{ (M}^{-\frac{1}{2}})$, $B = 0.329 \times 10^{-8} \text{ (M}^{-\frac{1}{2}} \text{ cm}^{-1})$. The reaction rate is related to the activity coefficients by the following expression (Frost and Pearson, 1961b)

$$k = k_0 \frac{\gamma_A \gamma_B}{\gamma_{A:B}} \quad (4.2.2)$$

where k_0 is the rate constant at infinite dilution, $\gamma_A \gamma_B$ and $\gamma_{A:B}$ are the activity coefficients of reactants A, B and the activated complex formed by the reactants A and B, respectively. Combining the equations 4.2.1 and 4.2.2 and assuming a mean value a for the distance of closest approach, one can derive the expression for the dependence of the rate constant on the ionic strength (Frost and Pearson, 1961b)

$$\log k = \log k_0 + \frac{2 Z_A Z_B a \sqrt{I}}{1 + B a \sqrt{I}} \quad (4.2.3)$$

Inserting known values into the equation 4.2.3 and assuming a mean value of closest approach for iron hexacyanide-cytochrome c of 18.5 Å (Schejter and Margalit, 1970) one obtains:

$$\log k = \log k_0 + 1.018 Z_A Z_B f(I) \quad (4.2.4)$$

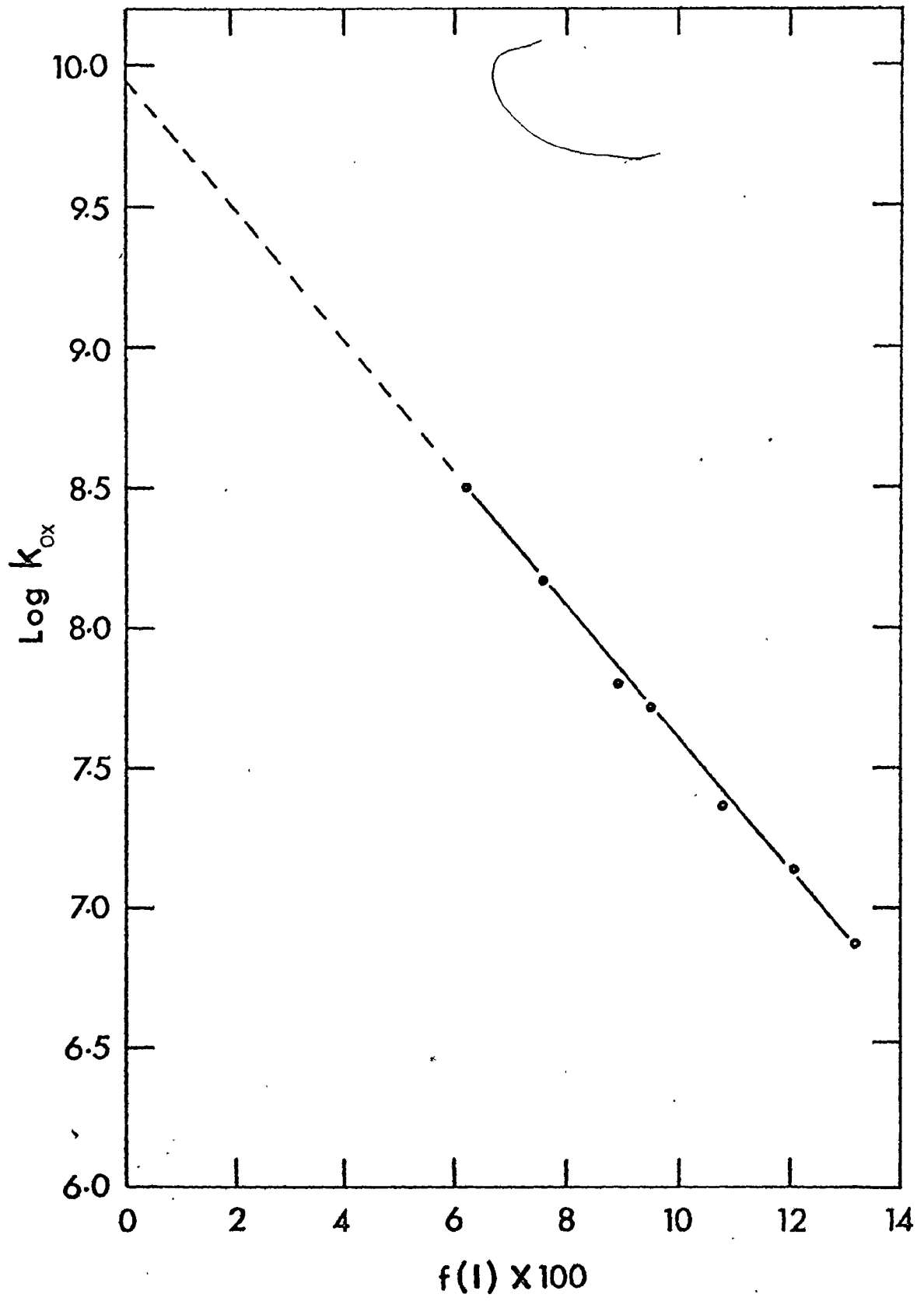
where $f(I)$ is defined:

$$f(I) \approx \frac{\sqrt{I}}{1 + 6 \sqrt{I}} \quad (4.2.5)$$

The ionic strength dependence of the rate constant for the oxidation of horse heart ferrocyanochrome c is plotted as a function of $f(I)$ in Figure 4.1. The value of the second-order rate constant (k_0) obtained from the extrapolation of the straight line to zero ionic strength

Figure 4.1. Variation of $\log k_{ox}$ vs $f(I) = \sqrt{I}/(1 + 6\sqrt{I})$
for horse heart cytochrome c.

The experimental values for k_{ox} are from Figure 3.8.
Buffer, tris-cacodylate; pH 7.0; temperature 24°C. The
straight line was drawn by eye.



was estimated to be $9^{12} \times 10^9 \text{ M}^{-1} \text{ sec}^{-1}$. This value is close to the value for a bimolecular diffusion-controlled reaction of $10^{10} \text{ M}^{-1} \text{ sec}^{-1}$ (North, 1966). The rate constant for a bimolecular diffusion-controlled reaction, without taking into account the electrostatic interactions, can be calculated using equation 4.2.6 (Alberty and Hammes, 1958):

$$k_o = \frac{4\pi N}{1000} (R_A + R_B) (D_A + D_B) \quad (4.2.6)$$

where N is the Avogadro's number, R_A, R_B are the radii of the reacting molecules and D_A, D_B the diffusion coefficients of reactants A and B, respectively. Ehrenberg and Paleus (1955) reported a diffusion coefficient for cytochrome c of $9.5 \times 10^{-7} \text{ cm}^2 \text{ sec}^{-1}$. Since the value of the diffusion coefficient for potassium ferricyanide was not known to us, the value for potassium ferrocyanide of $1.2 \times 10^{-5} \text{ cm}^2 \text{ sec}^{-1}$ (Handbook of Chemistry and Physics, Chemical Rubber Co., Cleveland, Ohio) was used for this calculation. This is a good approximation since the diffusion coefficient varies only slightly ($M^{-1/3}$) with the molecular weight. The value for $R_A + R_B$ was estimated before (18.5 Å). Inserting the experimental values into the equation 4.2.6 the value of $1.8 \times 10^{10} \text{ M}^{-1} \text{ sec}^{-1}$ was estimated for the rate constant of the bimolecular diffusion-controlled reaction between ferricyanide and ferrocytochrome c.

To take into account the effect of electrostatic interactions one has to multiply equation 4.2.6 by a

factor which has been theoretically derived by Alberty and Hammes (1958):

$$F = \frac{L/(R_A + R_B)}{\exp(L/(R_A + R_B)) - 1} \quad (4.2.7)$$

where $L = Z_A Z_B e^2 / \epsilon kT$; e being the electronic charge, ϵ the dielectric constant of the medium, k is Boltzmann's constant and T the temperature. The factor F is greater than 1 if two oppositely charged molecules interact and less than 1 if two similarly charged molecules interact. Assuming the charge on ferricyanide -3, the charge on ferrocyanochrome c +7.8 (see below), ϵ of water 80, the factor F was estimated to be 9. Thus, including the electrostatic interactions between ferricyanide and ferrocyanochrome c the estimated value for the biomolecular diffusion-controlled reaction is $16.2 \times 10^{10} \text{ M}^{-1} \text{ sec}^{-1}$. If we assume a total surface area of cytochrome c molecule of 3000 \AA^2 (Beetlstone, 1960) the reaction area (R.A.) on cytochrome c can be determined:

$$\text{R.A.} = 9.1^2 \times 10^9 \times 3000 \text{ \AA}^2 / 16.2 \times 10^{10} = 168 \text{ \AA}^2 \approx 170 \text{ \AA}^2$$

This value fairly well agrees with the surface area of the heme cleft (120 \AA^2) reported by Dickerson (1968).

The energy of activation for most diffusion-controlled reactions is found to be less than 3 kcal/mole (North, 1966). The energy of activation for the oxidation of ferrocyanochrome c by ferricyanide was measured by Morton *et al.* (1971) and

Cassatt and Marini (1974). Morton *et al.* (1971) observed that the oxidation of ferrocyanochrome c by ferricyanide was temperature independent and therefore the energy of activation was zero, whereas Cassatt and Marini (1974) estimated a value of 1.7 kcal/mole. These low values for the energy of activation would indicate that the oxidation of ferrocyanochrome c by ferricyanide is a diffusion controlled reaction, in agreement with our calculations.

From the slope of the curve in Figure 4.1, one can determine the effective charge on the region of horse heart ferrocyanochrome c involved in electron transfer. Assuming -3 for the charge of the ferricyanide ion, a value of +7.8 was determined for the effective charge on horse heart ferrocyanochrome c (pH 7.0). This value agrees with the value of 7-8 reported by Margoliash and Schejter (1966) for the total protein charge. From this one can conclude that most of the charges on the ferrocyanochrome c are involved in electrostatic interactions between ferricyanide and ferrocyanochrome c. It should be noted that the value for the closest approach is only estimated and if it is varied the slope of the curve and the effective charge will be changed as well. For example, if the mean value of the closest approach is increased to 20 Å, the effective charge on the protein would also increase to 8.5. Thus, the value for the effective charge

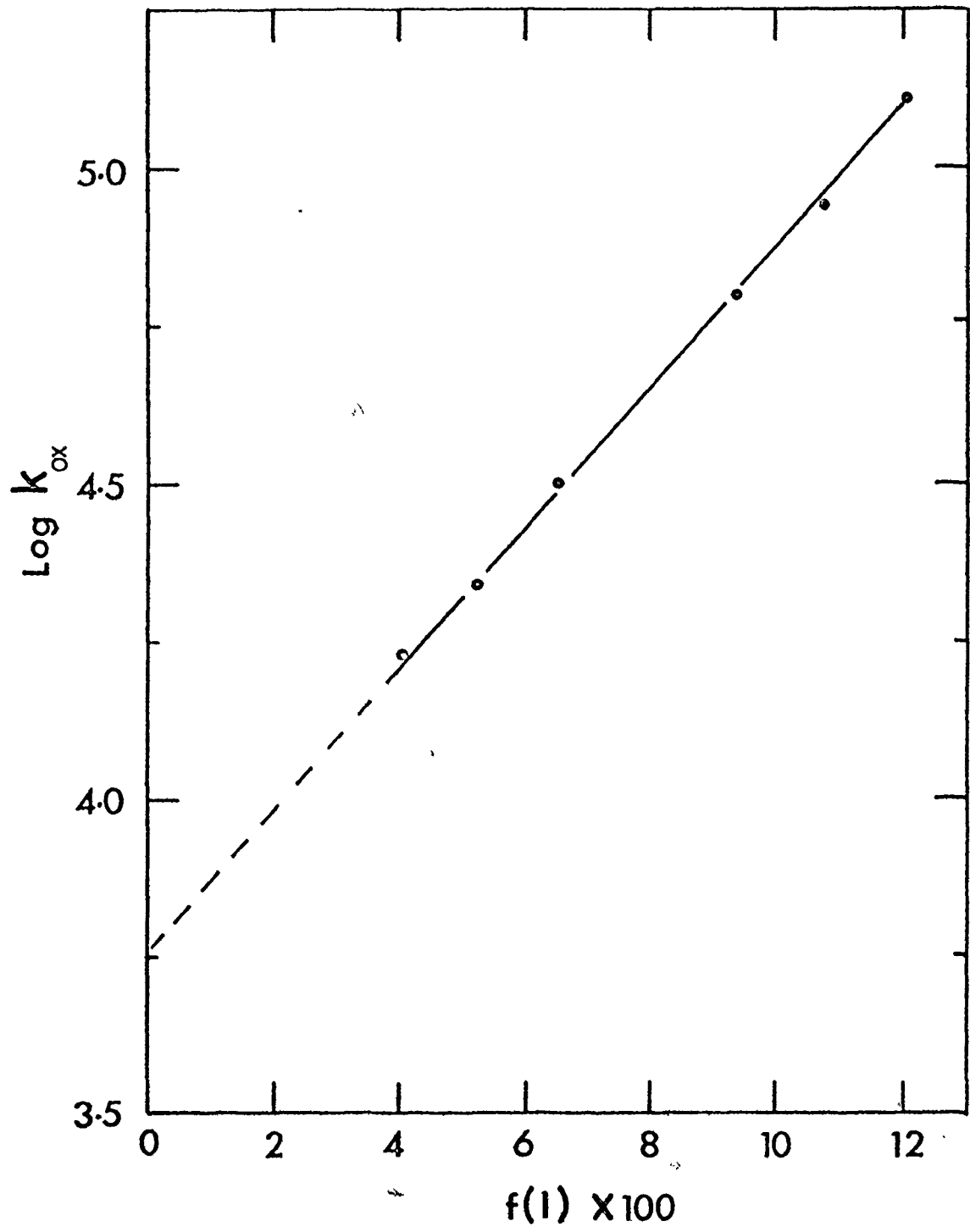
on horse heart ferrocytochrome c reported above should be taken only as an estimate and not as an exact value.

The rate of the electron transfer between *Pseudomonas aeruginosa* ferrocytochrome c and ferricyanide was also found to depend on the ionic strength. When the ionic strength dependence of the rate constant for oxidation of *Pseudomonas* ferrocytochrome c is replotted against the function $f(I)$ (equation 4.2.5) a straight line is obtained (Figure 4.2). The negative slope of the straight line indicates that the reacting molecules are similarly charged. From the extrapolation of the curve to zero ionic strength a value for k_0 of $5.75 \times 10^3 \text{ M}^{-1} \text{ sec}^{-1}$ was estimated. This is almost seven orders of magnitude smaller than the value of k_0 for horse heart cytochrome c.

Since the diffusion constant of cPs is almost the same as that of cHo (Hario *et al.* 1960) we can assume that except for the electrostatic effect, the ferricyanide ion collides with *Pseudomonas* cytochrome c at the same rate as it does with cHo ($1.8 \times 10^{10} \text{ M}^{-1} \text{ sec}^{-1}$). Due to the electrostatic repulsion between similarly charged ions the above value should be multiplied by $F = 0.05$ (the charge on cPs^{II} was taken as -3.7 , see below), giving the calculated value for the rate constant of a bimolecular diffusion-controlled reaction of $9 \times 10^8 \text{ M}^{-1} \text{ sec}^{-1}$. This value is much higher than the measured value. If this reaction is diffusion-controlled the probability

Figure 4.2. Variation of $\log k_{ox}$ vs $f(I) = \frac{\sqrt{I}}{1 + 6\sqrt{I}}$
for *P. aeruginosa* cytochrome c.

The experimental values for k_{ox} are from Figure 3.8.
Buffer, tris-cacodylate, pH 7.0; temperature, 24°C. The
straight line was drawn by eye.



that one collision will result in successful reaction is very low ($\sim 10^{-5}$). Since the heme group of cPs is identical with the heme group in cHo (Dickerson, 1971b) the large difference in k_o for cHo and cPs can be interpreted in terms of the involvement of the polypeptide chain in the electron transfer. Gupta (1973) observed a ten-fold difference between the rate of electron transfer for reduced-oxidized horse heart cytochrome c and reduced-oxidized *Candida krusei* cytochrome c. He attributed this difference to the different role of the polypeptide chains in the two proteins. We also assume that the different polypeptide chains of cHo and cPs form active sites of different activities although the mechanism is not yet clear.

From the slope of the curve the effective charge on cPs was found to be -3.7. Studies of the amino acid composition of *Pseudomonas* cytochrome c showed that the molecule should have a net charge of about -9 at pH 7.0 (Ambler, 1963a; Fanger *et al.*, 1967). The difference between the value for the effective charge obtained by the ionic strength dependence measurement and the net charge could be accounted for by the distribution of negative charges on the *Pseudomonas* cytochrome c molecule. The segment of the polypeptide chain that runs along the left edge of the heme crevice (amino acid residues 70 to 80) is highly charged in horse heart cytochrome c (three

out of ten amino acids are lysines), whereas the corresponding segment in *Pseudomonas* cytochrome c residues (51 to 61) contains only uncharged amino acids (Ambler, 1963b). This suggests that the "active site" and its proximity in *Ps* cytochrome c is less charged than the corresponding region in horse heart cytochrome c and that electrostatic interactions between ferricyanide and cPs^{II} are mainly due to charges distributed away from the active site.

It is difficult to explain the unusual dependence of the oxidation rate constant of *Micrococcus* ferrocyclochrome c on ionic strength. As mentioned before, there is ample evidence that the electrostatic interactions play an important role in the electron transfer. Despite its negative charge *Micrococcus* cytochrome c rapidly reacts with mammalian cytochrome oxidase (Smith *et al.*, 1966) which oxidizes basic mammalian cytochrome c. Smith *et al.* (1966) proposed that the electrostatic interactions involve not overall but localized charge on the cytochrome c molecule. The ionic strength dependence observed in this work could be explained by assuming two ionic strength dependent conformations of bacterial cytochrome c with different transfer properties. The two conformations would possess a different effective charge at the "active site": a positive charge when $I \gtrsim 0.015$ and a negative charge for $0 \lesssim I < 0.015$. Thus far we have no evidence that two ionic strength dependent conformations exist.

Since the ionic strength dependence of the oxidation of cMd^{II} by ferricyanide was measured using only a single preparation, these experiments must be repeated before any definite conclusion about the ionic strength dependence is drawn.

4.2.2. Effect of ionic strength on reduction

The effect of the ionic strength on the reduction of ferricytochrome c is more complex than its effect on oxidation. Data in Table 2 suggest that ionic strength has a large effect on the binding constant of ferrocyanide to ferricytochrome c. Decreasing the ionic strength increased the calculated association constant K_a ($K_a = 1/K_d$), a result which was also observed by Stellwagen and Cass (1975) using equilibrium dialysis. As pointed out by these authors, binding is determined by electrostatic interactions between ferrocyanide and ferricytochrome c. At higher ionic strengths the positively charged groups are more effectively shielded by counterions from the solution and as a result the binding of ferrocyanide is decreased. Once the complex is formed, the rate of the electron transfer to the heme iron (k_3) does not seem to be affected by ionic strength (Table 2). The reverse reaction (k_4) proceeds faster when a stronger complex between ferrocyanide and ferricytochrome c is formed.

The combined effects of ionic strength on the rate constant k_4 and on the association constant K_a govern the ionic strength dependence of k_{obs} as presented in Figure 3.19. Equation 3.3.3 states that the observed first-order rate constant varies with the substrate (ferrocyanide) concentration as well. For this reason k_{obs} vs \sqrt{I} was plotted at constant ferrocyanide concentration (Figure 3.19). Increasing the ionic strength of the medium decreases the observed first-order rate constant indicating that the reacting species are oppositely charged. The dissociation of the ferricyanide-ferrocytochrome c complex is again an ionic strength dependent process. Higher ionic strengths stabilize the complex between the reduced protein and ferricyanide (Table 2).

If we combine the effects of the ionic strength on all three steps we get the effect of ionic strength on the apparent equilibrium constant which can be measured independently. From the results presented in section 3.1 it is apparent that in the range of ionic strength from 0.05 M to 0.2 M the dependence of the apparent equilibrium constant on the ionic strength can be fitted to the Debye-Huckel theory. At ionic strengths higher than 0.2 M the linear relationship between $\log K_{eq}$ and $f(I)$ no longer exists. This may be due to interactions between the reacting molecules and the ions (tris, cacodylate) in solution. The reduction potential determined from the

extrapolation of the linear portion of the curve to zero ionic strength yields a value which is higher than previously reported. We attributed the higher value to the use of electro dialyzed cytochrome c from which ferricyanide and other ions presumably present in previously examined specimens have been removed.

4.3. Specific ion effects on electron transfer

4.3.1. Effects of ions on oxidation

The experimental results discussed in section 3.2.3 lead to the conclusion that the rate of electron transfer (k_{ox}^i) by ferrocyanochrome c, in the presence of any of the binding ions studied, is less than that for free cytochrome c (k_{ox}^f) prepared in non-binding tris-cacodylate buffer. The object of this section is to interpret the effect of ions on the rate of oxidation of ferrocyanochrome c. We attempted to derive from the experimental data the number of ions bound per cytochrome c molecule and the respective association constants assuming a simple, cooperative model.

The rate of appearance of ferricytochrome c when the mixture of free and liganded ferrocyanochrome c is present in the reaction mixture can be described by the following equation:

$$\frac{d(\text{cyt}^{\text{III}})}{dt} = \left\{ k_{\text{ox}}^{\text{f}} (\text{cyt}_{\text{f}}^{\text{II}}) + k_{\text{ox}}^{\text{i}} (\text{cyt}_{\text{i}}^{\text{II}}) \right\} (\text{Fe}^{\text{III}}) \quad (4.3.1)$$

where $(\text{cyt}_{\text{f}}^{\text{II}})$ and $(\text{cyt}_{\text{i}}^{\text{II}})$ represent the concentrations of free and liganded ferrocytochrome c and (Fe^{III}) is the concentration of ferricyanide (the initial concentration was held constant). We assume that the concentration of liganded ferrocytochrome c is proportional to the concentration of free ferrocytochrome c

$$(\text{cyt}_{\text{i}}^{\text{II}}) = X(i) (\text{cyt}_{\text{f}}^{\text{II}}) \quad (4.3.2)$$

where the function $X(i)$ depends on the equilibrium between liganded ferrocytochrome c and free ferrocytochrome c.

(The function $X(i)$ will be defined below.) The total concentration of ferrocytochrome c is:

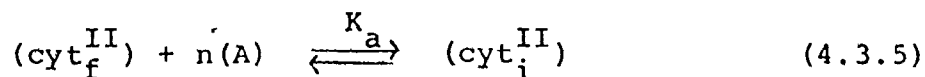
$$(\text{cyt}^{\text{II}}) = (\text{cyt}_{\text{f}}^{\text{II}}) + (\text{cyt}_{\text{i}}^{\text{II}}) \quad (4.3.3)$$

If we combine equations 4.3.4, 4.3.2 and 4.3.1 we obtain

$$\frac{d(\text{cyt}^{\text{III}})}{dt} = [(k_{\text{ox}}^{\text{f}} + k_{\text{ox}}^{\text{i}} X(i)) / (1 + X(i))] (\text{cyt}^{\text{II}}) (\text{Fe}^{\text{III}}) \quad (4.3.4)$$

The quantity in the square bracket (equation 4.3.4) will be the apparent (ie. measured) rate constant for the oxidation of the mixture of liganded and free ferrocytochrome c (k_{ox}). The function $X(i)$ can be derived by assuming a rapid equilibrium between free and liganded ferrocytochrome

c



The expression 4.3.5 assumes that n ions (A) bind cooperatively to cyt_f^{II} . This assumption may not be justified (in which case X is a more complicated function of A), but the data available would not seem to require a more complex treatment. Furthermore, this analysis assumes only two types of molecules cyt_i^{II} and cyt_f^{II} which react with ferricyanide at two different rates k_{ox}^i and k_{ox}^f . More complex treatments with additional forms are a possibility. The association constant of equation 4.3.5 can be expressed

$$K_a = \frac{(\text{cyt}_i^{\text{II}})}{(\text{cyt}_f^{\text{II}})(A)^n} \quad (4.3.6)$$

Therefore, the function $X(i)$ is given by:

$$X(i) = K_a (A)^n \quad (4.3.7)$$

Substituting equation 4.3.7 into equation 4.3.4 gives the apparent rate constant of oxidation at various ionic concentrations (but constant ionic strength):

$$k_{\text{ox}} = \left[k_{\text{ox}}^f + k_{\text{ox}}^i K_a (A)^n \right] / (1 + K_a (A)^n) \quad (4.3.8)$$

If we define $k_{\text{ox}}^i / k_{\text{ox}}^f = C$, equation 4.3.8 can be expressed as equation 4.3.9:

$$K_a (A)^n = \frac{1 - k_{\text{ox}}/k_{\text{ox}}^f}{k_{\text{ox}}/k_{\text{ox}}^f - C} \quad (4.3.9)$$

The function on the right of 4.3.9 will be defined as $H(k_{\text{ox}})$. The values for k_{ox}^{f} and k_{ox}^{i} can be estimated by measuring the rate constant for oxidation when $A \rightarrow 0$ and $A \rightarrow \infty$, respectively. The value of k_{ox}^{f} was obtained by measuring the rate of oxidation of ferrocyanide in non-binding (tris-cacodylate) buffer. With constant ionic strength, we could not obtain the condition $A \rightarrow \infty$, and therefore values for k_{ox}^{i} 's were obtained by "hand" extrapolation of the experimental curves to $A \rightarrow \infty$. (See Figures 3.10 A,B and 3.13.) The values of $7.5 \times 10^6 \text{ M}^{-1} \text{ sec}^{-1}$, $6 \times 10^6 \text{ M}^{-1} \text{ sec}^{-1}$ and $8.8 \times 10^6 \text{ M}^{-1} \text{ sec}^{-1}$ for k_{ox}^{i} were obtained for chloride, phosphate and potassium, respectively. This procedure is inaccurate and somewhat arbitrary, but fortunately the value for k_{ox}^{i} does not markedly affect the values for n and K_{a} . (For example; assuming $k_{\text{ox}}^{\text{i}} = 7.0 \times 10^6 \text{ M}^{-1} \text{ sec}^{-1}$ for chloride, the value for n will change less than 10% and the value for K_{a} less than 40%). The value for k_{ox}^{i} of 1×10^6 for picrate was estimated similarly (Figure 3.11). Since the value of k_{ox}^{i} for chloride at $I = 0.0485 \text{ M}$ could not be estimated with any confidence the analysis of it at this ionic strength was omitted. If we plot $\log H(k_{\text{ox}})$ vs $\log (A)$, values for n and K_{a} can be estimated. Such plots for picrate ($I = 0.0485 \text{ M}$), phosphate, chloride and potassium (all $I = 0.194 \text{ M}$) are presented in Figure 4.3. The values for n and K_{a} estimated from these are given in Table 3.

Figure 4.3. Plot of $\log H(k_{Ox})$ vs $\log (A)$ for chloride (o), phosphate (+), potassium (Δ) and picrate (Δ).

The solid lines were drawn with emphasis on the rate constants at intermediate concentrations since at limiting concentrations (e.g. points at $\log (A) \approx -2$) small errors cause large deviations.

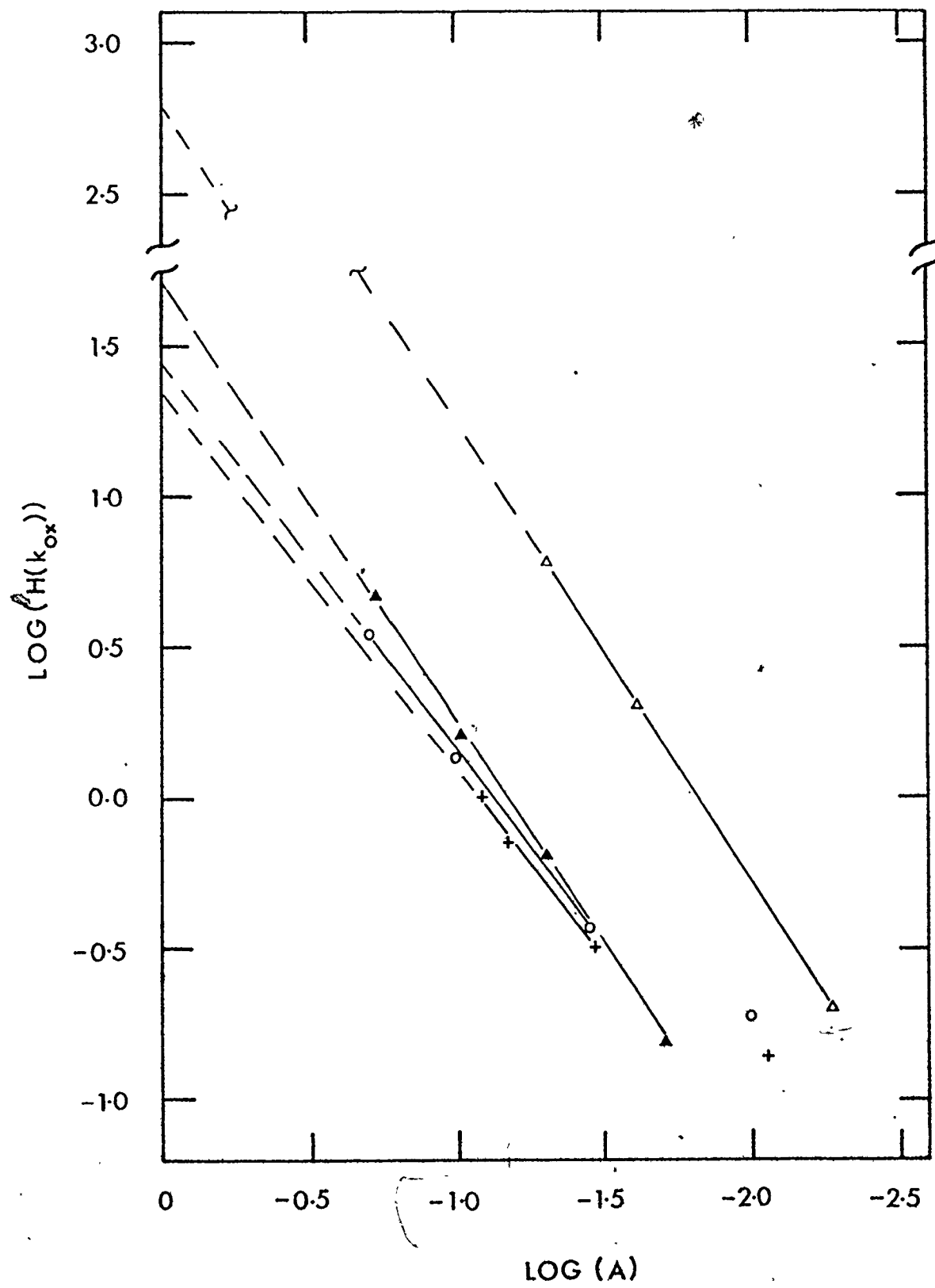


Table 3

The Number of Ions Bound to cyt^{II} (n) and Their Association Constants (K_a) as Estimated from Plots (Figure 4.3) Based on Measured Oxidation Rate Constants

Ion	Ionic strength (M)	n	K_a (M^{-1})	k_{Ox}^i ($M^{-1} \text{ sec}^{-1}$)
Picrate	0.0485	1.52	630.	1×10^6
Phosphate	0.194	1.24	21.8	6×10^6
Chloride	0.194	1.28	27.5	7.5×10^6
Potassium	0.194	1.5	50.1	8.8×10^6

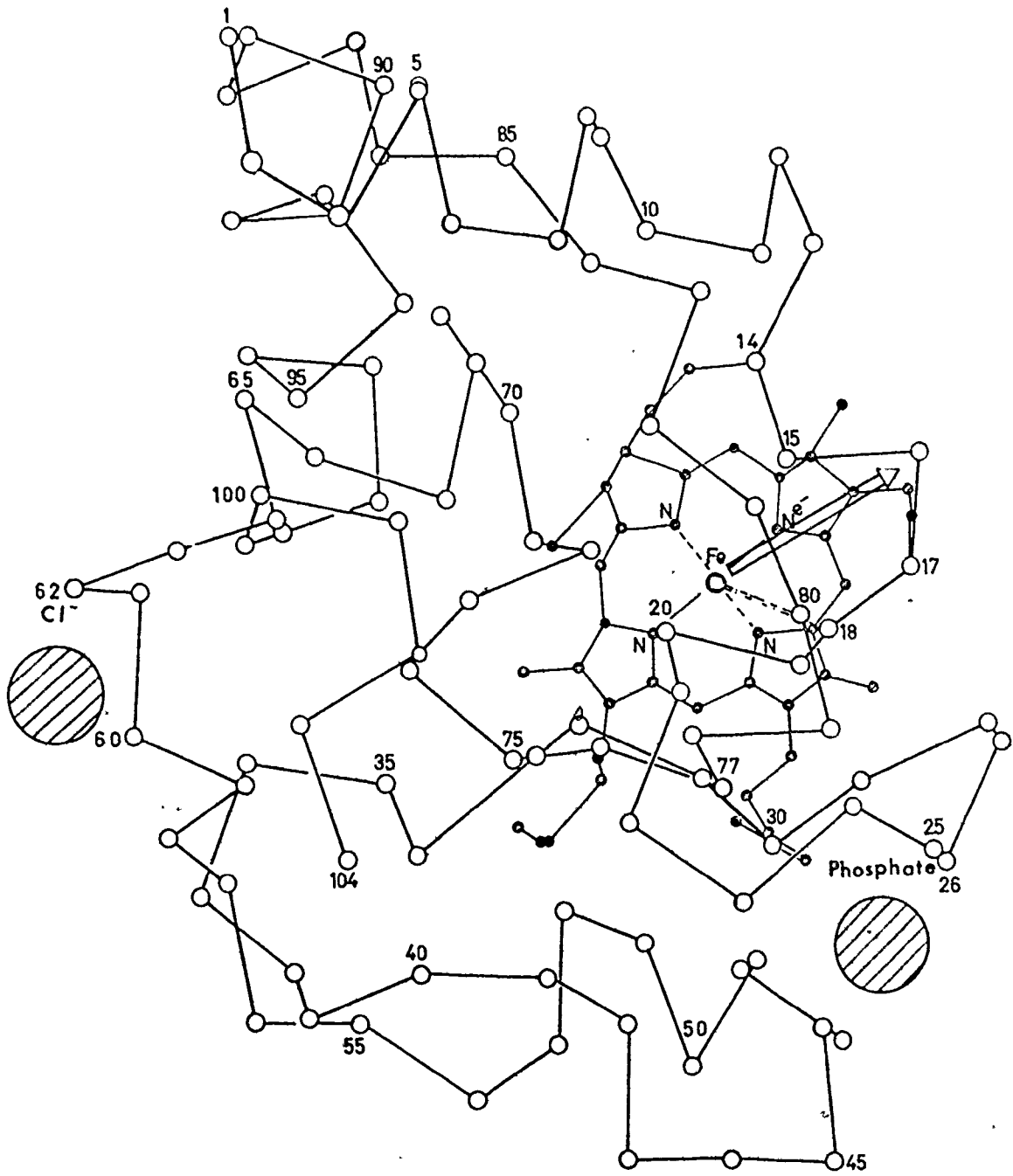
The results are subject to large errors, although the values in Table 3 were successfully used to calculate (equation 4.3.8) the curves through the experimental points in Figures 3.10, 3.11 and 3.13. They suggest that an average of more than one picrate, chloride, phosphate or potassium ion are associated with reduced cytochrome under the conditions of our experiment.

As noted in the Introduction (section 1.4), Stellwagen and Shulman (1973a) tentatively identified the site of the interaction of phosphate with ferrocyclochrome c. They suggested that a phosphate ion bound in the vicinity of histidine 26 which is a residue easily accessible to the solvent. Phosphate strongly affects the exchange rate of the imidazole amino proton of histidine 26, probably by perturbing the hydrogen bond between histidine 26 and carbonyl group of aspartic acid 31. The experiments by Stellwagen and Shulman (1973a) also suggested that chloride specifically interacts with ferrocyclochrome c by weakening the hydrogen bond between the ϵ -amino proton of lysine 60 and the carboxylate group of glutamic acid 62. The resonance line assigned to the ϵ -amino proton of lysine 60 was shifted by protons and also by negative ions like bromide and iodide. The binding sites for picrate and potassium have not been identified thus far.

An attempt will be made to explain the mechanism by which the bound ions affect the electron transfer to ferrocytochrome c. The explanation is based on observations by Fridovich (1963). In this discussion, we shall assume that the effect of ions on the rate of oxidation is due to the binding of phosphate and chloride at the sites proposed by Stellwagen and Shulman (1973a). Examination of the x-ray model of cytochrome c proposed by Dickerson *et al.* (1971) indicates that binding sites for both chloride and phosphate are located on the surface of the molecule far from the heme iron (Figure 4.4). The distances between the binding sites for chloride and phosphate, and the heme iron are of the order of 18 Å and 11 Å, respectively.

Distant effects of anions were previously interpreted by Fridovich (1963). Studies of the anion inhibition of acetoacetic decarboxylase led Fridovich to conclude that when an anion interacts with a binding site on the surface of the protein, disruption (rearrangement) of the hydration shell near the binding site occurs. This rearrangement of the hydration shell can induce either changes in the hydrogen bond network on the surface of the protein molecule or minor conformational changes near the binding site or both. The perturbation of the surface hydrogen bond(s) can be transmitted to another part of the protein (e.g. the iron atom in the case of


Figure 4.4. Assumed location of binding sites for chloride and phosphate on cytochrome c.



cytochrome c) through a hydrogen bond chain. Tanaka *et al.* (1975) proposed a hydrogen bond chain connecting glutamic acid 44 and histidine 18 which may play a role in enzymatic activity of cytochrome. This chain includes histidine 26 which is part of the binding site of phosphate. Tanaka *et al.* (1975) proposed that the perturbation induced by the binding of phosphate could be transmitted to the iron atom through the proposed hydrogen bond chain. We do not know of any proposed hydrogen bond chain that would transmit the perturbation due to chloride binding.

Binding of an ion is frequently followed by minor conformational changes near the binding site (for a review see Gurd, 1970). However, we do not know of any evidence such as differences in ORD, CD and absorption spectra, or changes in viscosity which would indicate that conformational changes of ferrocyanochrome c occur as a result of binding. Thus we can only speculate that distant binding of ions could have an indirect effect on the electron transport properties of cytochrome c.

There are three lines of evidence suggesting that the above model can be applied to interpret our data. First, the binding sites for phosphate and chloride are located on the surface of the molecule which is necessary if binding is to change the hydration shell of ferrocyanochrome c. Second, according to Fridovich (1963) both anions and cations should show similar effects. The



results for chloride, phosphate and potassium in Table 3 are in agreement with this statement. Third, if the hydration shell has an effect on the activity of the protein, then different solvents will affect the activity differently (Fridovich, 1963). When H₂O was replaced by D₂O the rate of oxidation of ferrocytochrome c was reduced by a factor of two (section 3.4.).

4.3.2. Effects of ions on reduction

The effects of ions on the reduction of ferricytochrome c by ferrocyanide will be discussed in terms of the equilibrium constants defined by equation 2.7.2.

Phosphate decreases both oxidation and reduction rates about equally (Figure 3.21), thus leaving the reduction potential unchanged. This is consistent with the results of electrophoretic measurements (Margoliash *et al.*, 1970) which showed that phosphate bound to both forms of cytochrome c. We conclude that phosphate not only binds to the same extent to both forms of cytochrome c, but affects the rate approximately equally in both forms.

Chloride and picrate, on the other hand, decrease the overall reduction rate much more than the overall oxidation rate. These two ions therefore interact differently with the two forms of cytochrome c. Chloride

(Stellwagen and Shulman, 1973; Margoliash *et al.*, 1970) and picrate (section 3.2.3.3. and 3.3.3.2.) bind to both forms of cytochrome c. We may assume that they bind with different affinities to different forms of cytochrome c so that in the range of concentrations used one form had substantially more ions bound.

To estimate the number of binding sites and their association constants for chloride and picrate the method developed by Palcic (1972) and Schejter and Margalit (1970) was used. If we define $K_{ap} = k_{ox}^r / k_{red}^r$ we can write (Palcic, 1972; Schejter and Margalit, 1970):

$$\frac{K_{ap} - K_{ap}^0}{K_{ap}^0} = K_a (A)^n \quad (4.3.11)$$

where K_{ap}^0 is the value of k_{ox}^r / k_{red}^r measured in non-binding buffer, K_a is the association constant and n the number of anions (A) bound per cytochrome c molecule. Again it is assumed that anions bind cooperatively to cytochrome c. If one plots $\log (K_{ap} - K_{ap}^0)$ vs $\log (A)$ (a Hill plot) one can estimate the number of binding sites and the association constants. Figure 4.5 shows Hill plots for picrate ($I = 0.0485$ M) and chloride at two ionic strengths ($I = 0.194$ M and $I = 0.0485$ M). From the slopes of the curves and the intercepts the values for n and K_a can be estimated. These are given in Table 4. A comparison between picrate and chloride binding at the ionic strength of 0.0485 M indicates that approximately two picrate

Figure 4.5. Plot of $\log [(K_{ap} - K_{ap}^{\circ}) / K_{ap}^{\circ}]$ vs $\log (A)$
for picrate at ionic strength of 0.0485 M (+)
and chloride at the ionic strength of 0.194 M
(o) and 0.0485 M (Δ).

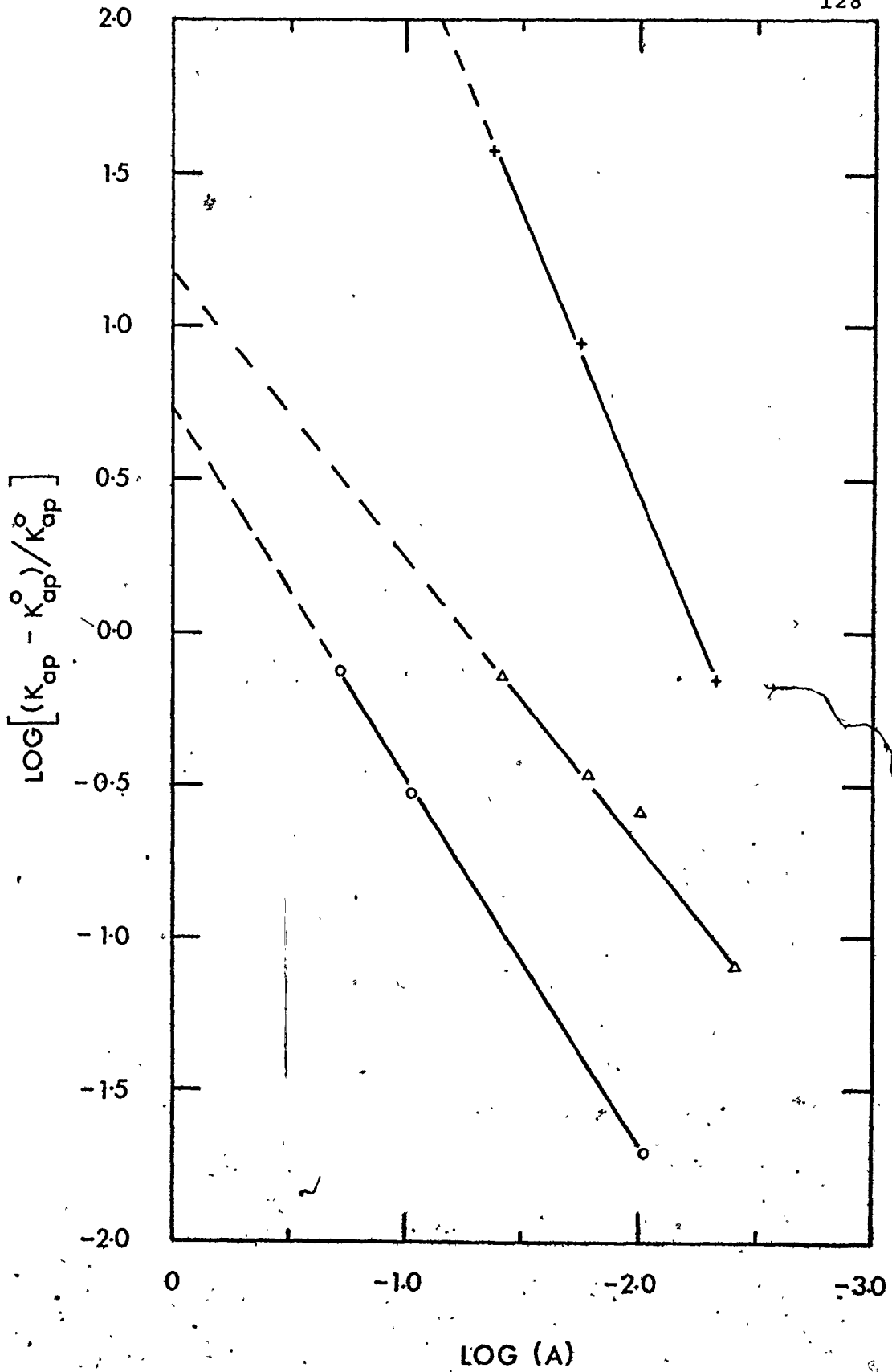


Table 4

The Number of Ions Bound to cyt^{III} (n) and Their Association Constants (K_a) as Determined from Hill plots (Figure 4.5) Based on Measurements of $(k_{\text{red}}^{\text{r}}/k_{\text{ox}}^{\text{r}})$

Ion	Ionic strength (M)	n	K_a (M^{-1})
Picrate	0.0485	1.8	5.25×10^3
Chloride	0.0485	1.0	14.4
Chloride	0.194	1.3	5.75

fons are bound to cyt^{III} as opposed to only one bound chloride ion. Palcic (1972) and Margalit and Schejter (1973) reported higher values for chloride binding at lower ionic strength ($n = 1.8$, ionic strength, 3.94×10^{-3} M and $n = 1.6$, ionic strength, 4×10^{-3} M, respectively). However, it was shown by Palcic (1972) that both the number of anion binding sites and their apparent association constant vary with the ionic strength. Therefore, our results can be considered as substantially in agreement with those previously reported.

Our results are also consistent with the results of the electrophoretic measurements carried out by Margoliash *et al.* (1970). They observed that the presence of chloride in buffer had a large effect on the electrophoretic mobility of ferricytochrome c but it did not affect the mobility of ferrocytochrome c. These results show that chloride more strongly interacts with the ferri- than the ferro- form of cytochrome c as has been observed in our measurements.

The results reported in Tables 3 and 4 were obtained by two different methods. The data in Table 3 were estimated by measuring the rate constants for oxidation of reduced cytochrome c whereas the data in Table 4 were estimated by using the ratio of the overall rate constants $k_{\text{red}}^{\text{r}}$ and k_{ox}^{r} . In both cases we assumed the same mechanism of ion binding (cooperative binding).

As can be seen from Tables 3 and 4, picrate has the largest n 's and K_a 's whereas chloride, although similar in both cases, shows smaller intersections (n, K_a) with cytochrome c.

4.4. Comparison between guanidinated and unmodified cytochrome c

Measurements of the oxidation of gn- ferrocytochrome c by ferricyanide (Figure 3.23) showed that this modification did not markedly alter the electron transfer properties. On the contrary, the oxidation of gn- ferrocytochrome c occurred even more rapidly than the unmodified protein. This is in agreement with previous findings which showed that gn- ferrocytochrome c reacted more rapidly with cytochrome oxidase than does the unmodified protein (Hettinger and Harbury, 1964). This could be interpreted by assuming an increase in the area of heme crevice exposed or an increase in the apparent positive charge.

The modification of ferricytochrome c did not alter the mechanism of the reduction as illustrated in Figure 3.24. In Table 5, the kinetic parameters for the reduction of gn- ferricytochrome c are compared with the corresponding parameters for unmodified cytochrome c. They are within 20% except the value for K_d (dissociation constant of the ferrocytochrome c - ferricyanide complex).

Table 5

Comparison Between the Kinetic Parameters $K_d = k_2/k_1$, k_3 , k_4 and $K_d' = k_5/k_6$ for Guanidinated and Unmodified Cytochrome c ($I = 0.1 \text{ M}$)*

Cytochrome	K_d (M)	k_3 (sec^{-1})	k_4 (sec^{-1})	K_d' (M^{-1})	K_{eq}
gn- cytochrome c	2×10^{-3}	68	200	1.1×10^{-6}	1.63×10^{-3}
unmodified cytochrome c	1.8×10^{-3}	70	250	8.6×10^{-6}	3.9×10^{-3}

* See section 3.3.1.

It appears from our data that gn- ferrocytochrome c forms a stronger complex with ferricyanide than does the unmodified protein.

The binding of chloride to gn- ferricytochrome c was analyzed as described in section 4.3. The number of chloride binding sites was estimated to be 0.8 which is somewhat lower than the number of binding sites for unmodified cytochrome c of 1.3. It was also observed by Palcic (1972) that guanidination reduced the binding of chloride to ferricytochrome c.

The results suggest that when the iron hexacyanides are used as electron acceptor and donor, positive charges and not lysines as such are necessary to maintain the electron transfer properties of native cytochrome c.

5. SUMMARY AND CONCLUSIONS

5.1. Oxidation of ferrocytochrome by ferricyanide

Study of the oxidation of ferrocytochrome c by ferricyanide confirmed the previous reports that this reaction follows an irreversible, second-order mechanism. The oxidation of horse heart ferrocytochrome c was found to be an extremely fast, reaction ($13.3 \pm 0.6 \times 10^6 \text{ M}^{-1} \text{ sec}^{-1}$ at $I = 0.194 \text{ M}$, pH 7.0, temperature 24°C). The effect of ionic strength on the rate of oxidation was analyzed in terms of Debye-Hückel theory. The results of this analysis suggested that oxidation of horse heart cytochrome c is a diffusion-limited reaction. The value of the rate of oxidation extrapolated to zero ionic strength was estimated to be $\sim 9 \times 10^9 \text{ M}^{-1} \text{ sec}^{-1}$. This value was 7% of the value calculated for a diffusion-controlled reaction. Since the area of the exposed heme edge is about the same fraction (4%) of the total surface area, we conclude that the electron transfer probably occurs through the exposed heme edge. An effective charge of + 7.8 units for horse heart cytochrome c was calculated, and this was close to the total charge of the protein molecule. The same analysis was applied to

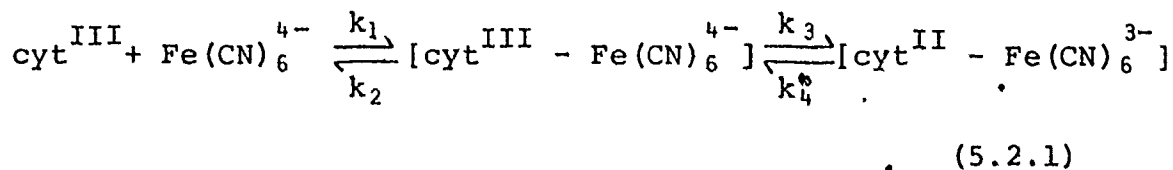
the ionic strength dependence of the oxidation of *P. aeruginosa* ferrocytochrome c. The extrapolated value (to $I = 0$) for the rate of oxidation was found to be seven orders of magnitude smaller than the value for horse heart cytochrome c. This reaction was not consistent with the diffusion-limited kinetics. The effective charge for *P. aeruginosa* cytochrome c was estimated to be -3.7 units (the protein's charge is not known precisely for this species). The ionic strength dependence of the oxidation of *M. denitrificans* ferrocytochrome c was unexpected and should be studied more thoroughly. If our results are correct, cMd would represent an interesting example of a protein whose properties dramatically change with change in the ionic strength of the environment.

The ions that were found by other techniques to bind to cytochrome c were also found to slow the rate of oxidation of horse heart ferrocytochrome c. We analyzed the effect of ions on the rate of oxidation by assuming cooperative binding. This analysis, indicated that, on the average, there are about 1.5 picrate, 1.2 phosphate, 1.3 chloride and 1.5 potassium ions associated with ferrocytochrome c (ionic strength 0.194 M, except picrate where $I = 0.485$ M, pH 7.0, temperature, 24°C). As proposed by other authors, the binding of these ions probably occurs on the surface of the molecule and in some cases far from the exposed heme edge. It is possible that the perturbation due to binding

of these ions could be transmitted to various parts of the molecule (the heme group, for example) via a hydrogen bond network or by conformational changes.

5.2. Reduction of ferricytochrome c by ferrocyanide,

The reduction of ferricytochrome c by ferrocyanide was found to be consistent with the following reaction mechanism:



with the measured values for $K_d (= k_1/k_2) = 2.9 \times 10^{-3} \text{ M}$, $k_3 = 190 \text{ sec}^{-1}$ and $k_4 = 70 \text{ sec}^{-1}$ at $I = 0.235 \text{ M}$, pH 7.0, temperature, 24°C . Complexation of ferricytochrome c and ferrocyanide has also been observed by other techniques. When we combined our stopped-flow results with steady-state measurements of the apparent equilibrium constant we determined a value for the dissociation constant of the $[\text{cyt}^{\text{II}} - \text{Fe}(\text{CN})_6^{3-}]$ complex of $K_d' = 5.6 \times 10^{-7} \text{ M}^{-1}$.

Ionic strength was found to have a large effect on the dissociation constants K_d and K_d' and on the rate constant k_4 . The overall effect of the ionic strength on the observed first-order rate constant was as expected for a reaction between two oppositely charged molecules: increasing the ionic strength of the medium decreased the

rate constant.

The effect of binding ions on the reduction of ferricytochrome c was discussed in terms of the ratio of forward to reverse rate constants (i.e., the apparent equilibrium constant), again assuming cooperative binding. The presence of phosphate did not affect the equilibrium constant. An analysis of chloride and picrate binding indicated that approximately one chloride and almost two picrate ions are associated with ferri- form of cytochrome c (I - 0.0485 M, pH = 7.0, temperature = 24°C).

Our data suggested that there were two different electron pathways for oxidation and reduction of cytochrome c by hexacyanides. Further work is suggested in order to prove this hypothesis. For example, chemical modification of specific amino acid residues may be used for this purpose.

5.3. Modification of the lysine residues of cytochrome c

Guanidination of the lysine residues of horse heart cytochrome c did not markedly alter its electron transfer properties. The oxidation of gn- ferrocytochrome c was found to proceed more rapidly than the oxidation of native ferrocytochrome c. The reduction of gn- ferricytochrome c, on the contrary, proceeds more slowly than the reduction of native ferricytochrome c. The

binding of chloride ion was somewhat diminished in gn-cytochrome c. The results suggested that positive charges and not lysine residues are necessary to maintain the electron transfer properties of cytochrome c.

APPENDIX I

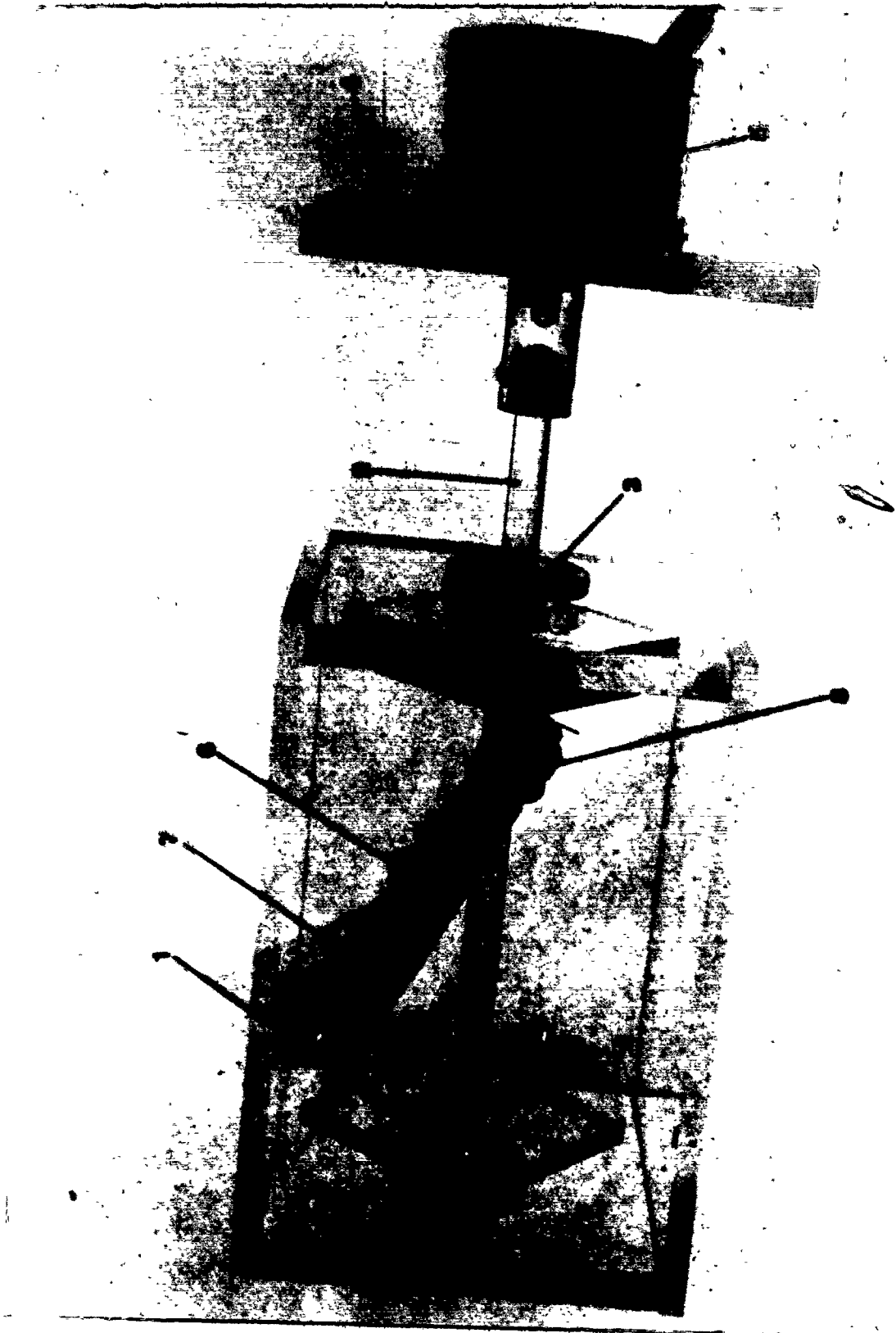
ROTATING DIALYZER

A rapid approach to equilibrium is necessary for efficient dialysis. The process can be accelerated by stirring on both sides of the membrane. This consideration led Feinstein (1952) to construct a rotating dialyzer. Feinstein showed that equilibrium was reached four times faster when the rotating dialyzer was used as compared to a free-floating dialysis bag. A disadvantage of his apparatus was that 45 liters of buffer were necessary to fill the dialyzing bath.

Figure I.1 shows a rotating dialyzer made of lucite. Only 1.6 litres of buffer are necessary. The lucite box (15 cm x 10.5 cm x 11 cm) was glued together with chloroform. Two plexiglass squares (6.5 cm) with six small holes in the corners are firmly glued to the driving shaft 11 cm apart. Four dialysis bags of approximate 25 ml each can be tied diagonally between the two squares. The dialysis bags contain 3 or 4 glass beads, 0.6 cm diameter and are closed at one end by a specially constructed plexiglass plug. Each dialysis bag makes an angle of 27° with the shaft, which is

Figure I.1. Rotating dialyzer.

1. Square lucite plate with holes in the corners to tie dialysis bags; 2. Driving shaft; 3. Circular plate forcing an O-ring against the wall to prevent leaking; 4. Plate supporting the electric motor; 5. Electric motor; 6. Dialysis bag; 7. Marbles; 8. Specially constructed plexiglass plug which allows one to open the bag without cutting it.



clamped to the electric motor turning at a speed of 6 rpm. When the dialysis bag is rotating, the glass beads roll up and down inside the bag stirring the contents of the dialysis bag.

APPENDIX II

ELECTRODIALYSIS

II.1 Principles of electro dialysis

Inorganic ions can be removed from a protein solution by electro dialysis. If direct current is passed through a cell containing a salt solution of a protein bounded by two ion-exchange membranes, desalting occurs.

Direct current causes electrolysis of a salt solution whereby the cations discharge at the cathode and the anions deposit at the anode. The cation (anion) exchange membrane functions as an ion filter, allowing only the passage of cations (anions) under the influence of the electric field and repelling the unwanted ions.

The rate of desalting ($-dc/dt$) can be described by the equation (Katz and Ellinger, 1962),

$$(-dc/dt) = \lambda E / (FRV) \quad (II.1)$$

where c is the concentration of dialyzable ions, E denotes the applied voltage, F designates the Faraday constant, R is the resistance of the sample cell and V is the volume of the sample solution. λ is called the electro-dialytic coefficient; it depends on the property and the

area of the ion-exchange membrane, the geometry of the electro dialysis cell, the temperature and the mixing of the sample solution. The equation states that the rate of desalting is proportional to the applied voltage and inversely proportional to the volume of the sample. Assuming that the applied voltage is constant and that the current through the cell is proportional to the concentration of dialyzable ions, the above equation (II.1) can be written in the form:

$$(-di/dt) = Ki$$

where K is a constant and i the current through the cell. The equation indicates that, under the above mentioned conditions, the current through the cell falls off exponentially with time. When a steady current is reached, the solution is depleted of ions and the pH of the solution is determined by the protein; that is the pH value equals the isoionic pH which for cytochrome c is about 10.

II.2. Apparatus

An electro dialysis unit similar to that described by Katz and Ellinger (1962) was constructed. The electro dialysis cell, which was made of lucite, has three compartments; two identical electrode vessels and the

sample compartment (Figure II.1). Tap water is directed toward the electrode to remove the electro dialysis products, and to cool the electrode compartment. The electrode vessels are fastened to the sample compartment with eight screws (four on each side) which squeeze the ion-exchange membranes between the sample compartment and the rubber O-rings located on the lower base plate of the electrode cells. The electrodes were made of 0.25 mm diameter platinum wire (Figure II.2A).

The sample compartment was made so that its length, and therefore the sample volume was variable (Figure II.2B). Two pairs of cylindrical inserts of different lengths were used; the longer inserts holding samples of 19 ml, and the shorter ones with the volume of 12 ml.

The solution in the sample cell was stirred magnetically to prevent salt and protein stratification.

A dc power supply (Heathkit, model IP-17) supplied the required voltage. The current through the cell was monitored with a chart recorder (Heathkit, model EUW-20M) connected across a 10 Ω resistor. The ion-exchange membranes were a gift from IONAC^{R*} (cation exchange MC-3470, anion exchange MA-3475R).

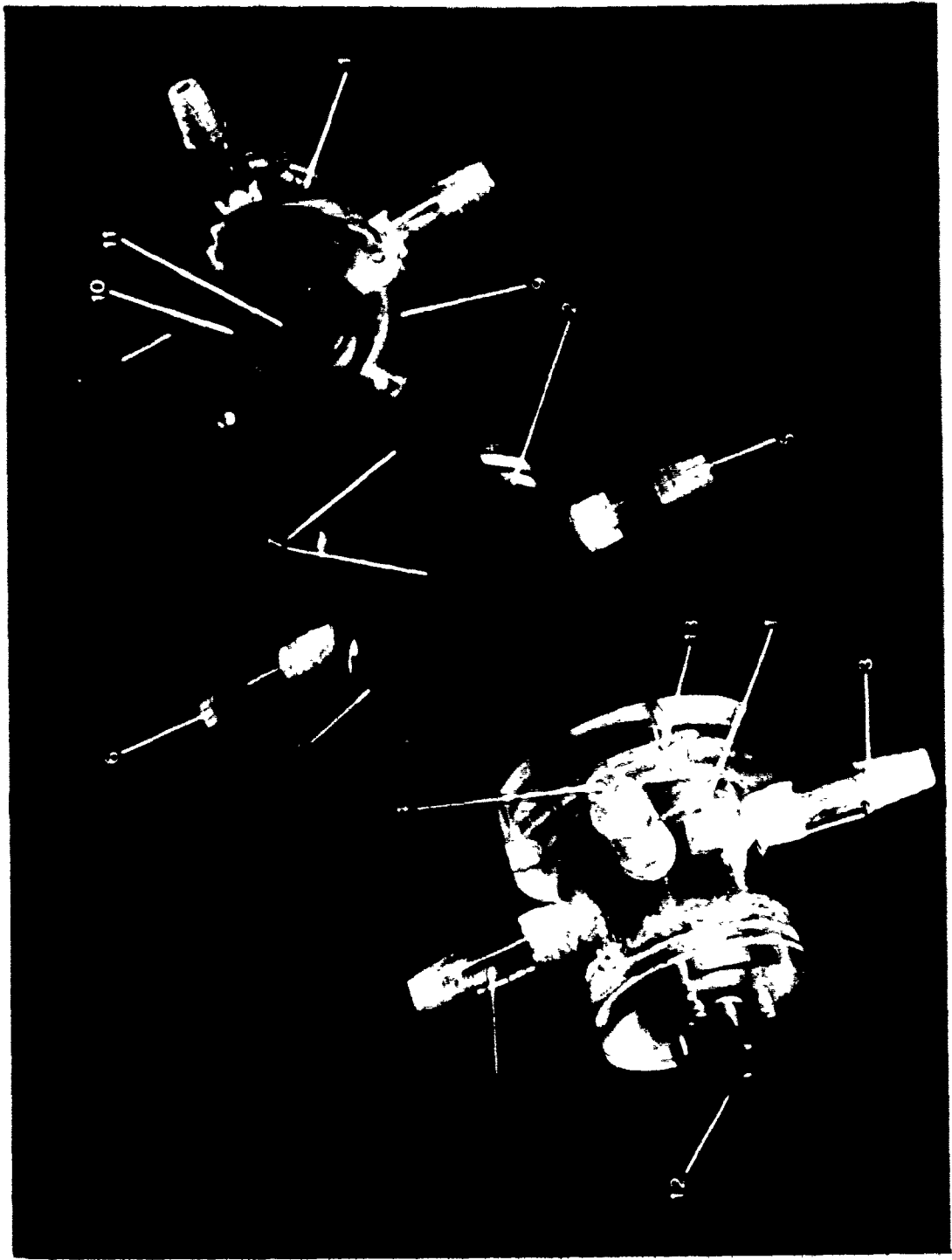
To test if the membrane functioned properly**, and the current passed in the right direction, double

* IONAC Chemical Co., Birmingham, N.J.

** After 5-10 electro dialysis runs the membranes were covered with a layer of protein and were discarded.

Figure II.1. Apparatus for electro dialysis.

1. Electrode compartment; 2. Sample compartment;
3. Cooling electrode water inlet; 4. Cooling electrode
water outlet; 5. Sample cooling water inlet; 6. Sample
cooling water outlet; 7. Sample ports; 8. Four tapped
holes (only one is indicated) for 4-40 stainless steel
screws spaced 90° apart (matched with holes 13); 9. Base
plate of the electrode cell; 10. Rubber O-ring; 11.
Coiled platinum electrode; 12. Banana plug; 13. Four
holes for 4-40 screws spaced 90° apart which hold the
three compartments together.



2

Figure II.2A. Cross sectional drawing of electrode compartment.

1. Banana plug; 2. Circular plate pressing an O-ring (3) against the housing of electrode compartment to prevent leaking; 4,5. Electrode water ports; 6. Base plate of the electrode compartment; 7. Platinum electrode wire; 8. Rubber O-ring.

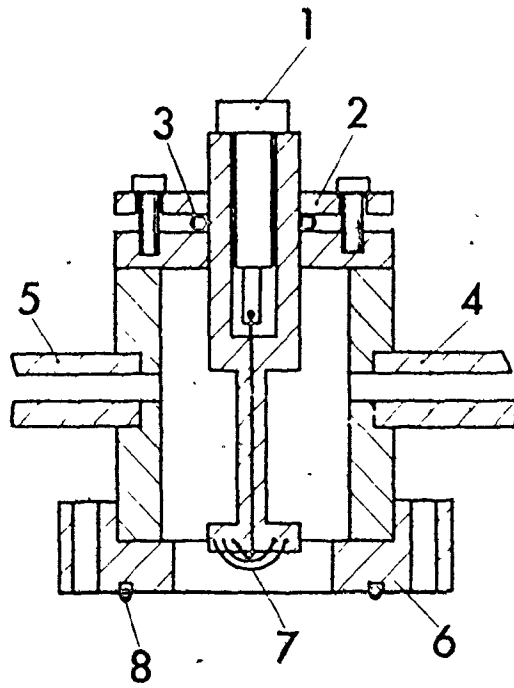
Figure II. 2B. Cross sectional drawing of sample compartment.

1. End plate; 2. Inside cylindrical insert; 3. Outside cylindrical insert; 4. Sample inlet; 5,6. Cooling water ports; 7. Rubber O-ring.

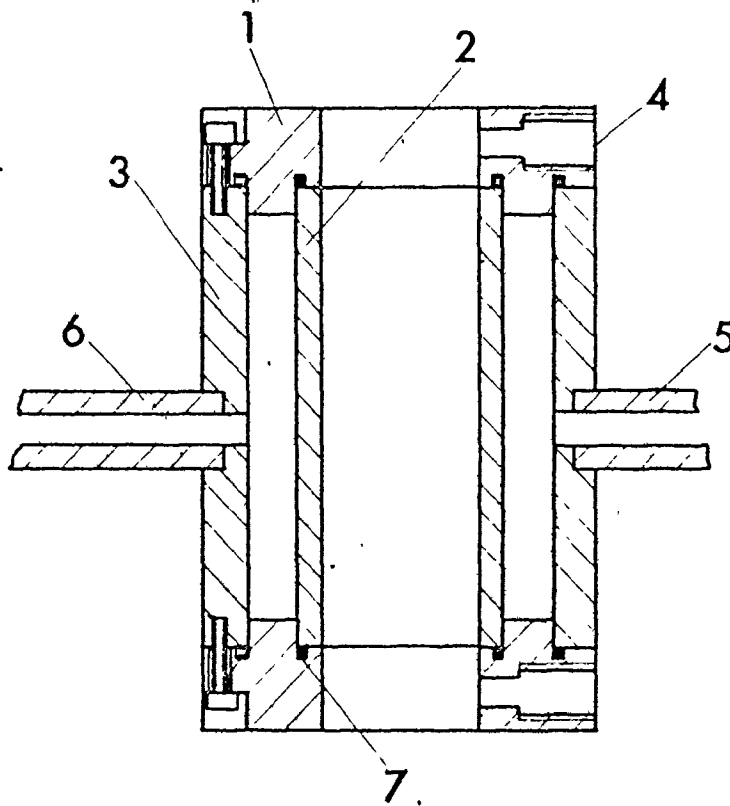
5

5

A



B



distilled water was electro-dialyzed. If a small current rapidly fell to a stable value the membranes were in good condition, and the current was in the right direction (otherwise the current through the cell increased rapidly).

APPENDIX III

STOPPED-FLOW PHOTOMETER

III.1. Apparatus

III.1.1. Principle of operation

Figure III.1 shows the entire stopped-flow system. The principle of operation of the stopped-flow photometer (SFP) can be followed by examining the flow system in Figure III.2. The reactants in the driving syringes are forced by a pneumatic drive through the delivery block into the mixer where rapid mixing takes place. The reacting mixture then passes through the observation chamber, having a light path of 2 cm, and enters the stopping syringe, driving its plunger backwards. The flow is stopped when the plunger of the stopping syringe strikes the preset mechanical barrier and simultaneously actuates a microswitch. When the microswitch is activated, it produces a voltage pulse which initiates the storing of the data in the memory of a transient recorder (see Figure III.1). The data stored in the memory is then transferred to the paper tape. The punched paper tape is fed into the computer and the data analyzed (Appendix IV).



Figure III.1. Stopped-flow system.

1. Oscilloscope; 2. Transient recorder; 3. Control panel; 4. High voltage power supply for photomultiplier tube; 5. Interface control; 6. Paper tape perforator; 7. Current-to-voltage converter; 8. Photomultiplier tube; 9. Flow system; 10. Monochromator and light source.

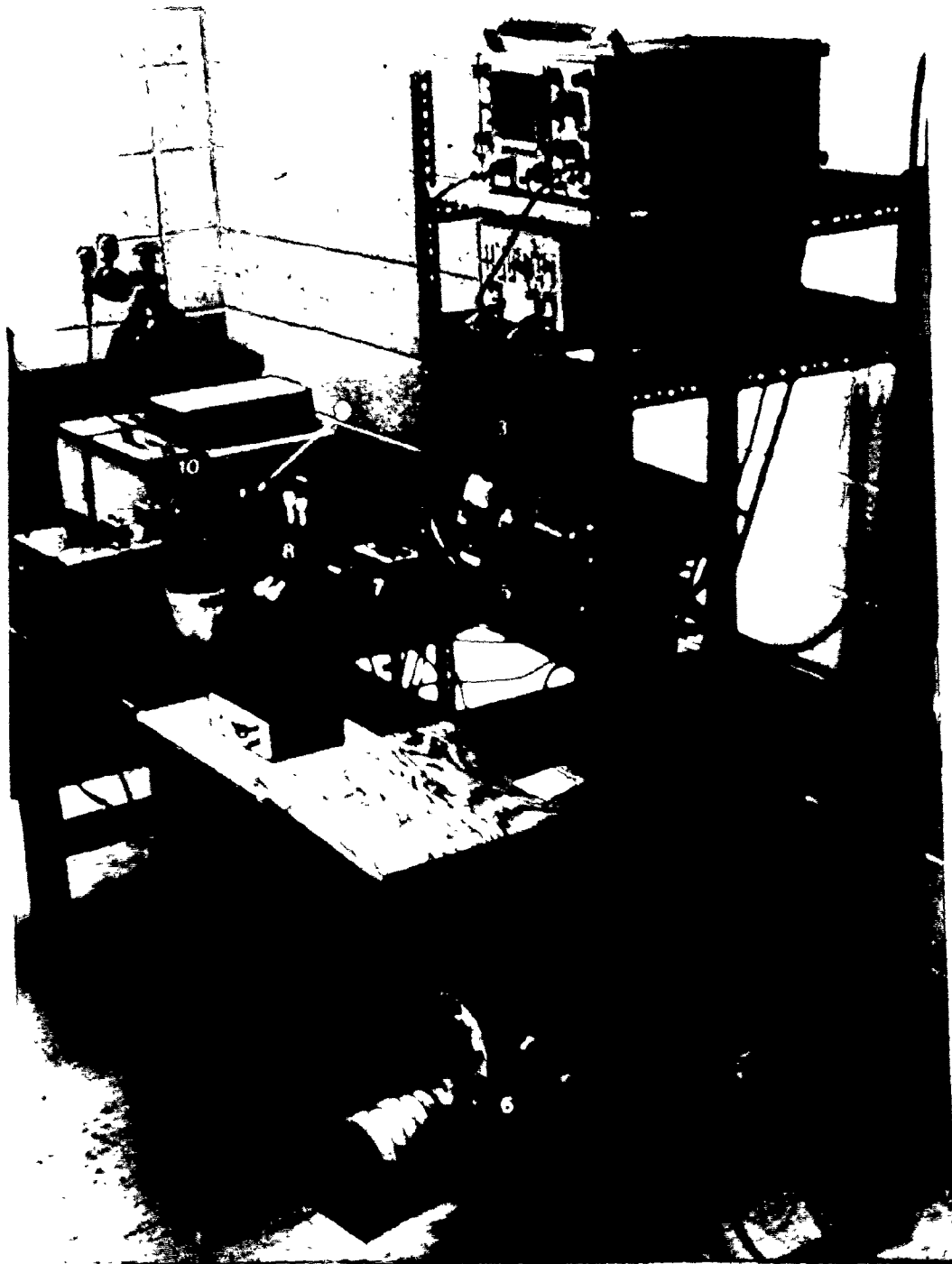
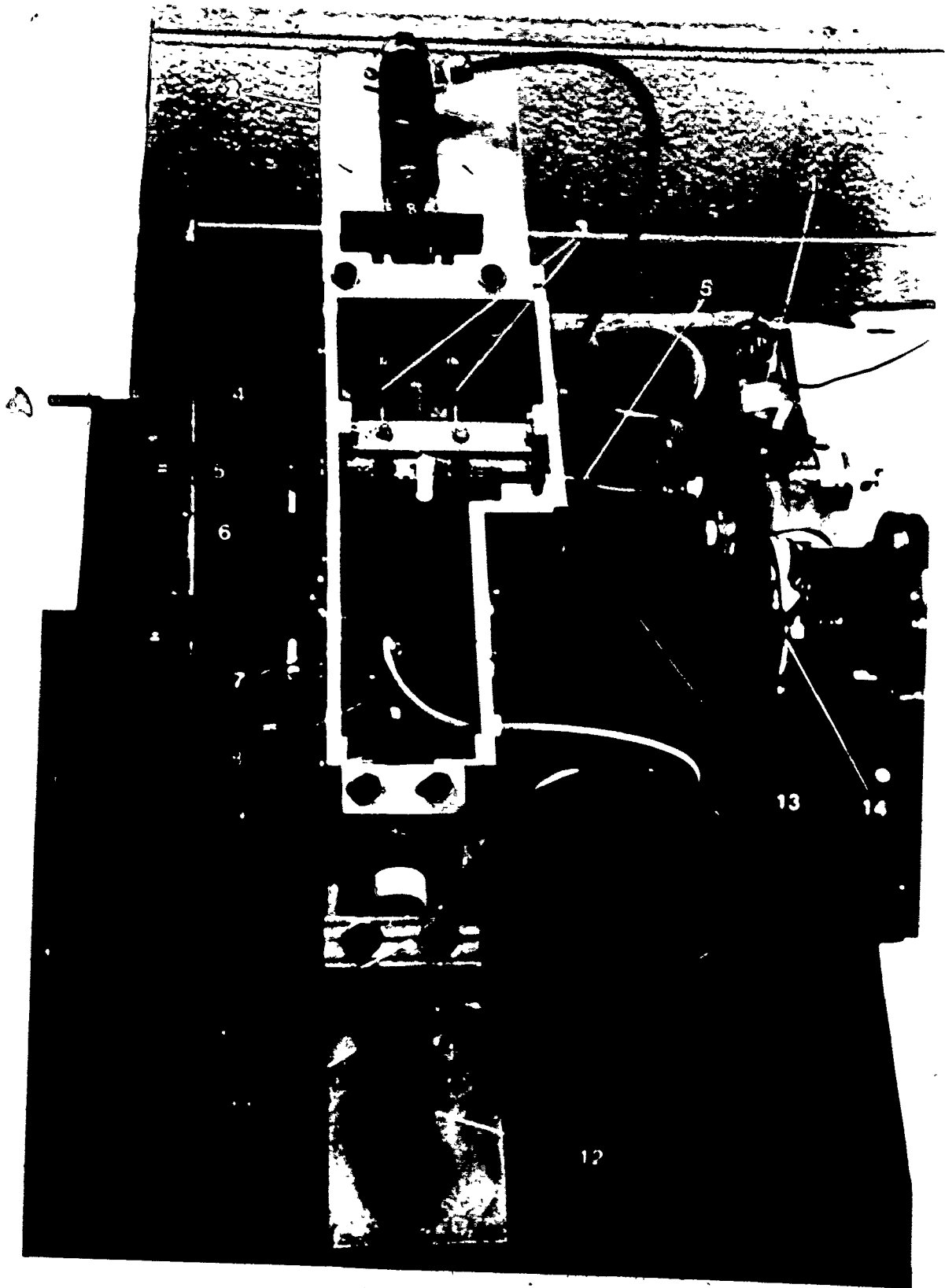


Figure III.2. Flow system.

1. Solenoid valve; 2. Hydraulic cylinder; 3. Driving syringes; 4. Three-way valves; 5. Valve handles;
6. Delivery block (lucite); 7. Observation chamber (lucite); 8. Drain valve; 9. Stopping syringe;
10. Stopping barrier; 11. Adjustable nut;
12. Microswitch; 13. Light guide; 14. Camera shutter;
15. Monochromator.

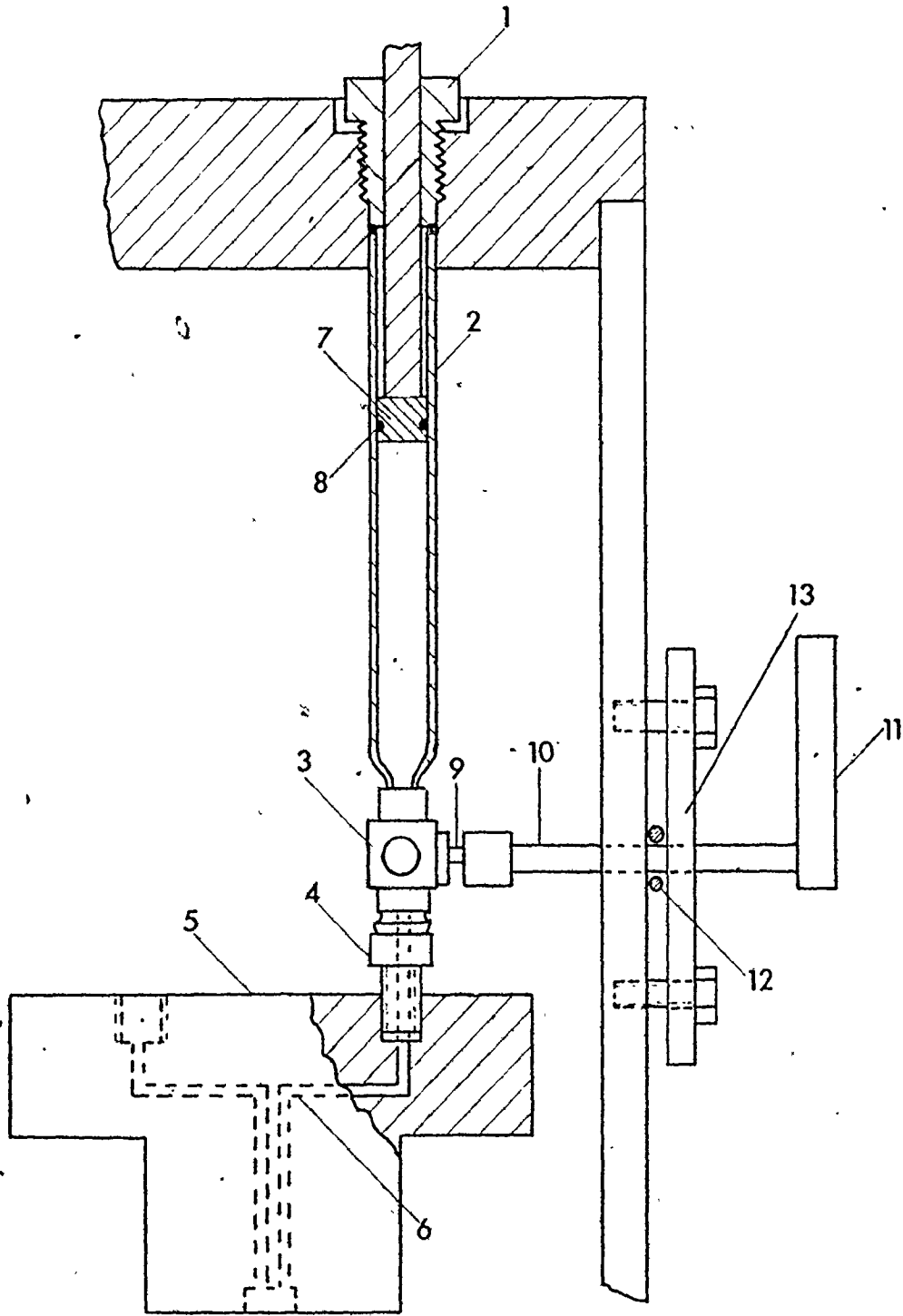


III.1.2. Flow system /

The flow system consists of water bath, pneumatic drive, the driving syringes, fluid delivery block, mixer, observation chamber, stopping syringe and stopping block (Figure III.2). The hydraulic cylinder (Airmate, Chicago, Ill., model P112-2), with its returning spring removed, is connected through a solenoid valve (Airco, Angola, Ind., model 36001) to a nitrogen gas cylinder. When the actuating switch is closed a capacitor (Figure III.5) discharges through the solenoid valve, opening it for approximately 90 msec and applying a pressure of 70 to 90 psi of N_2 to the piston of the hydraulic cylinder. The mounting of the driving syringes can be seen in the Figure III.3. The driving syringes (Hamilton, Co., Reno, Nev., model 1002) which are cut to the length of 8 cm are forced against a three-way valve (Hamilton, model 3MFF3) with a nylon screw fitting (Ballou, 1971). The connection between this three-way valve and the delivery block is made with a female luer adapter (Chromatronix, Inc., Berkeley, Calif., cat. no. 107 B9). The commercial teflon plunger tips are liquid-tight at room temperature, but they leak at lower temperatures (Ballou and Palmer, 1974). Therefore, they were replaced with teflon tips having a groove for a rubber O-ring. If the dimensions and the O-ring (Parker Seal Co., Culver City, Calif.,

Figure III.3. Mounting of syringes.

1. Nylon screw fitting; 2. 2.5 ml syringe; 3. Three-way valve; 4. Female luer adapter; 5. Delivery block; 6. Fluid delivery holes; 7. Teflon plunger tip; 8. Rubber O-ring; 9. Valve shaft; 10. Extension shaft; 11. Handle to operate the valve from outside the bath wall; 12. Rubber O-ring; 13. Circular plate pressing the O-ring against the wall to make the hole liquid tight.



cat. no. 2-007) are carefully chosen, this arrangement offers less resistance than the original plungers. When the plungers become tight, the O-rings are replaced.

To operate the three-way valves from outside, the commercial valve handles were removed. A 5 cm long extension shaft was made which connects the valve shaft (the two shafts were clamped together with a set screw) with a handle on the outside of the bath wall (Figure III.3).

The delivery block (Figure III.2) allows the transport of reactants from the driving syringes to the mixer. The block is screw fastened to the base plate. All fluid delivery holes are 1.58 mm in diameter.

It is of the utmost importance that the mixing of the reactants is completed as fast as possible. Tests of several different designs showed that a mixer should induce an opposite rotatory motion of reactants (Smith, 1973). Gibson-type mixers (Gibson and Milnes, 1964) were made with holes of smaller diameters to produce a smaller dead volume (Figure III.4A). This type of mixer has two sets of four tangential jets which swirl the reactants in opposite directions.

Four threaded rods and four nuts squeeze the mixer between the delivery block and the observation chamber. Two teflon washers assure leakproof connection. Observation chambers with light paths from 1.58 mm to

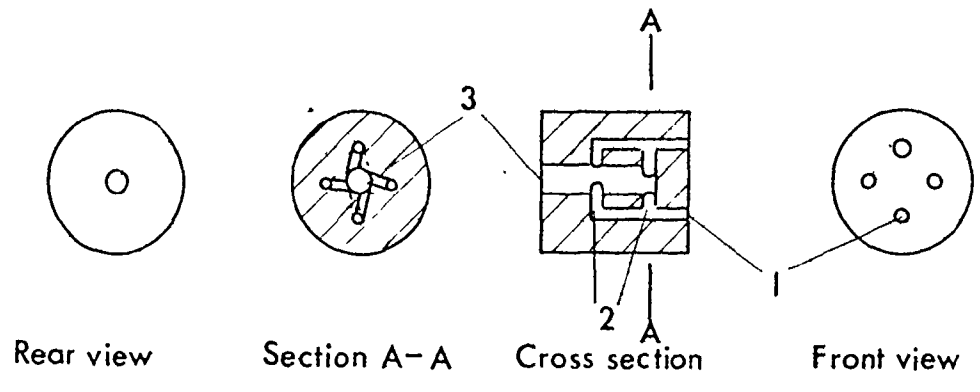
Figure III.4A. Diagramatic view of the mixer.

1. Entry holes 0.8 mm in diameter; 2. Tangential jets 0.36 mm in diameter; 3. Exit hole 1.58 mm in diameter.

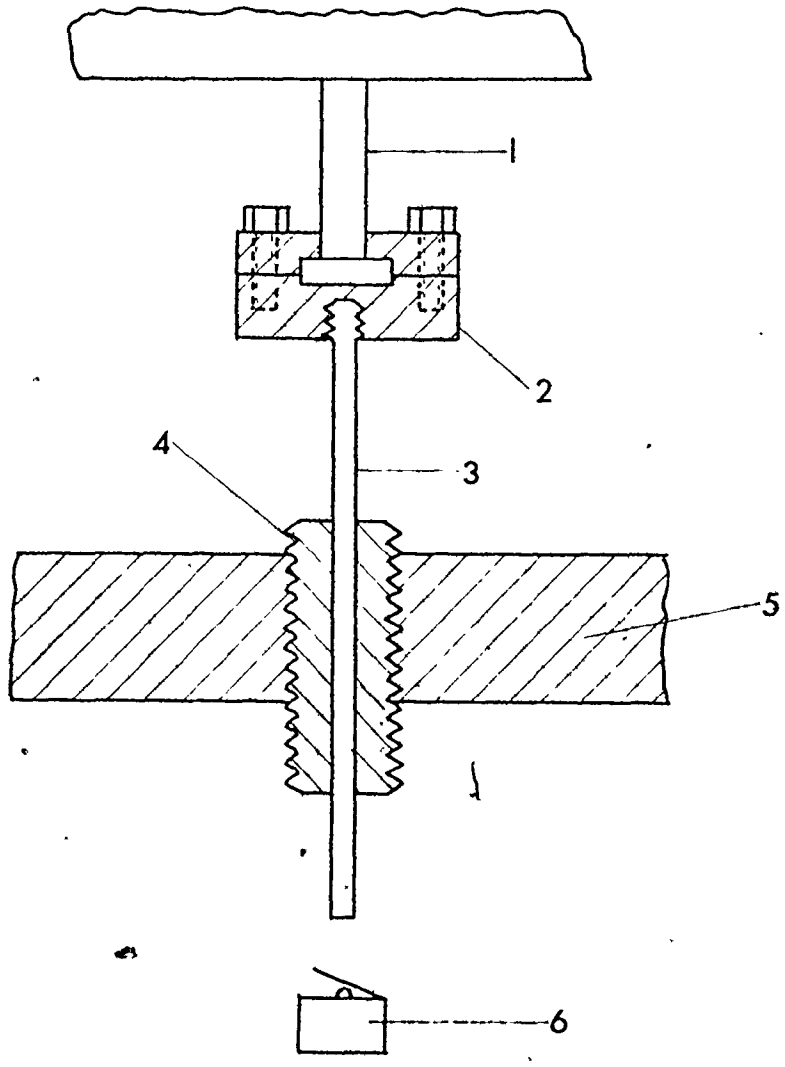
Figure III.4B. Stopping syringe assembly.

1. Plunger of the stopping syringe; 2. Teflon disc enclosing the end of the plunger; 3. Iron rod; 4. Adjustable nut; 5. Stopping barrier; 6. Microswitch.

A



B



3 cm can be used, but to this time all experiments have been made with a 2 cm light path.

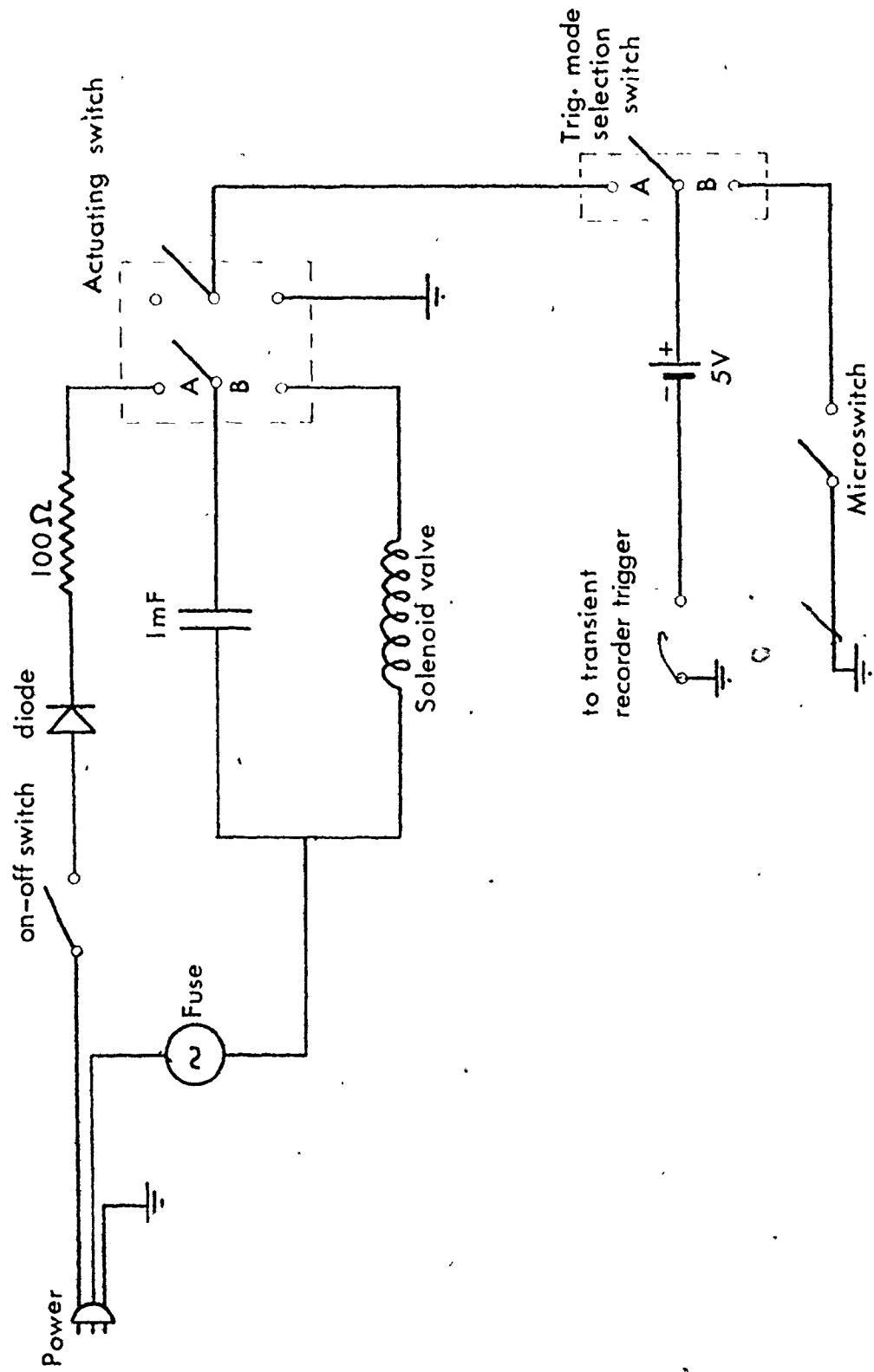
The stopping syringe assembly is shown in Figure III.4B. The volume of the reactants is controlled by the position of an adjustable nut. A total volume of 0.4 ml (0.2 ml of each reactant) is sufficient to flush the reacted mixture. When the flow is stopped, an iron bar activates an adjustable microswitch (Microswitch Inc., Freeport, Ill., model 1SM1 with JS-2 actuator). Triggering can also be activated before the flow starts (pre-flow triggering). When preflow triggering is employed, the trigger pulse is sent forward when the actuating button is activated (Figure III.5). The record of reaction run will include the mixing process as well as the reaction. This triggering mode is useful when the performance of the system is examined.

The spent reaction mixture is drained through the three-way valve located between the observation chamber and the stopping syringe.

The walls of the thermal bath are screw-mounted on the base plate, and the joints are sealed with silicon seal. For the temperature-dependent measurements, the entire flow system is immersed in water which is circulated and thermostated by a thermostating bath (Brinkmann Instruments, Lauda, model K-2/R). The temperature is measured with a thermometer inserted into a hole in the delivery block.

Figure III.5. Actuating and triggering circuit.

When the actuating switch is in the position A the 1 mF capacitor is charging, when it is in the position B the capacitor is discharging through the solenoid valve (the flow starts). By means of the triggering mode selection switch one can choose pre-flow triggering (A) or stopped-flow triggering (B).



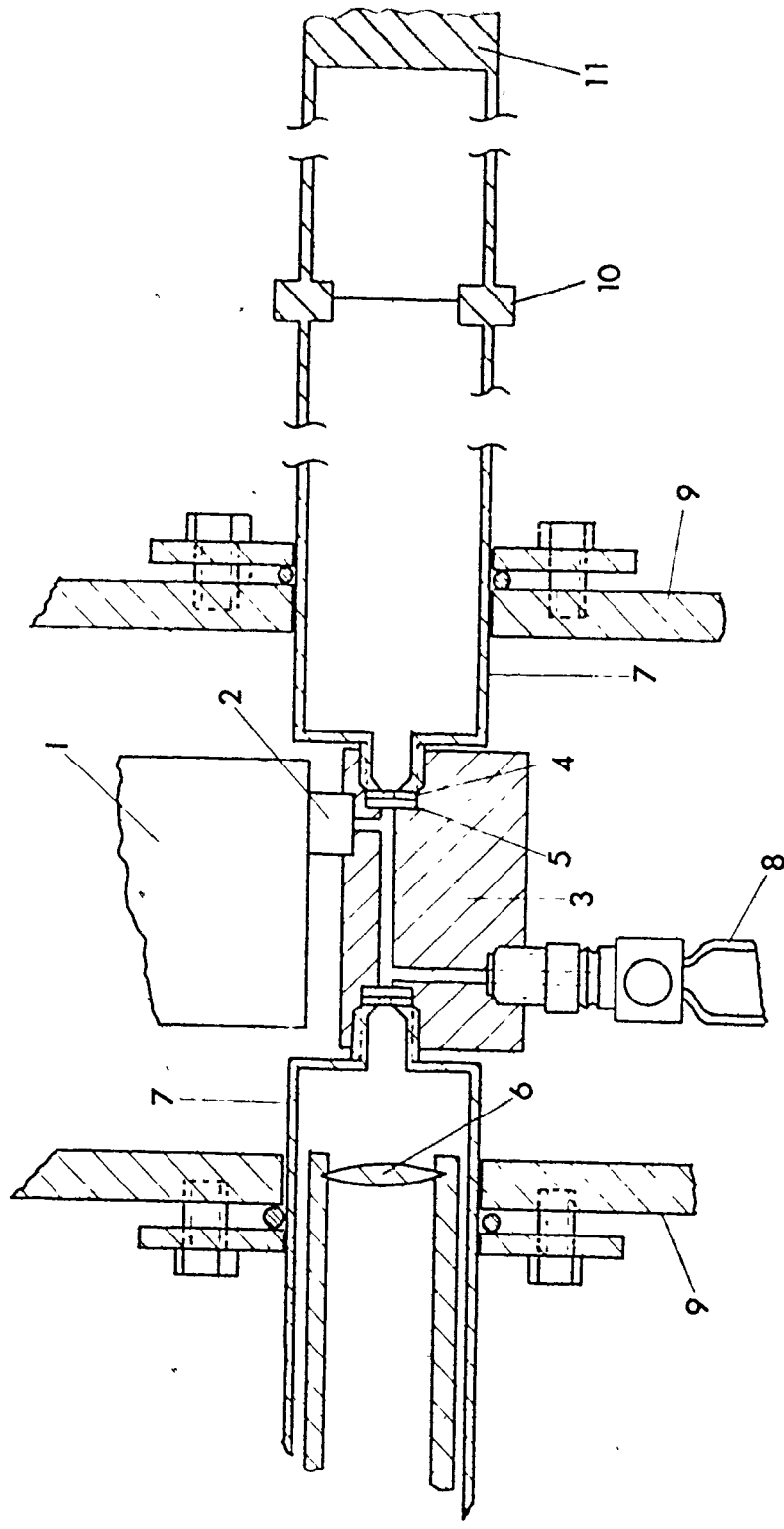
III.1.3. Optical system

Light from UV-VIS. light source (Heath Co., Benton Harbor, Mich., model EU-701-50) passes through the grating monochromator (Heath, model EU-700) and is focused on the center of the cuvette with a double convex lens with a focal length of 2 cm (Baush and Lomb, Rochester, N.Y., cat. no. 31-05-63-021) (Figure III.6). Quartz discs 1.58 mm thick and 8 mm diameter (Quartz Scientific, Inc., East Lake, Ohio) serve as windows. The light guides are screwed into the threaded holes forcing the windows against the body of the observation cuvette. The bottom flats of the threaded holes should be machined very accurately (milling machine with 3/8" end mill should be used), otherwise the windows leak and/or the breakage of windows may occur. In order not to scratch or break the windows teflon washers with a central hole of 1.4 mm were placed between the light guides and the quartz windows.

The transmitted light is detected by a photomultiplier tube (EMI, type 9558 QB, S-20 response). The voltage on the 11-dynode chain was supplied by a regulated power supply (EMI, Brandenburg, model 472-R). The best signal/noise was obtained when the voltage was about 800 V. A camera shutter positioned in front of the photomultiplier tube serves to isolate the

Figure III.6. Optical system.

1. Delivery block; 2. Mixer; 3. Observation chamber;
4. Teflon washer; 5. Quartz window; 6. Lens;
7. Light guide; 8. Stopping syringe; 9. Bath walls;
10. Camera shutter; 11. Photomultiplier tube.



photomultiplier tube from the light source.

III.1.4. Electronics

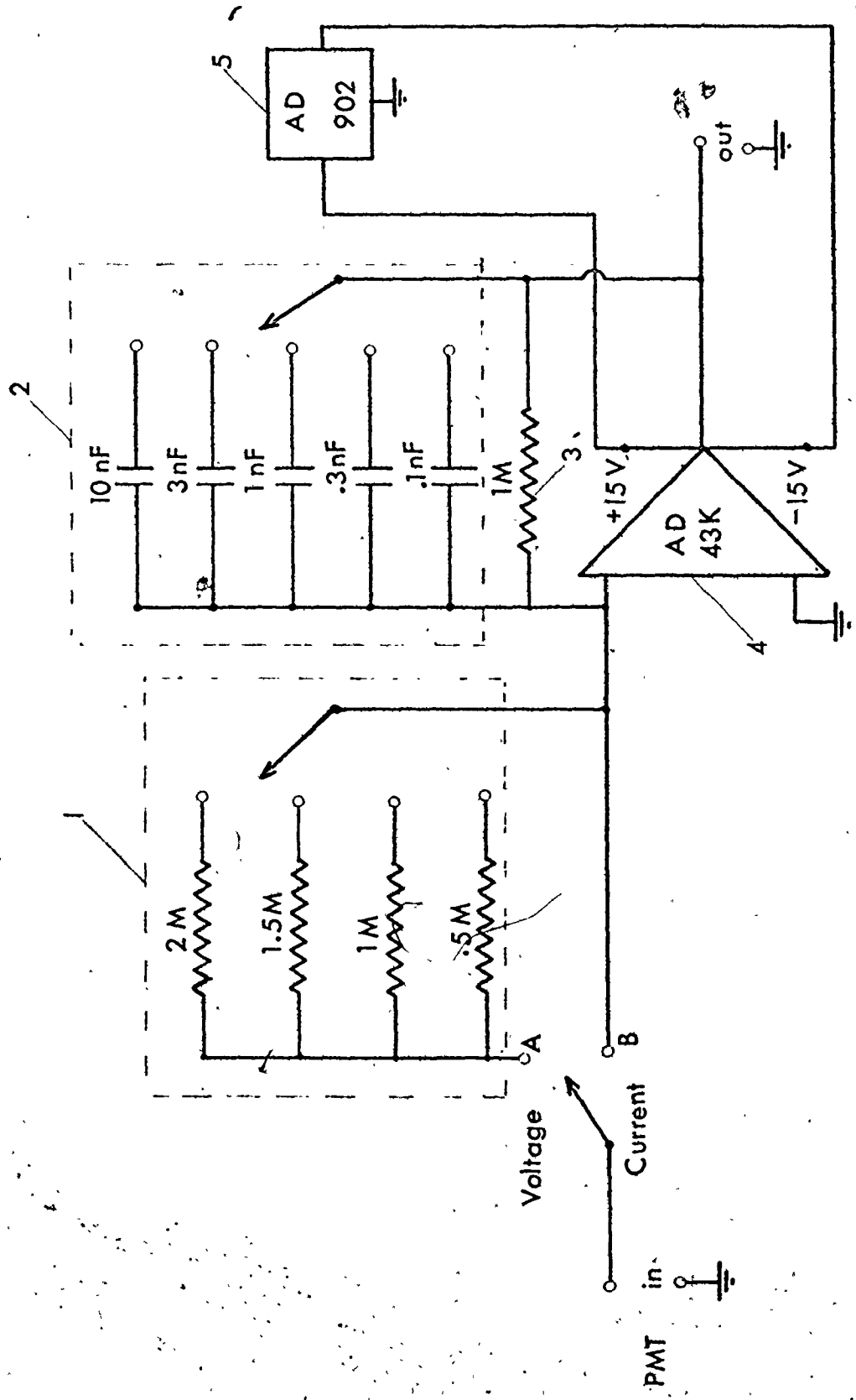
The current produced by the photomultiplier tube is converted into a voltage signal by a current-to-voltage converter (Malmstadt, Enke, and Toren, 1963), (Harvey, 1969). An ultra low noise, low drift operational amplifier (Analog Devices, Norwood, Mass., model 43K) (Ballou, 1973) was used to build the current-to-voltage converter powered by a dual power supply (Analog Devices, model 902) (see Figure III.7). With a feedback resistor of 1 megaohm 1 μ A is converted to 1 V by the current-to-voltage converter.

The current-to-voltage converter can also be used as a voltage amplifier. In this case the voltage pulse passes through the input resistor. This is convenient when the electronic circuit is to be checked and calibrated.

The signal from the photomultiplier tube is filtered by a capacitor connected in parallel across the operational amplifier. The time constant could be varied from 0.1 msec to 10 sec. The current-to-voltage converter was placed just behind the photomultiplier tube in order to avoid noise which would be generated by long cables.

Figure III.7. Current-to-voltage converter.

- 0
1. A series of resistors used when the current-to-voltage converter is employed as voltage amplifier;
 2. Filtering capacitors;
 3. Feedback resistor;
 4. Operational amplifier;
 5. Power supply.



The current-to-voltage converter is connected to a transient recorder (Biomation, Palo Alto, Calif., model 802). The transient recorder is triggered by the signal from the microswitch on the stopping syringe. The signal is sampled and converted into an eight bit binary record at 1024 points. The memory content is displayed on an oscilloscope (Advance, Hainault, Essex, G. Britain, model OS1000A). Successful runs are further analyzed. An interface control constructed by the Computer Centre, McMaster University transfers the memory contents to a sequence of binary data on paper tape driven by a paper tape perforator (Tally Corp., Kent, Wash., model 420 with PD60 driver). The memory contents could also be transferred directly to an X-Y recorder (Hewlett Packard, model 7005B).

III.2. Evaluation of performance

III.2.1. Applicability of Beer-Lambert law

The voltage output from the photomultiplier tube is proportional to the transmitted light. The transmittance T is related to the absorbancy A by the Beer-Lambert law:

$$A = - \log T = \epsilon c d$$

where ϵ is the extinction coefficient, c the concentration

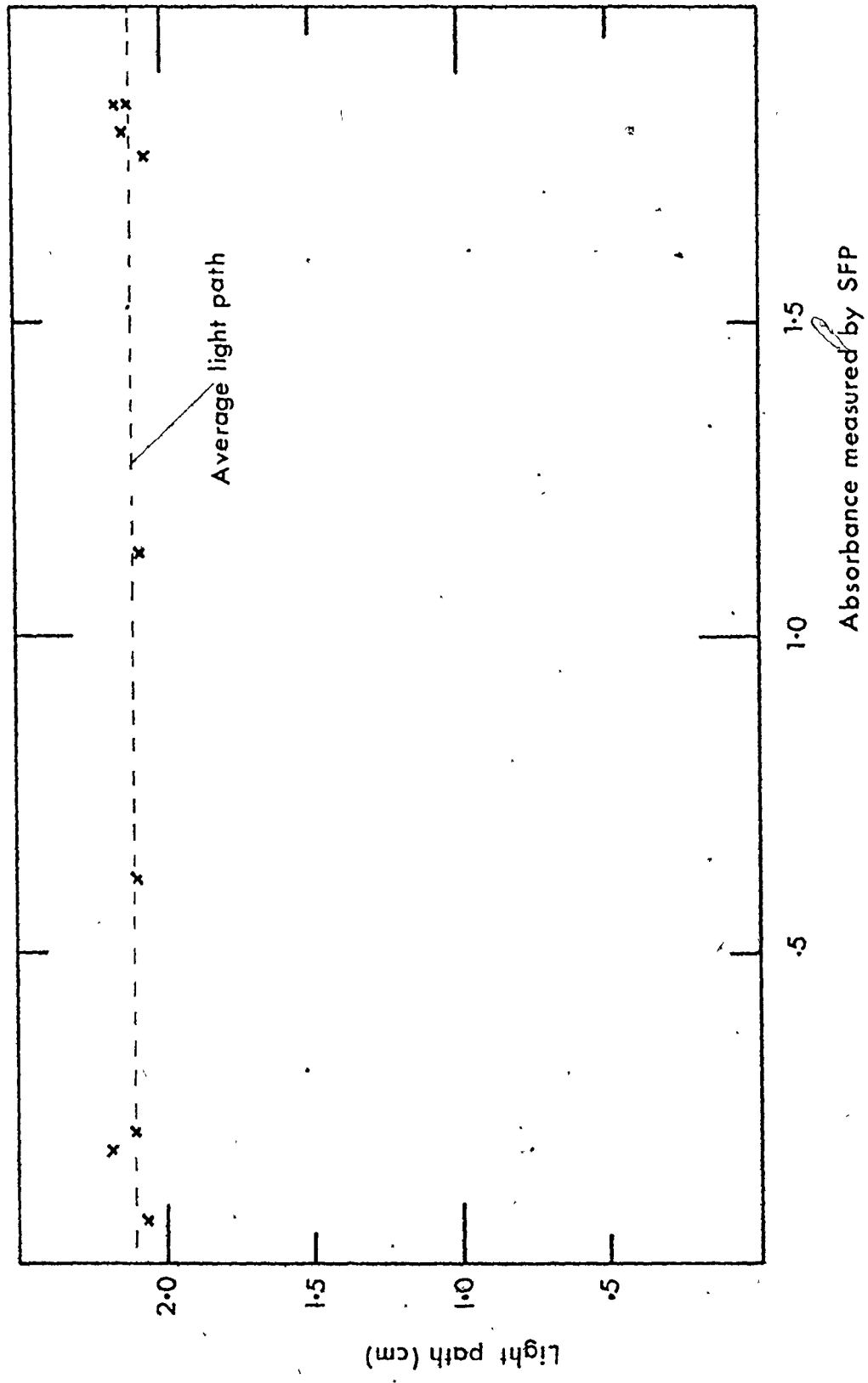
and d the light path. To correctly express a kinetic measurement as the change in the concentration as a function of time, one must have linearity between measured absorbance and concentration. Deviation from the Beer-Lambert law occurs when different parts of the beam traverse different light paths. To avoid such deviations, the holes in the washers between the windows and the light guides were made smaller than the hole in the observation chamber (see Figure III.6). The linearity between the concentration and the absorbance can be tested by putting solutions of known absorbance (measured by a Unicam 1800 spectrophotometer) into the SFP and determining the absorbance measured by the SFP. At the same time, one can determine the effective light path of the SFP. The light path d_s of the SFP can be calculated by:

$$d_s = A_s (d/A)$$

where A_s is the absorbance measured by SFP, A the absorbance measured by the spectrophotometer and d the light path of the spectrophotometer. Figure III.8 shows the variation of the effective light path as a function of the absorbance measured by the SFP. As can be seen from the graph, the light path is constant for the absorbance values between 0 and 2. The average value for the effective light path was found to be 2.05 ± 0.02 which is close to 2.035 cm as measured by a micrometer.

Figure III.8. Calculated light path as a function of absorbancy measured by the stopped-flow photometer.

Various concentrations of phenol red solution were measured at $\lambda = 550$ nm.



The value 2.05 cm was used for all calculations.

III.2.2. Mixing efficiency

The efficiency of mixing is the major factor determining the time resolution of the apparatus. It depends on the rate of flow of reactants and on the diameters of the jet holes in the mixer. Mixing of the reactants should be completed before the reacting mixture enters the observation cell, i.e. it should be completed within the transport time. The efficiency of mixing can be studied by following a diffusion-controlled reaction, such as proton transfer, which proceeds much faster than the stopped-flow mixing. Any inhomogeneity in mixing of the two reactants will result in sharp deviations from constant transmittance since the reaction is completed in the mixer. Solutions of sodium hydroxide containing phenol red and hydrochloric acid were mixed in the SFP and the transmittance was monitored at $\lambda = 550$ nm. Runs made in pre-flow triggering mode did not reveal any deviations from a straight trace on the oscilloscope indicating that mixing was completed within the transport time of the apparatus.

The volumes of the reactants delivered from each syringe should be the same when identical driving syringes are used. Inaccuracies in mixing can result

from different internal syringe diameters and from non-uniform driving. The accuracy of mixing was tested by mixing solutions of known absorbancy with water. The absorbancy of the solution should be exactly one half of the absorbancy before mixing. Thirty independent measurements showed that the deviation from the value of $\frac{1}{2}$ was less than 0.5%.

III.2.3. Dead time

Mixing and transport of the reacting solutions does not occur instantaneously. To decrease the time of these processes the driving pressure can be increased, but this usually impairs the performance. High pressure, exerted momentarily on the solution, can cause the reduction of the local pressure to the degree where water vaporization occurs (Chance, 1964). As a result a stream of bubbles (cavitations) is formed behind the mixer which can be observed on the scope as irregular fluctuations in the transmittance. High pressure can also cause degassing of the solution, and disturbances when flow is stopped. These problems limit the usefulness of the SFP for studying reactions which occur faster than 2-3 msec. Since the reaction begins as soon as the two solutions come in contact, the very early part of the reaction is missed. The dead time

is defined as the time interval between the beginning of the reaction and the first point of observation ($t = 0$). It depends on the flow velocity, the efficiency of mixing and the dimensions of the observation chamber. It can be determined by measuring a rapid pseudo-first order reactions as a function of concentration (Hammes and Haslam, 1968).

As discussed in Appendix IV, the kinetic runs are analyzed by means of a computer program. One of the program input parameters is the total absorbancy change measured independently. The change in the absorbancy from $t = -TD$ to $t \rightarrow \infty$ is taken to be the same as the total change in absorbancy measured by the spectrophotometer. The computer generates a theoretical curve which is the best fit to the experimental points including the initial absorbancy point at $t = -TD$ (Figure III.9). In this way the computer estimates the dead time. The reduction of potassium ferricyanide with various concentrations of ascorbate in 0.1 M phosphate buffer, pH 7.5, was employed to determine the dead time of the SFP. The average value was found to be 1.5 ± 0.4 msec at driving pressure of 70 to 80 psi.

III.2.4. Summary of performance

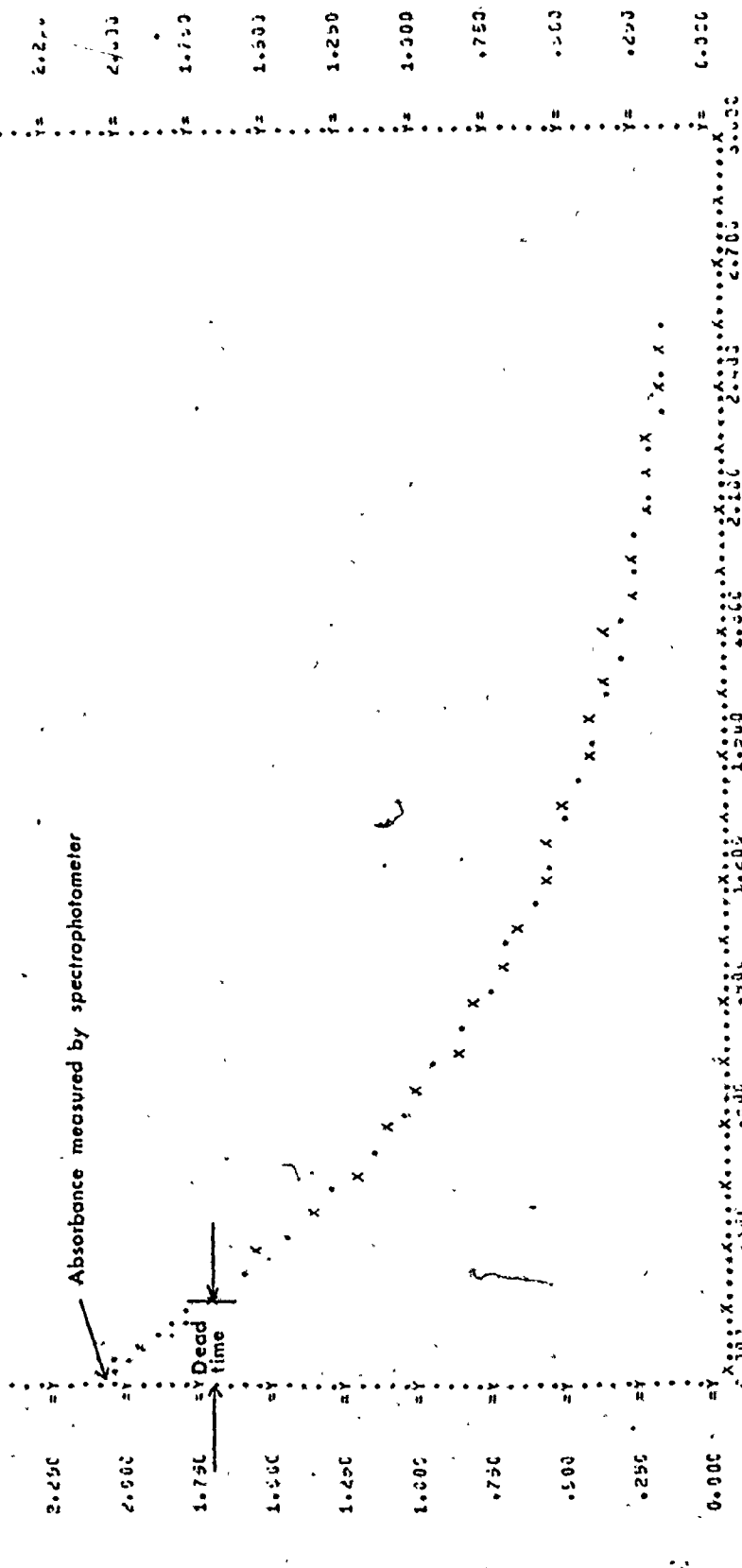
The absorbancy vs time (ascorbate reduction of ferricyanide) measured when the SFP is operated in the

Figure III.9. Computer analysis of a kinetic run.

Y-axis absorbance, X-axis time in sec. The dead time estimated by the computer was $TD = 1.352$ msec.

(Reaction: reduction of potassium ferricyanide (0.41 mM) by ascorbate (0.1 M) in 0.1 M phosphate buffer, pH 7.5). The dots are the computer-calculated fit, the x's are the experimentally measured points.

SUBJECT LIMIT, X=1.000000, XMAX= 2.500000, YMIN= 0.000000, YMAX= 2.500000, TO PULSED PLJITEL, A USESITES, X= 2.500000, Y= 2.500000



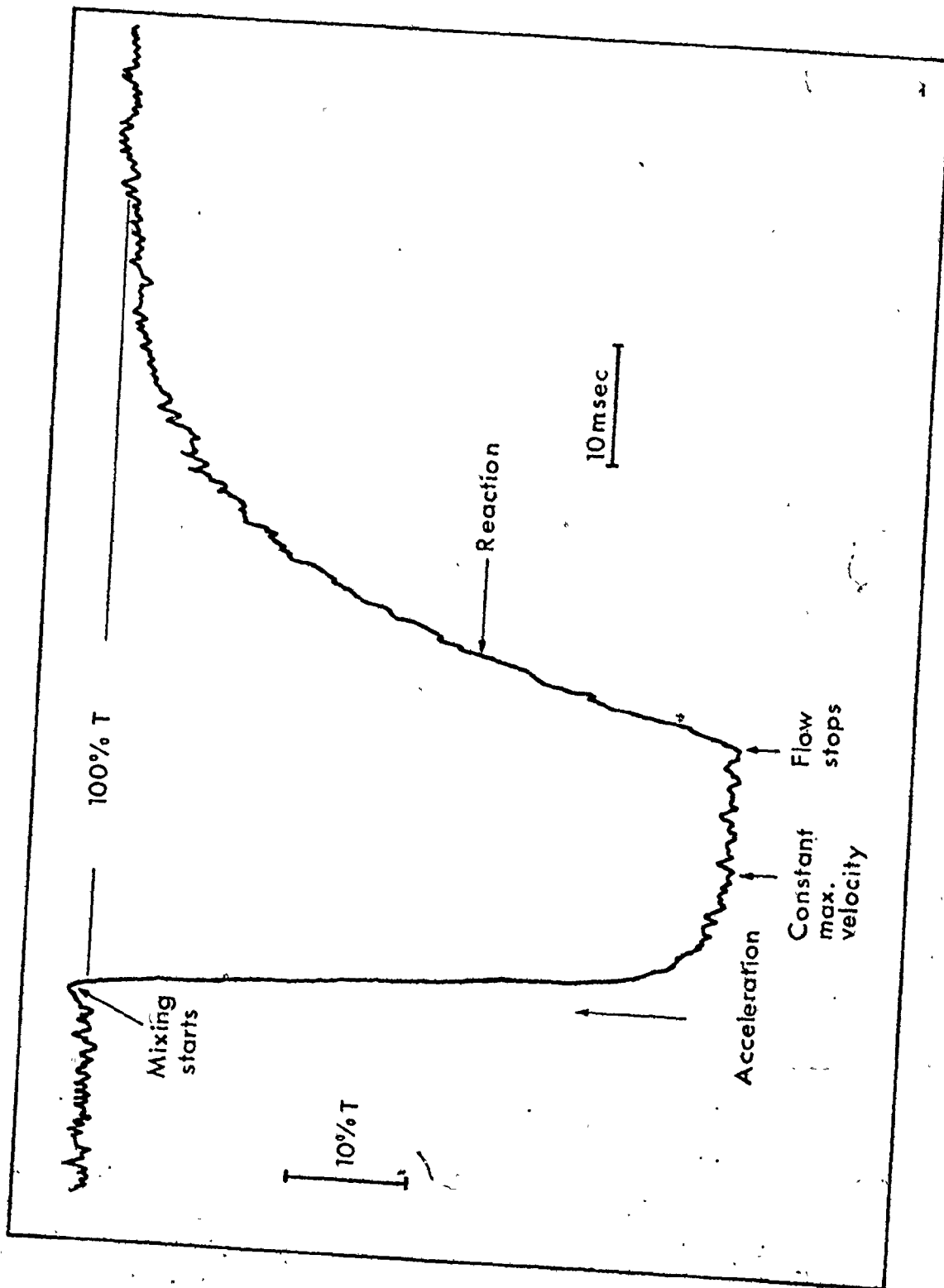
SCALING--- X VALUES TIMES 10 TO POWER -2, Y VALUES TIMES 10 TO POWER -1
 A(T), THEORY () AND EXPERIMENT (X)
 AQ= 2.500E-01, Q= 1.235E+03, QJ= 0.
 AIZ= 2.500E-01, IIZ= 3.352 (0.227), KI= 2.14E+04 (0.00002)

pre-flow triggering mode, can be seen in Figure III.10. The observation chamber was initially filled with a completely reacted solution. The plungers are accelerated and assume maximum constant velocity after approximately 10 msec. The average flow velocity was estimated to be 25 ml/sec (at a driving pressure of 80 psi) which corresponds to a linear velocity of approximately 12 m/sec. It should be pointed out that the velocity at the point of stopping is higher than the average flow velocity. During the last 10 msec before the flow stops, the transmittance is constant without any mixing artifacts. At the point where the flow stops no backshock effects can be seen - a frequent phenomenon when high pressures are used. The last part of the kinetic run is the observed part of the reaction between potassium ferricyanide and ascorbic acid, and finally the transmittance approaches the level it had before the discharge.

The SFP has been in operation for the last two years and some performance figures can be discussed. The smallest change in absorbance which still yields useful results is 0.03 per cm. Most frequently the SFP is used to study first order and second order (reversible and irreversible) reactions. The fastest first order reaction depends on the dead time of the apparatus. The largest first order rate constant measured was over 500 sec^{-1} . The second order reaction depends also on

Figure III.10. Transmittance changes during discharge.

Reaction: reduction of potassium ferricyanide (0.41 mM) by ascorbate (0.1 M) in 0.1 M phosphate buffer, pH 7.5. The reaction was measured at $\lambda = 420$ nm, time constant 0.1 msec, driving pressure 75 psi, $T = 24^{\circ}\text{C}$. A description of the events during the discharge is given in the text.



the change of the extinction coefficient during the reaction. With a change in the extinction coefficient of $2.0 \times 10^4 (\text{M cm})^{-1}$, the highest second rate constant was determined to be $3 \times 10^8 (\text{M sec})^{-1}$.

The reproducibility of the analysis was tested by measuring seven consecutive reactions between potassium ferricyanide and ascorbate of two different concentrations (see Table III.1).

Table III.1

First-order Rate Constants and Dead Times for Reduction
of Ferricyanide (0.41 mM) by Ascorbate in 0.1 M
Phosphate Buffer pH 7.0, 24°C

Ascorbate conc. (M)	Rate constant (sec ⁻¹)	Dead time (msec)
.05	118.5	1.67
.05	116.2	1.46
.05	111.6	1.36
.1	243.2	1.33
.1	232.0	1.20
.1	216.3	1.44
.1	226.4	1.61

APPENDIX IV

IV.1. Analysis of the kinetic runs

The program, developed to analyze the kinetic runs was written in Fortran language by Dr. R.A. Morton. The computations were carried out on a CDC-6400 computer (Computer Centre, McMaster University). Although this program was not produced by the author it will be briefly described to give a general idea of the method.

The analysis of the kinetic run consisted of two steps. The first step was the conversion of the experimental data to the absorbance vs time curve, i.e. $A(t)$ vs t . The second step involved calculating the reaction parameters by fitting a theoretical curve to the absorbancy values.

In order to calculate the absorbance change as a function of time two runs - the kinetic run (run K) and the calibration run (run C) were made. The transient recorder has a built-in switched time base function which enables one to store at two different sweep rates. When the kinetic run was made the experimental conditions were selected so that the first 900 channels (approximately) of the 1024 channels of the transient recorder memory

were swept at a fast rate appropriately chosen for each particular reaction. The remaining channels were swept at a slow rate to record the equilibrium level of the reaction. This is illustrated in Figure IV.1A. The calibration run (run C) was taken at a very slow sweep time rate (5 sec). Approximately 3 sec after the initiation of the run, the camera shutter in front of the PMT was closed, causing the photomultiplier current to drop to the dark current level $y(D)$ (see Figure IV.1A). These two runs (K and C) could be recorded at two different sensitivities if necessary. Where both runs were recorded at the same input scale, the transmittance at time t ($T(t)$) divided by its equilibrium value (T_{eq}) can be expressed by:

$$T(t)/T_{eq} = [y(t) - y(D)] / [y(eq) - y(D)] \quad (IV.1)$$

If one includes different amplifications (K for run K and C for run C) after some rearrangements one gets:

$$T(t)/T_{eq} = 1 + C[y_K(t) - y_K(eq)] / K[y_C(eq) - y_C(D)] \quad (IV.2)$$

The difference between the absorbancy at time t and its equilibrium value is given by:

$$\Delta A(t) = A(t) - A_{eq} = -\log \left\{ 1 + C[y_K(t) - y_K(eq)] / K[y_C(eq) - y_C(D)] \right\} \quad (IV.3)$$

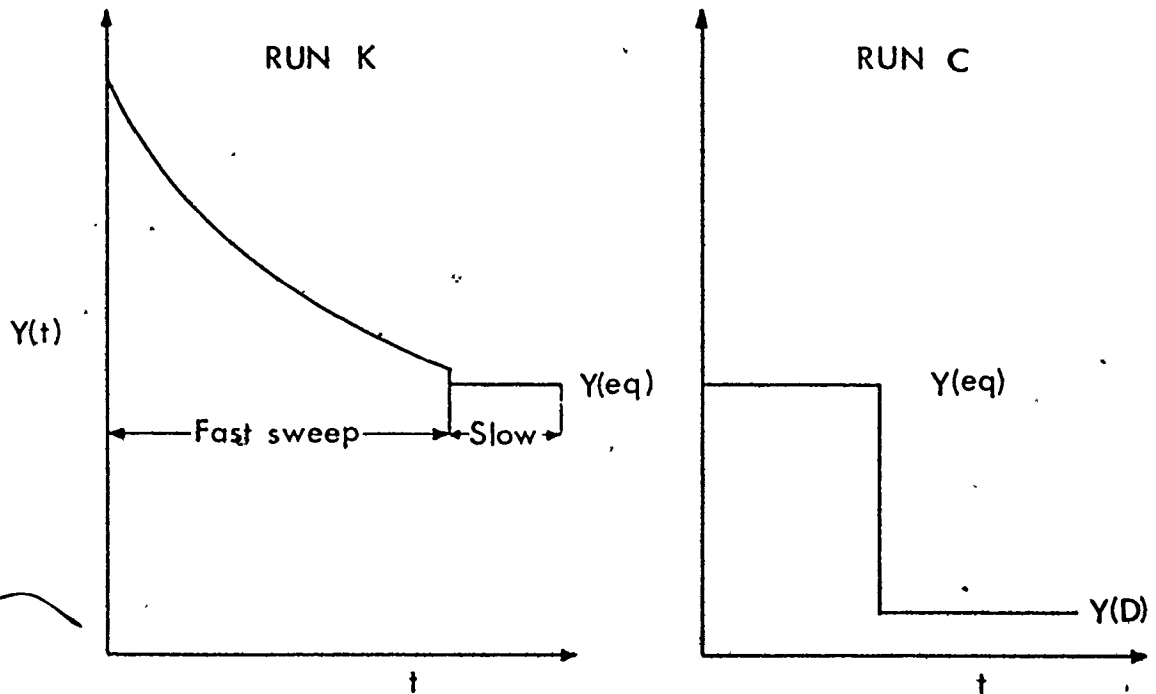
Figure IV.1A. Schematic representation of a stopped-flow experiment.

Runs K and C were recorded with the same amplification. Y(t) represents the phototube current.

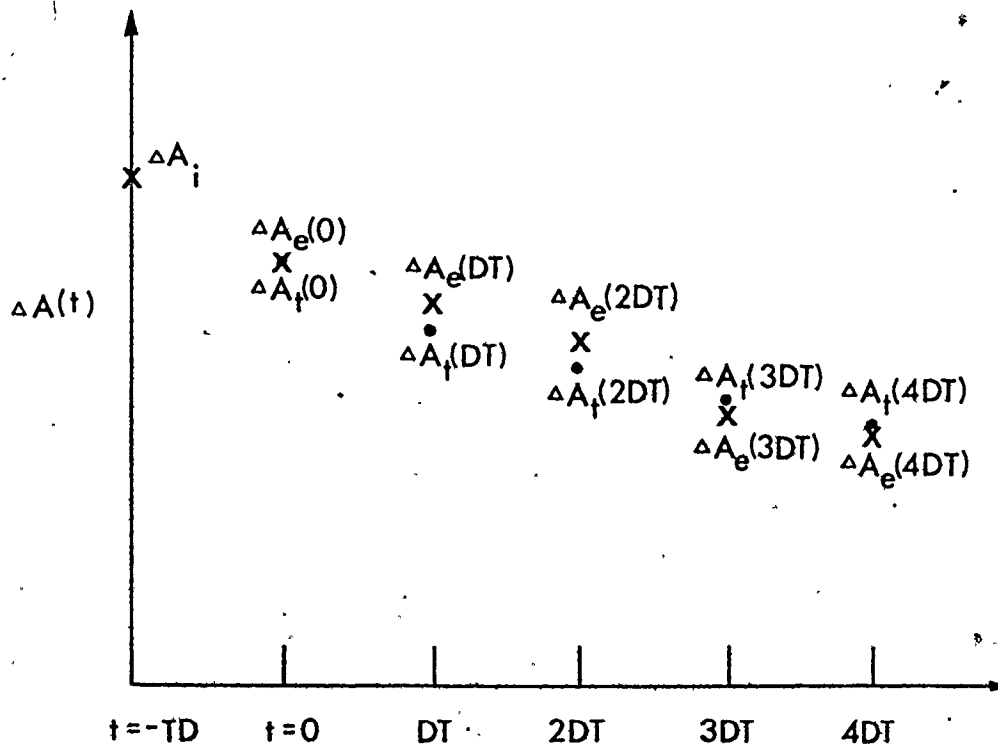
Figure IV.1B. Schematic representation of the computer fitting of the experimental curve.

ΔA_e , experimental values (X); ΔA_t , theoretical values (o); ΔA_i , the total absorbancy change determined by the spectrophotometer.

A



B



In order to average out the noise present in the experimental curve, it was smoothed by linear interpolation. A least square subroutine was used to calculate a straight line through sets of ten points and the centre value was used for further calculations. The kinetic runs were taken with various RC filtering in order to decrease the noise. Since this filtering distorts the curve, the program was written to correct for the time constant, the value $\Delta A'(t)$ being replaced by $\Delta A(t)$:

$$\Delta A(t) = \Delta A'(t) + RC(dA(t)/dt) \quad (\text{IV.4})$$

where R is the feedback resistance and C the capacitance of the filtering. The values of $\Delta A(t)$ so calculated at discrete time intervals formed the raw data for curve fitting.

By taking the logarithm of the absorbancy curve, one can determine if the reaction followed the first (or pseudo first) order kinetics. A least square procedure was employed to calculate a straight line through $\log \Delta A(t)$ vs t, points, calculating the observed pseudo-first rate constant and the half time of the reaction.

Frequently, we were interested in reactions which followed a second-order mechanism. In order to fit the experimental points to this mechanism, the following algorithms were incorporated in the program. Consider second-order reaction equation IV.5;



The rate of disappearance of P is expressed by equation

IV.6:

$$\frac{dP}{dt} = \frac{dQ}{dt} = -k_1 (P_0 - x)(Q_0 - x) + k_2 (R_0 + x)(S_0 + x) \quad (\text{IV.6})$$

where x represents the decrease in the concentration of reactant P in a given time and P_0 , Q_0 , R_0 and S_0 are the initial concentrations of the reactants P, Q, R and S.

If one re-defines:

$$P = P_0 - x$$

$$Q = Q_0 - x$$

$$R = R_0 + x$$

$$S = S_0 + x$$

equation IV.6 reduces to equation IV.7:

$$\frac{dP}{dt} = -k_1 PQ + k_2 RS \quad (\text{IV.7})$$

The change in absorbancy (ΔA) due to the reaction at time t is:

$$\Delta A(t) = (\epsilon_P P_0 + \epsilon_Q Q_0 + \epsilon_R R_0 + \epsilon_S S_0 + x\Delta\epsilon) \quad (\text{IV.8})$$

Combining equations IV.7 and IV.8 one can derive a differential equation for $\Delta A(t)$:

$$-\frac{d\Delta A(t)}{dt} = c_1 [\Delta A(t)]^2 + c_2 \Delta A(t) \quad (\text{IV.9})$$

where c_1 and c_2 are defined:

$$c_1 = (k_2 - k_1) / \Delta\epsilon \quad \text{and}$$

$$c_2 = 2\Delta A_i (k_1 - k_2) / \Delta\epsilon - \Delta A_i [k_1 (P_0 + Q_0) + k_2 (R_0 + S_0)]$$

ΔA_i is the value of the absorbancy change at $t = -TD$, where TD designates the dead time of stopped-flow photometer (see Figure IV.1B). The solution of this differential equation is:

$$\Delta A(t) = (c_2 e^{c_2 t}) / (1 - c_1 e^{c_1 t}) \quad (\text{IV.10})$$

where

$$G = \Delta A(0) / (c_1 \Delta A(0) + c_2)$$

with $\Delta A(0)$ being the value of the absorbancy change at $t = 0$, i.e. the first point detected by the stopped-flow photometer.

The parameters necessary to carry out the fitting of the experimental data to equation IV.10 are:

- 1) an initial guess for k_1 and its lower and upper limits.
- 2) an initial guess for the dead time and its upper and lower limits.
- 3) the measured value of ΔA_i which was allowed to vary ($\pm 5\%$) to produce the best fit within these limits.

Using these initial values, the computer calculated $\Delta A(t)$ (IV.10) at discrete time intervals (see Figure IV.1B). By changing the rate constant (k_1), the dead time (TD) and the value

of the absorbancy change at $t = -TD$, ΔA_i , the difference between the theoretical and the experimental values can be minimized. This optimization was carried out by a subroutine called Simplex (Nedler and Mead, 1965). The search for the optimum values of k_1 , TD and ΔA_i was stopped when the standard error (defined by equation IV.11) became smaller than a pre-set value (v).

$$\left[\frac{1}{N} \sum_{i=1}^N (\Delta A_c(t_i) - \Delta A_t(t_i)) \right]^2 < v \quad (\text{IV.11})$$

where N is the number of the points. Once k_1 is known, k_2 was calculated from the equilibrium relation:

$$k_2 = k_1 (P_o - x_{eq})(Q_o - x_{eq}) / (R_o + x_{eq})(S_o + x_{eq}) \quad (\text{IV.12})$$

where x_{eq} is the extent of the reaction at the equilibrium, and is related to ΔA_i by:

$$x_{eq} = -\Delta A_i / \Delta \epsilon$$

Finally, the program estimated the dead time of the apparatus using the equation IV.10 and printed the theoretical curve and experimental points.

Variances of the optimized kinetic parameters were obtained as follows: In the case of pseudo-first order reaction, a least squares procedure was used. Finding the uncertainty in the estimation of the rate constant is equivalent to estimating the variance of the slope. The variance of the slope σ_s^2 is given by the

sum of the product of the variance σ_i^2 of each data point (y_i) with the effect that data point has on the slope (Bevington, 1969):

$$\sigma_s^2 = \sum_i \sigma_i^2 \left(\frac{\partial S}{\partial y} \right)^2 \quad (\text{IV.13})$$

If one defines $\ln \Delta A(t) = y(t)$, the variance of the slope is given by:

$$\sigma_s^2 = \frac{1}{N-2} \sum_i (y_i - y_i^t)^2 / \sum_i (t_i - \bar{t})^2 \quad (\text{IV.14})$$

where N is the number of data points, $(y_i - y_i^t)$ is the difference between the experimental and calculated value of y at time t_i , and \bar{t} is the mean of t_i .

The variances of the parameters determined by fitting the data to a second-order mechanism were determined similarly. In this case, $y(t)$ represents the absorbancy change as a function of time. The relationship between the variance of a parameter (the rate constant, for example) α (σ_α^2) and the variance in the absorbancy σ_y^2 can be expressed:

$$\sigma_y^2 = \sigma_\alpha^2 \sum_i \left(\frac{\partial y}{\partial \alpha} \right)^2 \quad (\text{IV.15})$$

The variance of y is :

$$\sigma_y^2 = \frac{1}{N-2} \sum_i (y_i - y_i^t)^2 \quad (\text{IV.16})$$

The second term in equation IV.15 was estimated according to equation IV.17 by incrementing α a small amount and calculating the effect on $y_i(t)$:

$$\sum_i \left(\frac{\partial y_i}{\partial \alpha} \right)^2 = \frac{1}{\Delta \alpha^2} \sum [y_i(\alpha + \Delta \alpha) - y_i(\alpha)]^2 \quad (\text{IV.17})$$

From σ_y^2 and $\sum_i \left(\frac{\partial y_i}{\partial \alpha} \right)^2$, σ_α^2 was calculated by equation IV.15.

REFERENCES

- ALBERTY, R.A. and Hammes, G.G. (1958). *J. Phys. Chem.* 62, 154.
- AMBLER, R.P. (1963a). *Biochem. J.* 89, 341.
- AMBLER, R.P. (1963b). *Biochem. J.* 89, 349.
- ASHIDA, T., Ueki, T., Tsukihara, T., Sugihara, A., Takano, T. and Kakudo, M. (1971). *J. Biochem.* 70, 913.
- ASHIDA, T., Tanaka, N., Yamane, T., Tsukihara, T. and Kakudo, M. (1973). *J. Biochem.* 73, 463.
- BALLOU, D.P. (1971). *Ph. D. Thesis*, University of Michigan, Ann Arbor, Mich. USA.
- BALLOU, D.P. (1973). *Private communication*.
- BALLOU, D.P. and Palmer, G.A. (1974). *Anal. Chemistry* 46, 1248.
- BARLOW, G.H. and Margoliash, E. (1966). *J. Biol. Chem.* 241, 1473.
- BEEBLESTONE, J. (1960). *Arch. Biochem. Biophys.* 89, 35.
- BEVINGTON, P.R. (1969). *Data Reduction and Error Analysis for the Physical Sciences*. McGraw Hill, N.Y. p. 56ff.
- BOYD, W.C. (1965). *J. Biol. Chem.* 240, 4097.
- BRANDT, K.G., Parks, P.C., Czerlinski, G.H. and Hess, G.P. (1966). *J. Biol. Chem.* 241, 4180.

- CAMPION, R.J., Deck, C.F., King, P. and Wahl, A.C. (1967).
Inorg. Chem. 6, 672.
- CASSATT, J.C. and Marini, P.C. (1974). *Biochemistry*
13, 5323.
- CASTRO, C.E. (1971). *J. Theor. Biol.* 33, 475.
- CASTRO, C.E. and Davis, H.F. (1969). *J. Am. Chem. Soc.*
91, 5405.
- CHANCE, B. (1964). *Rapid Mixing and Sampling Techniques*
in Biochemistry, edited by Chance, B., Einsenhardt,
R.H., Gibson, Q.H. and Lonberg-Holm, K.K., Academic
Press (1964), p. 39.
- CREUTZ, C. and Sutin, N. (1974). *J. Biol. Chem.* 249, 6788.
- DEVAULT, D. and Chance, B. (1966). *Biophys. J.* 6, 825.
- DICKERSON, R.E. (1968). IN: *Structure and Function of*
Cytochromes, edited by Okunuki, K., Kamen, M.D.
and Sekuzu, I. University Park Press, Baltimore.
p. 437.
- DICKERSON, R.E., Takano, T., Eisenberg, D., Kallai, O.B.,
Swanson, L., Cooper, A. and Margoliash, E. (1971a).
J. Biol. Chem. 246, 1511.
- DICKERSON, R.E. (1971b). *J. Mol. Biol.* 57, 1.
- DICKERSON, R.E. (1974). *Ann. N.Y. Acad. Sci.* 227, 599.
- DIXON, H.B.F. and Thompson, C.M. (1968). *Biochem. J.*
107, 427.
- DULTZ, G. and Sutin, N. (1963). *Inorg. Chem.* 2, 917.

- EATON, W.A., George, P. and Hanania, G.I.H. (1967).
J. Phys. Chem. 71, 2016.
- EHRENBERG, A. and Paleus, S. (1955). *Acta Chem. Scand.*
9, 1193.
- EWAL, R.X. and Bennett, L.E. (1974). *J. Am. Chem. Soc.*
96, 940.
- FANGER, M.W., Hettinger, P.T. and Harbury, H.A. (1967).
Biochemistry 6, 713.
- FEINSTEIN, R.N. (1952). *J. Lab. Clin. Med.* 40, 313.
- FERGUSON-MILLER, S., Brautigan, D. and Margoliash, E.
(1976). *J. Biol. Chem.* 251, 1104.
- FRIDOVICH, I. (1963). *J. Biol. Chem.* 238, 592.
- FROST, A.A., and Pearson, R.G. (1961a). *Kinetics and
Mechanism, 2nd edition* p.150. John Wiley and
Sons, Inc.
- FROST, A.A. and Pearson, R.G. (1961b). *Kinetics and
Mechanism, 2nd edition* p.127. John Wiley and
Sons, Inc.
- GIBSON, Q.H. and Milnes, L. (1964). *Biochem. J.* 91, 161.
- GIBSON, Q.H. (1969). *Methods of Enzymology*, Vol. 16,
ed. Kustin, K., Academic Press, p. 187.
- GREEN, A.A. (1933). *J. Am. Chem. Soc.* 55, 2331.
- GRIMES, C.J., Piszkiwicz, D. and Fleisher, E.B. (1974).
Proc. Nat. Acad. Sci. USA 71, 1408.
- GOOD, N.E., Wignat, G.D., Winter, W. and Connolly, T.N.
(1966). *Biochemistry* 5, 467.

- GUPTA, R.K., Loenig, S.H. and Redfield, A.G. (1972).
J. Mag. Res. 7, 66.
- GURD, F.R.N. (1970). IN: *Physical Principles and
Techniques of Protein Chemistry*, ed. Leach, S.J.,
part B, p. 365.
- HALPERN, J. (1961). *Quart. Rev. (London)* 15, 207.
- HAMMES, G.G. and Haslam, J.L. (1968). *Biochemistry* 7,
1519.
- HANANIA, G.I.H., Irvine, D.H., Eaton, W.A. and George, P.
(1967). *J. Phys. Chem.* 71, 2022.
Handbook of Chemistry and Physics, The Chemical Rubber Co.,
Cleveland, Ohio.
- HANSTEIN, W.G. and Hatefi, Y. (1974). *Proc. Nat. Acad. Sci.
USA* 71, 288.
- HARVEY, R.A. (1969). *Anal. Biochem.* 29, 58.
- HAVSTEEN, B.H. (1965). *Acta Chem. Scand.* 19, 1227.
- HETTINGER, T.P. and Harbury, H.A. (1964). *Proc. Nat.
Acad. Sci. USA* 52, 1469.
- HODGES, H.L., Holwerda, R.A. and Grey, H.B. (1974).
J. Am. Chem. Soc. 96, 3132.
- HOPFIELD, J.J. (1974). *Proc. Nat. Acad. Sci. USA* 71,
3640.
- KAKADE, M.L. and Liéner, I.E. (1969). *Anal. Biochem.*
27, 273.
- KATZ, S. and Ellinger, F. (1962). *Biochemistry* 2, 406.
- KEILIN, D. (1930). *Proc. Roy. Soc. London Biol. Sci.* 106,
418.

- KERESZTES-NAGY, S. and Klotz, I.M. (1965). *Biochemistry* 4, 919.
- KOLTHOFF, I.M. and Tomsicek, W.J. (1935). *J. Phys. Chem.* 39, 945.
- KOWALSKI, A. (1969). *J. Biol. Chem.* 244, 6619.
- LIBBY, W.F. (1952). *J. Phys. Chem.* 56, 863.
- LUMRY, R., Smith, E.L. and Glantz, R.R. (1951). *J. Am. Chem. Soc.* 73, 4330.
- MALMSTADT, H., Enke, C.G. and Toren, E.C. (1963). *Electronics for Scientists*, p. 431, Benjamin Publishing Co., New York.
- MARCUS, R.A. (1955). *J. Chem. Phys.* 24, 966.
- MARCUS, R.A. (1959). *Can. J. Chem.* 37, 155.
- MARCUS, R.A. (1963). *J. Phys. Chem.* 67, 853.
- MARGALIT, R. and Schejter, A. (1970). *FEBS, Lett.* 6, 278.
- MARGALIT, R. and Schejter, A. (1973a). *Eur. J. Biochem.* 32, 492.
- MARGALIT, R. and Schejter, A. (1973b). *Eur. J. Biochem.* 32, 500.
- MARGOLIASH, E. and Frohwirt, N. (1959). *Biochem. J.* 71, 570.
- MARGOLIASH, E. and Schejter, A. (1966). *Adv. Prot. Chem.* 21, 113.
- MARGOLIASH, E. and Walasek, O.F. (1967). IN: *Methods in Enzymology*, Vol. 10, eds. Eastbrook, R.W. and Pullman, M.E., Academic Press, New York, pp. 339.

- MARGOLIASH, E., Barlow, G.H. and Byers, V. (1970).
Nature 228, 723.
- MARGOLIASH, E., Ferguson-Miller, S., Tulloss, J., Kang,
C.G., Feinberg, B.A., Brautingan, D.L. and
Morrison, M. (1973). *Proc. Nat. Acad. Sci. USA*
70, 3245.
- MCARDLE, J.V., Gray, H.B., Creutz, C. and Sutin, N. (1974).
J. Am. Chem. Soc. 96, 5737.
- MCELORY, J.D., Mauzerall, D.C. and Feher, G. (1974).
Biochem. Biophys. Acta. 333, 261.
- MEANS, G.E. and Feeney, R.E. (1971). *Chemical Modification
of Proteins*, p. 93, Holden-Day, Inc. San Francisco.
- MILLER, W.G. and Cusanovich, M.A. (1975). *Biophys.
Struct. Mechanism* 1, 97.
- MORTON, R.A., Overnell, J. and Harbury, H.A. (1970).
J. Biol. Chem. 245, 4653.
- NELDER, J.A. and Mead, R. (1965). *Computer J.* 7, 308.
- NEWTON, T.W. (1968). *J. Chem. Education* 45, 571.
- NICHOLLS, P. (1974). *Biochim. Biophys. Acta* 346, 261.
- NORTH, A.M. (1966). *Quart. Rev. Chem. Soc.* 20, 421.
- OKUYAMA, T. and Satake, K. (1960). *J. Biochem.* 47, 454.
- PALCIC, K. (1972). *M.Sc. Thesis*, McMaster University,
Hamilton, Ontario, Canada.
- POWER, S.D., Choucair, A. and Palmer, G. (1975). *Biochem.
Biophys. Res. Comm.* 66, 103.
- REDFIELD, A.G. and Gupta, R.K. (1971). *Cold Spring
Harbor Symp. Quant. Biol.* 36, 405.

- SALEMME, F.R., Kraut, J. and Kamen, M.D. (1973). *J. Biol. Chem.* 248, 7701.
- SALEMME, F.R., Freer, S.T., Xuong, Ng. H., Alden, R.A. and Kraut, J. (1973a). *J. Biol. Chem.* 248, 3910.
- SCHEJTER, A. and Margalit, R. (1970). *FEBS Lett.* 10, 179.
- SCHOLES, P.B. and Smith, L. (1968). *Biochim. Biophys. Acta* 153, 363.
- SCHOLES, P.B., McLain, G. and Smith, L. (1971). *Biochemistry* 10, 2072.
- SMITH, L. and Minnaert, K. (1965). *Biochim. Biophys. Acta* 105, 1.
- SMITH, L., Newton, N. and Scholes, P. (1966). *Hemes, and Hemoproteins*, eds. Chance, B., Eastbrook, R. and Yonetani, T., p. 395, Academic Press, New York.
- SMITH, M.H. (1973). *Biophys. J.* 13, 817.
- SMITH, L., Davies, H.C., Reichlin, M. and Margoliash, E. (1973). *J. Biol. Chem.* 248, 237.
- STELLWAGEN, E. and Shulman, R.G. (1973a). *J. Mol. Biol.* 75, 683.
- STELLWAGEN, E. and Shulman, R.G. (1973b). *J. Mol. Biol.* 80, 559.
- STELLWAGEN, E. and Cass, R.D. (1975). *J. Biol. Chem.* 250, 2095.
- STRICKLAND, S., Palmer, G. and Massey, V. (1975). *J. Biol. Chem.* 250, 4048.
- SUTIN, N. and Yandell, J.K. (1972). *J. Biol. Chem.* 247, 6932.

- SUTIN, N. (1976). (Submitted to *Advances in Chemistry*).
- SWANSON, R., Trus, B.L., Mandel, H., Mandel, G., Kallai, O.B. and Dickerson, R.E. (1976). *J. Biol. Chem.* In press.
- TAKANO, T., Kallai, O.B., Swanson, R. and Dickerson, R.E. (1973). *J. Biol. Chem.* 248, 5234.
- TAKANO, T., Trus, B.L., Mandel, N., Mandel, G., Kallai, O.B., Swanson, R. and Dickerson, R.E. (1976). *J. Biol. Chem.* In press.
- TANAKA, N., Tamane, T., Tsukihara, T., Ashida, T. and Kakudo, M. (1975). *J. Biochem.* 77, 147.
- TAUBE, H. and Myers, H. (1954). *J. Am. Chem. Soc.* 76, 2103.
- TIMKOVICH, R. and Dickerson, R.E. (1973). *J. Mol. Biol.* 79, 39.
- VERNON, L.P. (1956). *J. Biol. Chem.* 222, 1035.
- WADA, K. and Okunuki, K. (1969). *J. Biochem.* 66, 249.
- WILGUS, H. and Stellwagen, E. (1974). *Proc. Nat. Acad. Sci. USA.* 71, 2892.
- WINFIELD, M.E. (1965). *J. Mol. Biol.* 12, 600.
- WOOD, F.E. and Cusanovich, M.A. (1975). *Bioinorg. Chem.* 4, 337.
- YAMANAKA, T. and Okunuki, K. (1963). *Biochim. Biophys. Acta* 67, 379.
- YAMAZAKI, I. (1962). *J. Biol. Chem.* 237, 224.
- YANDELL, J.K., Fay, D.P. and Sutin, N. (1973). *J. Am. Chem. Soc.* 95, 1131.

ZABINSKI, R.M., Tatti, K. and Czerlinski, G.H. (1973).

J. Biol. Chem. 249, 6125.